AI in Thyroid Cancer Diagnosis: Techniques, Trends, and Future Directions

Yassine Habchi [1], Yassine Himeur [2,*,†], Hamza Kheddar [3,†], Abdelkrim Boukabou [4,†], Shadi Atalla [2,†], Ammar Chouchane [5,†], Abdelmalik Ouamane [6,†] and Wathiq Mansoor [2,†]

[1] Institute of Technology, University Center Salhi Ahmed, BP 58 Naama, Naama 45000, Algeria; habchi@cuniv-naama.dz

[2] College of Engineering and Information Technology, University of Dubai, Dubai 14143, United Arab Emirates; satalla@ud.ac.ae (S.A.); wmansoor@ud.ac.ae (W.M.)

[3] LSEA Laboratory, Electrical Engineering Department, University of Medea, Medea 26000, Algeria; hamza.kheddar@gmail.com

[4] Department of Electronics, University of Jijel, BP 98 Ouled Aissa, Jijel 18000, Algeria; aboukabou@univ-jijel.dz

[5] Department of Electrical Engineering, University of Yahia Fares Medea, Medea 26000, Algeria; chouchane.ammar@univ-medea.dz

[6] Laboratory of LI3C, Mohamed Khider University, Biskra 07000, Algeria; ouamaneabdealmalik@univ-biskra.dz

* Correspondence: yhimeur@ud.ac.ae

† These authors contributed equally to this work.

Abstract: Artificial intelligence (AI) has significantly impacted thyroid cancer diagnosis in recent years, offering advanced tools and methodologies that promise to revolutionize patient outcomes. This review provides an exhaustive overview of the contemporary frameworks employed in the field, focusing on the objective of AI-driven analysis and dissecting methodologies across supervised, unsupervised, and ensemble learning. Specifically, we delve into techniques such as deep learning, artificial neural networks, traditional classification, and probabilistic models (PMs) under supervised learning. With its prowess in clustering and dimensionality reduction, unsupervised learning (USL) is explored alongside ensemble methods, including bagging and potent boosting algorithms. The thyroid cancer datasets (TCDs) are integral to our discussion, shedding light on vital features and elucidating feature selection and extraction techniques critical for AI-driven diagnostic systems. We lay out the standard assessment criteria across classification, regression, statistical, computer vision, and ranking metrics, punctuating the discourse with a real-world example of thyroid cancer detection using AI. Additionally, this study culminates in a critical analysis, elucidating current limitations and delineating the path forward by highlighting open challenges and prospective research avenues. Through this comprehensive exploration, we aim to offer readers a panoramic view of AI's transformative role in thyroid cancer diagnosis, underscoring its potential and pointing toward an optimistic future.

Keywords: thyroid carcinoma detection; thyroid cancer segmentation; machine learning; deep learning; convolutional neural networks

1. Introduction

1.1. Background

The adoption of AI in healthcare has become a pivotal development, profoundly reshaping the landscape of medical diagnosis, treatment, and patient care. AI's exceptional capabilities, including pattern recognition, predictive analytics, and decision-making skills, enable the development of systems that can analyze complex medical data at a scale and precision beyond human capacity [1]. This, in turn, augments early disease detection, facilitates accurate diagnoses, and aids personalized treatment planning. Moreover, AI-driven predictive models can forecast disease outbreaks, enhance the efficiency of hospital

operations, and significantly improve patient outcomes [2]. Additionally, AI has the potential to democratize healthcare by bridging the gap between rural and urban health services and making high-quality care more accessible. Hence, the importance of AI in healthcare is profound and will continue to grow as technology advances, leading to more sophisticated applications and better health outcomes for patients worldwide [3,4]. However, the trust serves as a mediator, influencing the impact of AI-specific factors on user acceptance. Researchers have investigated how security, risk, and trust impact the adoption of AI-powered assistance [5]. They have conducted empirical tests on their proposed research framework and found that trust plays a pivotal role in determining user acceptance.

Cancer, a leading cause of death, affects various body parts, as depicted in Figure 1a. Among different types, thyroid carcinoma is one of the most common endocrine cancers globally [6,7]. Concerns are mounting over the escalating incidence of thyroid cancer and associated mortality. Research indicates that thyroid cancer incidence is higher in women aged 15–49 (ranked fifth globally) than in men aged 50–69 years [8–10].
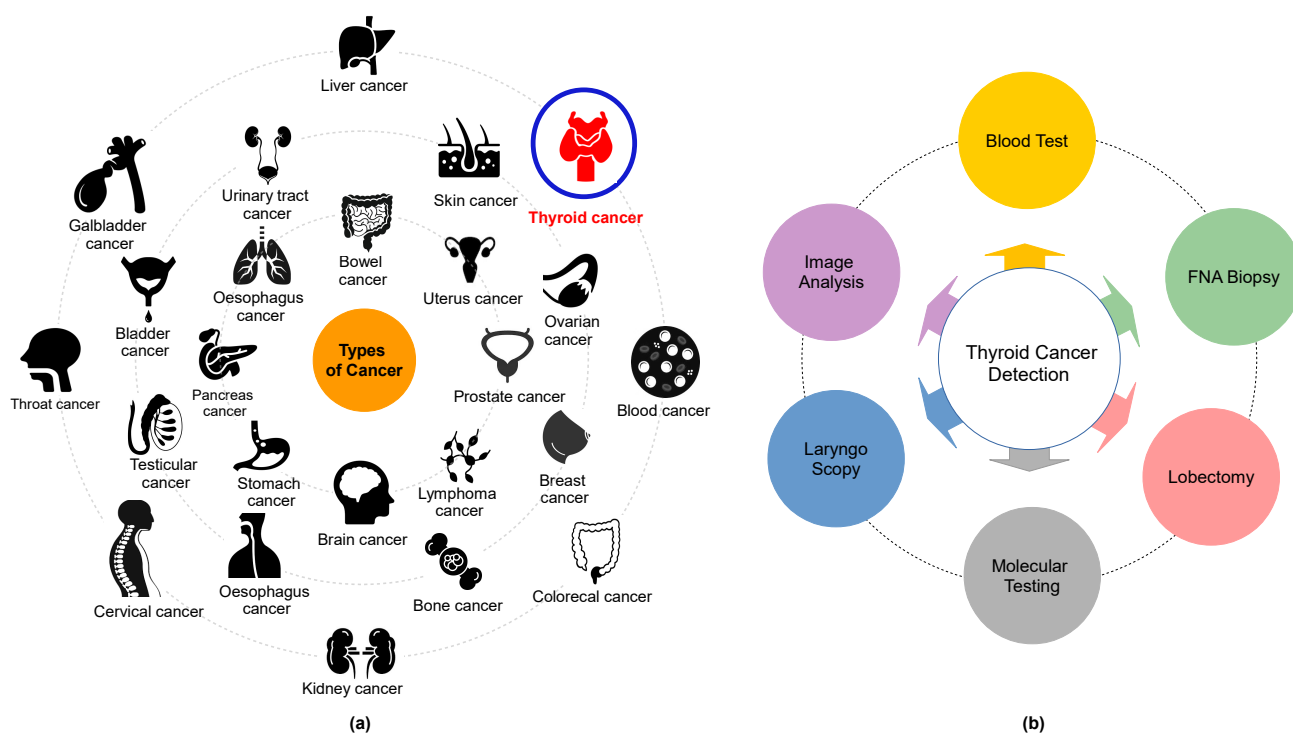

Figure 1. (**a**) Some of the common types of cancer and (**b**) thyroid cancer detection methods.

According to existing global epidemiological data, the rapid growth of abnormal thyroid nodules is driven by an accelerated increase in genetic cell activity, where the normal functioning and activity of cells in an organism are heightened or intensified. This condition can be categorized into four primary subtypes: papillary carcinoma (PTC) [11], follicular thyroid carcinoma (FTC) [12], anaplastic thyroid carcinoma (ATC) [13], and medullary thyroid carcinoma (MTC) [14]. Influential factors such as high radiation exposure, Hashimoto's thyroiditis, psychological and genetic predispositions, and advancements in detection technology can contribute to the onset of these cancer types. These conditions might subsequently lead to chronic health issues, including diabetes, irregular heart rhythms, and blood pressure fluctuations [15–17]. Although the quantity of cancer cells is a significant indicator for assessing both invasiveness and poor prognosis in thyroid carcinoma, obtaining results is often time-consuming due to the requirement to observe cell appearance. Therefore, the detection and quantification of cell nuclei are considered alternative biomarkers for assessing cancer cell proliferation.

The utilization of computer-aided diagnosis (CAD) systems for analyzing thyroid cancer images has seen a significant increase in popularity in recent years. These systems, renowned for enhancing diagnostic accuracy and reducing interpretation time, have become an invaluable tool in the field. Among these technologies, radionics, when used in conjunction with ultrasonography imaging, has become widely accepted as a cost-effective, safe, simple, and practical diagnostic method in clinical practice. Endocrinologists frequently conduct US scans in the 7–15 MHz range to identify thyroid cancer and evaluate its anatomical characteristics. The American College of Radiology has formulated a Thyroid Imaging, Reporting, and Data System (TI-RADS) that classifies thyroid nodules into six categories based on attributes such as composition, echogenicity, shape, size, margins, and echogenic foci. These classifications range from normal (Thyroid Imaging, Reporting, and Data System (TIRADS)-1) to malignant (TIRADS-6) [18–20]. Several open-source applications are available for assessing these thyroid cancer features [21,22]. However, the identification and differentiation of nodules continue to present a challenge, largely reliant on radiologists' personal experience and cognitive abilities. This is due to the subjective nature of human eye-based image recognition, the poor quality of captured images, and the similarities among US images of benign thyroid nodules, malignant thyroid nodules, and lymph nodes.

Moreover, ultrasonography imaging is often a time-intensive and stressful procedure, which can result in inaccurate diagnoses. Misclassifications among normal, benign, malignant, and indeterminate cases are typical [23–28]. A fine-needle aspiration biopsy (FNAB) is typically conducted for a more precise diagnosis. However, FNAB can be an uncomfortable experience for patients, and a specialist's lack of knowledge can potentially convert benign nodules into malignant ones, not to mention the additional financial burden [29,30] (refer to Figure 1b). Selecting their characteristics is the primary challenge in distinguishing between benign and malignant nodules. Numerous studies have explored the characterization of conventional US imaging for various types of cancers, including retina [31,32], breast cancer [33–37], blood cancer [38,39], and thyroid cancer [40,41]. However, these methods remain insufficiently accurate for the reliable classification of thyroid nodules.

The incorporation of AI technology plays a pivotal role in reducing subjectivity and enhancing the accuracy of pathological diagnoses for various intractable diseases, including those affecting the thyroid gland [42,43]. This enhancement is achieved through an improved interpretation of ultrasonography images and faster processing times. Machine learning (ML) and deep learning (DL) have surfaced as potential solutions for automating the classification of thyroid nodules in applications such as US, fine-needle aspiration (FNA), and thyroid surgery [44,45]. This potential has been underscored in numerous studies, such as [43,46–50]. Furthermore, there are ongoing studies examining the use of this innovative technology for cancer detection, where its effectiveness hinges on the volume of data and the precision of the classification process.

The motivation to write a review on "AI in thyroid cancer diagnosis" stems from the increasing prevalence of thyroid cancer, a significant endocrine malignancy where early and accurate detection is pivotal for patient outcomes. As technological advancements in AI and machine learning burgeon, their integration into medical diagnostics—spanning imaging, pathology, and genomics—offers potential improvements in detection accuracy and efficiency. Traditional thyroid carcinoma diagnostic methods, such as fine-needle aspiration biopsies, sometimes present inconclusive results; AI promises less-invasive alternatives with possibly superior precision. This review amalgamates insights from the intersection of computer science, radiology, pathology, and endocrinology, propelling multidisciplinary collaboration. It also spotlights AI's clinical implications, guiding clinicians in leveraging its capabilities for patient care, while delineating future research directions. Furthermore, this review underscores the economic and healthcare benefits, from cost savings to reduced waiting times. At the same time, it is imperative to address AI's inherent challenges, including data privacy and ethical considerations, ensuring its balanced integration into healthcare. In essence, the review offers a comprehensive panorama of AI's

current and potential role in thyroid carcinoma detection, benefiting both researchers and medical practitioners.

1.2. Our Contribution

This review provides a comprehensive examination of the application of AI methods in detecting thyroid cancer. The objective of AI-based analysis in the medical field is increasingly shifting towards enhancing diagnostic accuracy, and this review aims to illustrate this trend, particularly in thyroid cancer detection. We first provide an overview of the existing frameworks and delve into the specifics of various AI techniques. These include supervised learning methods, such as DL, artificial neural networks, traditional classification, and PMs, as well as USL methods, such as clustering and dimensionality reduction. We also explore ensemble methods, including bagging and boosting. Recognizing the importance of quality datasets in AI applications, we scrutinize several TCDs, addressing their features, as well as feature selection and extraction methods used in various studies. We then outline the standard assessment criteria used to evaluate the performance of AI-based thyroid cancer detection methods. These range from classification and regression metrics to statistical metrics, machine vision metrics, and ranking metrics. Finally, we discuss future research directions, emphasizing areas that require more attention to overcome existing barriers and improve the use and deployment of thyroid cancer detection solutions. In conclusion, we underscore the potential of AI in advancing thyroid cancer detection while also noting the need for a continuous critical evaluation to ensure its responsible and effective use.

Accordingly, the principal contributions of our paper are as follows:

- An overview of existing frameworks and specifics of various AI techniques, including supervised learning (DL, artificial neural networks, traditional classification, and PMs) and USL (clustering and dimensionality reduction) methods, as well as ensemble methods (bagging and boosting).
- An examination of multiple TCDs, exploring the characteristics of these datasets, as well as the methods employed for selecting and extracting features in different research studies.
- An outline of standard assessment criteria used to evaluate the performance of AI-based thyroid cancer detection methods, encompassing classification and regression metrics, statistical metrics, computer vision metrics, and ranking metrics.
- A critical analysis and discussion highlighting limitations, hurdles, current trends, and open challenges in the field.
- A discussion of future research directions, emphasizing areas requiring more attention to overcome existing barriers and improve thyroid cancer detection solutions.
- An emphasis on the potential of AI in advancing thyroid cancer detection while advocating a continuous critical evaluation for responsible and effective use.

Additionally, the principal contributions of the proposed review compared to other existing surveys are summarized in Table 1.

Table 1. The significant contributions of the proposed review on thyroid cancer classification in comparison with other related studies.

Ref	Year	PPY	TCDS	AIA	Open Challenges			Future Directions					
					TCDA	RDLA	PP	XAI	EFC-AI	RL	PS	IoMIT	RS
[51]	2021	✓	✓	✗	✗	✗	✗	✗	✗	✗	✗	✗	✗
[52]	2021	✓	✓	✗	✗	✗	✗	✗	✗	✗	✗	✗	✗
[53]	2021	✓	✓	✗	✗	✗	✗	✗	✗	✗	✗	✗	✗
[54]	2021	✓	✓	✗	✗	✗	✗	✗	✗	✗	✗	✗	✗
[55]	2021	✓	✓	✗	✗	✗	✗	✗	✗	✗	✗	✗	✗
[56]	2022	✓	✓	✗	✗	✗	✗	✗	✗	✗	✗	✗	✗
[57]	2022	✓	✓	✗	✗	✗	✗	✗	✗	✗	✗	✗	✗
[58]	2022	✓	✓	✗	✗	✗	✗	✗	✗	✗	✗	✗	✗
[59]	2022	✓	✓	✗	✗	✗	✗	✗	✗	✗	✗	✗	✗
Ours	-	✓	✓	✓	✓	✓	✓	✓	✓	✓	✓	✓	✓

Abbreviations: edge, fog, and cloud networks based on AI (EFC-AI).

1.3. Road Map

The rest of this paper is organized as follows. Section 2 follows, providing an overview of existing frameworks utilized in this field, and discussing their respective advantages and limitations. Section 3 presents various TCDs used in AI-based analyses, explaining their relevance and uniqueness. In Section 4, the paper delves into the vital aspect of "Features", discussing feature extraction and selection methods in AI models used for thyroid cancer detection. Section 5 outlines the standard assessment criteria used to evaluate the performance of these models. An actual instance of AI-based thyroid cancer detection is presented in Section 6 to provide a real-world context to the theoretical aspects discussed earlier. The paper then proceeds to a critical analysis and discussion in Section 7, where challenges, limitations, and areas for improvement in the current approaches are discussed. In Section 8, potential future research directions are proposed, highlighting areas where further exploration and innovation can lead to advancements in AI-based thyroid cancer detection. The paper concludes with Section 9, summarizing the main findings and discussions, thereby providing a comprehensive conclusion to the discussions presented in the earlier sections.

2. Overview of Existing Frameworks

This section showcases the various AI-based methods utilized for diagnosing thyroid gland (TG) cancers. In the illustration, Figure 2 presents a proposed categorization of the thyroid cancer diagnosis techniques relying on AI.
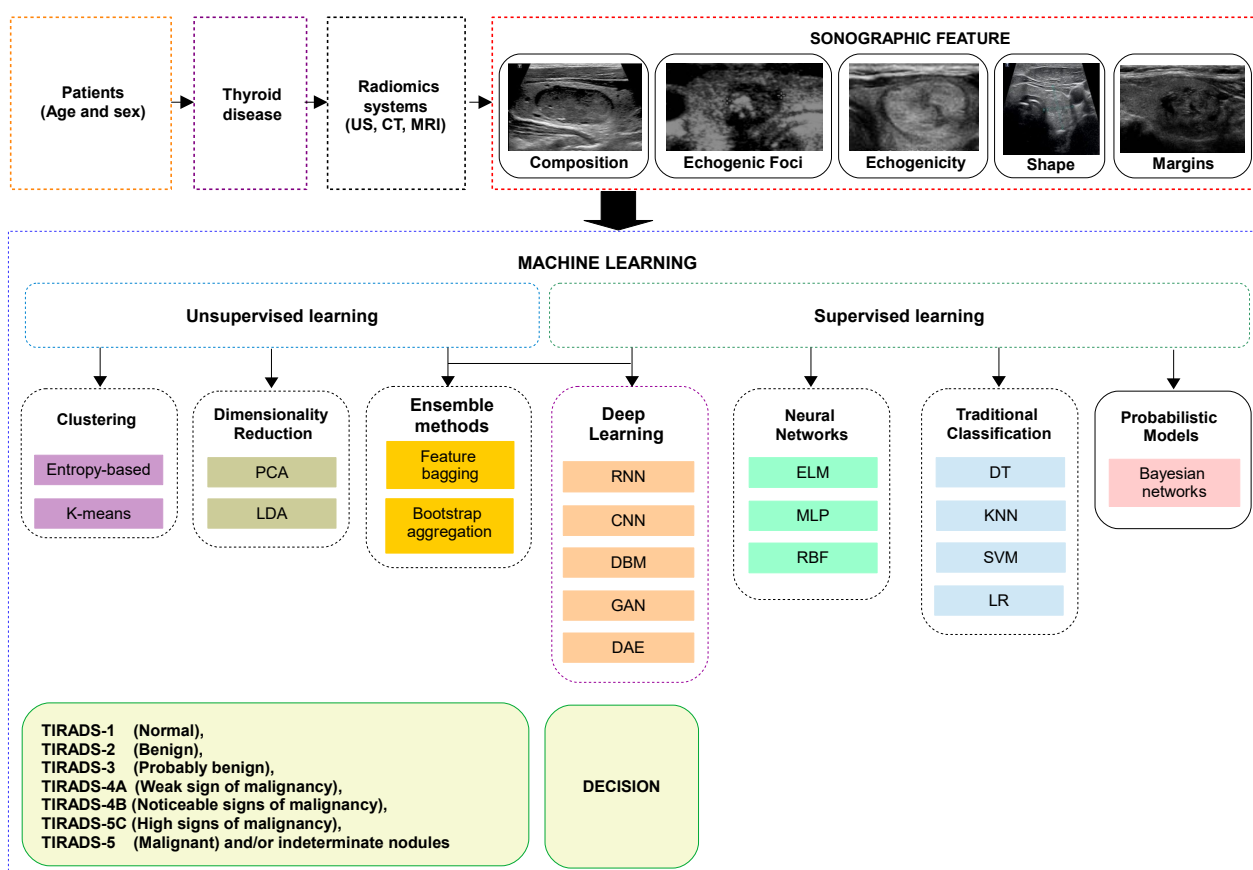

Figure 2. Taxonomy of the thyroid cancer detection schemes based in AI.

2.1. Objective of AI-Based Analysis (O)

This article focuses on the application of AI in thyroid cancer detection. In order to better understand the purpose behind each framework, it is crucial to identify the objective of each approach.

O1. Classification: Thyroid carcinoma classification refers to the categorization of thyroid cancers based on their histopathological features, clinical behavior, and prognosis. There are several types of thyroid carcinomas, each of which has distinct characteristics. The primary categories include: (i) PTC: The most common type, accounting for about 80% of all thyroid cancers. PTC tends to grow very slowly, but it often spreads to lymph nodes in the neck. Despite this, it is usually curable with treatment; (ii) FTC: the second most common type, FTC can invade blood vessels and spread to distant parts of the body, but it is less likely to spread to lymph nodes; (iii) MTC: This type of thyroid cancer starts in the thyroid's parafollicular cells, also called C cells, which produce the hormone calcitonin. Elevated levels of calcitonin in the blood can indicate MTC; (iv) ATC: A very aggressive and rare form of thyroid cancer, ATC often spreads quickly to other parts of the neck and body. It is difficult to treat.

The classification of thyroid carcinomas is crucial in determining the most effective course of treatment for each patient. Various factors such as tumor size, location, and the patient's age and overall health are also taken into consideration when forming a treatment plan. Advances in AI and machine learning are helping to automate and improve the accuracy of thyroid carcinoma classification, with many models trained to classify tumors based on medical images or genetic data. Liu et al. [60] report on incorporating a support vector machine (SVM) for cancer detection. Similarly, Zhang et al. [61,62] propose deep neural network (DNN)-based strategies for segregating and categorizing benign and malignant thyroid nodules in ultrasound imagery. Furthermore, the bidirectional LSTM (Bi-LSTM) model, as presented by Chen et al. [63], demonstrates a notable accuracy in classifying thyroid nodules. These classification systems constitute structured hierarchies instrumental in organizing knowledge and workflows in the specific domain of thyroid cancer.

O2. Segmentation: The segmentation of thyroid carcinoma refers to the process of identifying and delineating the region of an image that corresponds to a thyroid tumor. The goal of segmentation is to separate the areas of interest, in this case, the thyroid tumor, from the surrounding tissues in medical images. This can be done manually by an expert radiologist, or it can be automated using machine learning algorithms [64,65]. Segmentation is a crucial step in medical image analysis because it helps to accurately determine the location, size, and shape of the tumor, which are vital parameters for diagnosis, treatment planning, and prognosis prediction. A variety of methods can be used to perform image segmentation, including thresholding, edge detection, region-growing methods, and more complex machine learning and DL techniques.

In the case of thyroid carcinoma, the segmentation can be challenging due to the high variability in the appearance and shape of the tumors, their proximity to other structures in the neck, and the presence of noise or artifacts in the images. Therefore, robust and reliable segmentation algorithms are needed to ensure accurate and consistent results. AI methods, including convolutional neural networks (CNNs) and the U-Net architecture, are being increasingly used for thyroid carcinoma segmentation because of their ability to learn and generalize from large quantities of data, thus improving the accuracy and reliability of the segmentation process.

O3. Prediction: The prediction of thyroid carcinoma involves the use of various diagnostic tools, tests, and techniques—often employing machine learning models—to anticipate the probability of a patient developing thyroid cancer. This predictive analysis can be based on several factors, including but not limited to (i) genetic predisposition: individuals with a family history of thyroid cancer are at a higher risk; (ii) gender and age: thyroid cancer is more common in women and people aged between 25 and 65; (iii) radiation exposure: exposure to high levels of radiation, especially during childhood, increases the risk of developing thyroid cancer; (iv) diet and lifestyle: a lack of iodine in the diet and certain lifestyle factors may contribute to an increased risk. In a medical context, prediction does not necessarily mean a certain future outcome, but rather it points to an increased risk or likelihood based on current data and predictive models. For thyroid carcinoma, predictive tools and tests are typically used in conjunction with each other to achieve more accurate

results. For instance, machine learning algorithms can be trained on historical medical data to predict the likelihood of a nodule being benign or malignant, aiding in early detection and more effective treatment planning. Various studies have been proposed to predict thyroid cancer. For instance, in [66], the authors employed the use of an artificial neural network (ANN) and a logistic regression (LR) to make predictions. Another study [67] detailed the creation of a predictive machine using a CNN to analyze 10,068 microscopic thyroid cancer images from South Asian populations. The thyroid cancer images were a part of pharmacogenomic datasets, encompassing genomics and a variation analysis of individual differences associated with the predisposition to the disease.

2.2. Preprocessing

Dimensionality reduction (DR) is a technique used in the field of ML, particularly in the preprocessing and feature engineering phases, that transforms data from a high-dimensional space into a lower-dimensional space. This technique is popular for classification due to its cost-effectiveness and ability to eliminate unnecessary data patterns and minimize redundancy. For instance, DR was used to diagnose thyroid disease (TD) using cytological images [68].

Principal component analysis (PCA) is a multivariate statistical preprocessing method that transforms variables into a reduced set of uncorrelated variables. This approach reduces the number of variables and minimizes redundant information while preserving the relationships among the data as much as possible. PCA has been widely used in cancer detection and classification of benign and malignant thyroid cells. For example, in [69], PCA was utilized to select the optimal set of wavelet coefficients from the application of the double-tree complex wavelet transform (DTCW) on noisy thyroid images, which were then classified using a random forest (RF). In [70], PCA was applied to data from 399 patients with three types of thyroid carcinoma (papillary, follicular, and undifferentiated) in Morocco, enabling a classification based on factors such as sex, age, type of carcinoma, and region.

2.3. Supervised Learning (SL)

SL is a method of machine learning where an algorithm is trained to classify or predict the condition based on labeled data, which, in this case, are medical data related to thyroid cancer. The aim of supervised learning is to differentiate between the different forms of thyroid cancer through the use of annotated data and examples. For example, these data can include ultrasound images, radiomic features, genetic markers, patient demographics, or any other information that may be relevant to the diagnosis or prognosis of thyroid cancer. The labeled data may indicate whether each instance corresponds to a case of thyroid cancer or not, or it may provide more detailed labels such as the stage of the cancer or the type of thyroid carcinoma.

In a classification setting, the supervised learning algorithm could be trained to distinguish between benign and malignant thyroid nodules based on certain characteristics extracted from medical imaging data. The labels in the training data would specify whether each nodule is benign or malignant. After training, the algorithm can then be used to classify new, unlabeled nodules. Similarly, a regression-based supervised learning algorithm might be trained to predict the progression or the prognosis of thyroid cancer based on various patient-specific features. The labels here would correspond to a continuous outcome variable, such as the survival time of the patient or a measure of disease progression. It is important to note that the performance of these methods heavily relies on the quality and quantity of the available data. The more accurate and comprehensive the data, the better the algorithm will perform in predicting or classifying new instances. Additionally, supervised learning models in healthcare, including thyroid carcinoma detection, need to be validated on separate test datasets and in real-world clinical settings to ensure their robustness and reliability [71,72].

Traditional Classification (TCL)

TCL employs a range of methods to address data-related challenges, and it is important to note that there is no universally applicable algorithm that suits every situation. The choice of the right algorithm depends on several factors, including the particular problem at hand, the number of variables involved, the most suitable model for the task, and other pertinent factors. Below is a brief summary of some of the most commonly used machine learning algorithms.

T1. K-nearest neighbors (KNN): The KNN algorithm is a type of nonparametric supervised machine learning method used for regression and classification. The method relies on the utilization of K training samples for predictions. In a study conducted by Chandel et al. in [73], the KNN method was applied to classify thyroid disease based on TSH, T4, and goiter parameters. Liu et al. [74] also employed the fuzzy KNN approach to differentiate between hyperthyroidism, hypothyroidism, and normal cases. There is a growing interest in larger datasets for future research, as noted in [75].

T2. Support vector machine (SVM): An SVM is a machine learning method used for classification and regression tasks. In a study published in [76], an SVM approach was proposed for differentiating benign from malignant thyroid nodules by utilizing 98 thyroid nodule (TN) samples (82 benign and 16 malignant). Another study in [77] employed six SVMs to classify nodular thyroid lesions by selecting the most important textural characteristics. The authors reported that the proposed method achieved the correct classification. In [78], a generalized discriminant analysis and wavelet carrier vector machine system (GDA-WSVM) was introduced for diagnosing TN, consisting of feature extraction, classification, and testing phases.

T3. Decision trees (DT): DT learning is a method for data mining that uses a predictive model for decision-making, where the output values are represented by the leaves and the input variables are represented by branches. This approach has been applied to uncover underlying thyroid diseases as demonstrated in various studies such as [79–82].

T4. Logistic regression (LR): In [83], the LR model was used to determine the specific characteristics of thyroid microcarcinoma in 63 patients, based on the combination of contrast-enhanced ultrasound (CEUS) and conventional US values. Another study, conducted in northern Iran and reported in [84], applied LR to analyze 33,530 cases of thyroid cancer. LR is a widely used binomial regression model in machine learning.

2.4. Unsupervised Learning (USL)

In AI and computer science, USL involves analyzing data without pre-existing labels or annotations. It aims to uncover the underlying structures in the unlabeled data. Unlike supervised learning, which uses labeled data to calculate a success score, USL lacks this labeling, making it difficult to assess the accuracy of the results. While USL algorithms can perform more complex tasks compared to supervised ones, they can also be more unpredictable, adding unintended categories and introducing noise instead of structure. Despite these challenges, USL remains a valuable tool for exploring AI, as it enables the discovery of patterns and relationships in data that might not be immediately apparent [85,86].

Clustering (C)

The purpose of this method is to segment a set of thyroid cancer data into various homogeneous groups that possess similar characteristics, making it easier to classify the unlabeled datasets into benign and malignant. This detection approach has gained significant attention in various medical studies for its simplicity, including in the detection of DNA copy number changes [87], breast cancer recognition [88], cancer gene detection [89], skin cancer diagnosis [90], and brain tumor detection [91]. Additionally, clustering can also help identify cancer without precise definitions [92]. The clustering technique was used in [93] to identify factors that impact the normal functioning of TG, and DBSCAN and PCA were

applied to manage the clusters and reduce dimensionality. An automated clustering system for thyroid diagnosis was developed in [94] to prescribe the appropriate drug datasets for hyperthyroid, hypothyroid, and normal cases. The efficiency of fuzzy clustering for thyroid and liver datasets from the UCI repository was analyzed in [95], where the FPCM and PFCM algorithms were applied and compared.

C1. K-means (KM): The K-means (KM) method is a technique for data partitioning and a combinatorial optimization challenge. It is commonly utilized in USL, in which observations are separated into K groups. In [96], the authors explore the utilization of an ANN and improvised K-means method for normalizing raw data. The study used thyroid data from the UCI dataset containing 215 instances.

C2. Entropy-based (EB): In [97], a parameter-free calculation framework named DeMine was developed to predict microRNA regulatory modules (MRMs). DeMine is a three-step method based on information entropy. Firstly, the miRNA regulation network is transformed into a synergistic miRNA–miRNA network. Then, miRNA clusters are detected by maximizing the entropy density of the target cluster. Finally, the coregulated miRNAs are integrated into the corresponding clusters to form the final MRMs. The proposed method not only provides improved accuracy but also identifies more miRNAs as potential tumor markers for tumor diagnosis.

2.5. Deep Learning (DL)

DL is a subset of ML and AI that is based on ANNs with representation learning. ANNs are defined as a class of information processing systems comprised of interconnected nonlinear elements known as neurons. These networks have proven to be effective in addressing complex issues since they can store and retrieve information. An ANN with many hidden layers is commonly referred to as a DNN. The depth of the network allows it to capture increasingly abstract and high-level features as you progress through the layers. It can automatically learn, generate, and improve representations of data by employing large neural networks with many layers, hence the term "deep" learning. In thyroid cancer, DL has been deployed to perform different tasks, including: (i) Image classification—DL algorithms such as CNNs can be trained to classify thyroid ultrasound images. For instance, they can differentiate between benign and malignant nodules based on their shape, texture, and other characteristics [98–100]. This approach can significantly reduce the time and effort required for manual interpretation, thus aiding in the early detection and treatment of thyroid cancer. (ii) Pathological analysis—DL can also be utilized to analyze histopathological or cytopathological slide images, helping in the detection and classification of cancerous cells. (iii) Genomic data analysis—with the advent of genomic medicine, DL models can be employed to analyze genetic variations that may predispose individuals to thyroid cancer. (iv) Radiomics—DL models can be used to extract high-dimensional data from radiographic images, allowing for more precise and personalized treatment planning. (v) Predictive analysis—using electronic health records and other patient data, DL models can be used to predict the likelihood of a patient developing thyroid carcinoma, allowing for preventive measures to be taken if necessary. Figure 3 illustrates the different classifications of thyroid cancer using DL.

2.5.1. Extreme Learning Machine (ELM)

The ELM model features a layer of hidden nodes with a randomized weight distribution. The weights between the hidden node inputs and outputs are learned in a single step, resulting in a more efficient learning process compared to other models. The ELM has been proven to be an effective method in the diagnosis of TD, as evidenced in several studies such as [101–104].
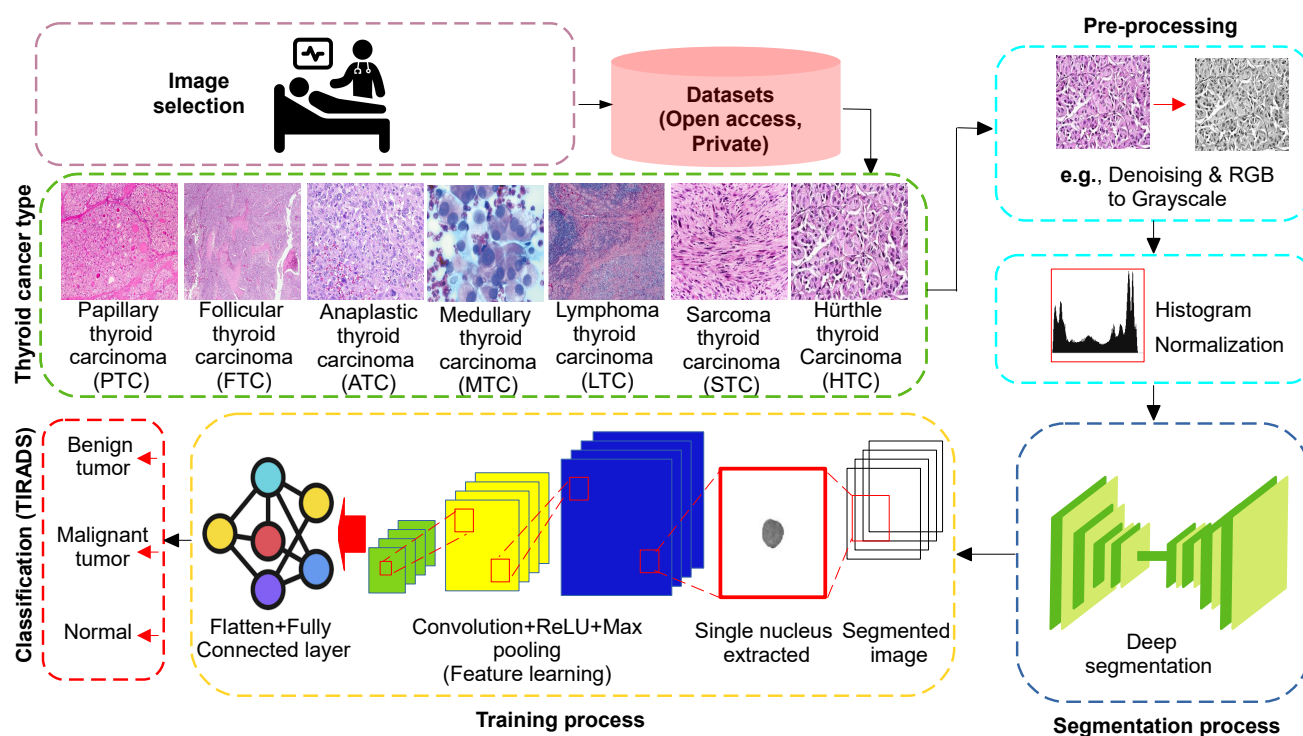
Figure 3. General DL system for thyroid cancer detection and classification.

2.5.2. Multilayer Perceptron (MLP)

MLP represents a category of feedforward networks where data are processed from the input layer through to the output layer. Each layer in this network comprises a varying number of neurons. Rao et al. [105] introduced an innovative approach for thyroid nodule classification, utilizing an MLP with a backpropagation learning algorithm. In their model, the MLP included four neurons in the input layer, three neurons in each of the ten hidden layers, and a single neuron in the output layer. Hosseinzadeh et al. [106] conducted a separate study with the objective of improving the accuracy of TD diagnosis through MLP networks. The research compared their findings with the existing literature on thyroid cancer classification and found MLP networks to be superior. Isa et al. [107] delved into the exploration of activation functions within MLP networks. Their goal was to identify the optimal activation function for the accurate classification of incurable diseases such as TD and breast cancer. The study evaluated multiple activation functions, including logarithmic, sigmoid, neural, sinusoidal, hyperbolic tangent, and exponential functions. The research found the hyperbolic tangent function to be the most effective for TD classification, using the backpropagation algorithm as the training algorithm. This result was further corroborated by Mourad et al. [108].

2.5.3. Radial Basis Function (RBF)

In [109], ML is applied to the classification of TN, where the MLP and RBF activation functions are utilized. The RBF activation function is found to outperform the MLP in terms of the structural classification of thyroid nodules. This approach highlights the effectiveness of activation functions in approximating functions, classifying, and predicting time series data, especially in the diagnosis of thyroid cancer.

2.5.4. Denoising Autoencoder (DAE)

DAEs can be beneficial for thyroid carcinoma classification by effectively learning representations from ultrasound or histopathological images. A DAE is a specific type of artificial neural network trained to reconstruct input data, often used for the purposes of dimensionality reduction or feature learning. The process for utilizing DAEs for thyroid carcinoma

classification generally follows these steps (i) preprocessing, (ii) noisy input creation, (iii) DAE training, (iv) feature extraction, and (v) classification. In [110], the authors implemented six autoencoder algorithms in the training process for PTC classification, including fixing weights and fine-tuning the network. The encoding layers and the complete autoencoder were used to embed the network. Another study [111] employed DAEs and stacked DAEs to extract features and identify informative genes in thyroid cancer.

2.5.5. Convolutional Neural Network (CNN)

CNNs are a class of DL models that have shown extraordinary performance in various image processing and analysis tasks, including the classification of medical images. CNNs are especially adept at processing gridlike data, such as an image, where spatial relationships between the pixels are crucial to understanding the image content. The past few years have seen considerable effort invested in developing CNN-based methodologies for detecting thyroid cancer, especially for the automated identification and classification of nodules in ultrasound imagery [112]. The ConvNet model, a widely adopted framework within the neural network realm, emphasizes the use of convolution operations over matrix multiplications [113]. Various CNN architectures such as LeNet [114], AlexNet [115], VGG [100], ResNet [116], GoogLeNet [117], Squeeze Net [118], and DenseNet [119] are distinguished by their incorporation of key components including convolutional, pooling, and fully connected layers.

In a study conducted by [120], the potential of CNN models to prognosticate thyroid cancer was explored using 131,731 ultrasound images taken from 17,627 thyroid cancer patients. Another research effort [121] employed VGG16, Inception, and Inception-Resnet models to differentiate malignant tissues within a set of 451 thyroid images from the DDTI dataset. To mitigate the challenge of data scarcity, the images were augmented before classification. A comparison of DCNN diagnostic performance with expert radiologists in distinguishing thyroid nodules within ultrasound images was carried out by [122], involving a test set of 15,375 TN ultrasound images. They utilized CNNE1 and CNNE2 models, derived from deep convolutional neural network (DCNN), for differentiating between malignant and benign TN. The study [123] proposed a CNN-based DL technique for detecting and classifying TN and breast nodules, with the results contrasted against those from ultrasound imaging. Table 2 presents a summary of recent CNN-based thyroid cancer classification contributions.

Table 2. Summary of CNN research conducted in the diagnosis of thyroid cancer. Accuracy, sensitivity, and specificity are provided in percentages (%) for better comparison.

Ref.	Year	Country	NP	NM	NF	NN	NBN	NMN	TP	TN	FP	FN	ACC	Sens.	Spec.
[124]	2021	China	102	00	102	104	57	47	38	07	07	50	44.12	43.18	50.00
[125]	2021	China	102	25	77	103	73	33	27	12	06	61	36.79	30.68	66.67
[126]	2021	Koria	325	61	264	325	257	68	48	52	20	205	30.77	18.97	72.22
[127]	2021	China	2775	726	2049	2775	2472	303	271	363	32	2109	22.85	11.39	91.90
[127]	2021	China	163	48	115	175	67	108	86	09	22	58	54.29	59.72	29.03
[128]	2020	China	2489	614	1875	2489	1021	1468	1280	258	188	763	61.79	62.65	57.85
[129]	2020	USA	571	234	337	651	500	151	133	214	18	287	53.22	31.67	92.24
[130]	2020	China	166	46	100	209	109	100	87	16	13	93	49.28	48.33	55.17
[122]	2020	Korea	200	49	151	200	102	98	90	41	08	61	65.50	59.60	83.67
[131]	2020	Korea	340	79	261	348	252	96	31	25	65	227	16.09	12.02	27.78
[132]	2019	Korea	106	29	77	2018	132	86	69	23	17	109	42.20	38.76	57.50
[133]	2019	China	171	32	139	180	85	95	86	50	09	35	75.56	71.07	84.75

Abbreviations: number of patients (NP); number of males (NM); number of females (NF); number of nodules (NN); number of benign nodules (NBN); number of malignant nodules (NMN); true negative (TN); true positive (TP); false negative (FN); false positive (FP).

2.5.6. Recurrent Neural Network (RNN)

RNNs are a class of artificial neural networks where connections between nodes form a directed graph along a sequence, thus enabling them to use their internal state (memory) to process variable-length sequences of inputs. This unique feature makes RNN particularly suitable for tasks where temporal dependencies are essential, such as time-series analysis, language translation, and speech recognition. In the context of thyroid carcinoma classification, RNNs can be utilized to analyze sequential or time-dependent data, such as the development of a patient's clinical signs over time, the evolution of a tumor seen in a series of medical images, or changes in the gene expression related to the progression of thyroid cancer. For instance, in the study by Chen et al. (2017) [134], the authors propose a hierarchical RNN approach for classifying thyroid nodules based on historical ultrasound reports. This hierarchical RNN is composed of three layers, with each layer incorporating an individually trained long short-term memory (LSTM) network. The study's findings indicate that the hierarchical RNN model surpasses basic models in terms of computational efficiency, control accuracy, and robustness, making it an effective tool for diagnosing TN. These advantageous attributes stem from the inherent memory mechanisms of RNNs, which allow them to remember previous states through feedback loops. This memory capability renders RNNs a popular choice for applications in cancer detection.

2.5.7. Restricted Boltzmann Machine (RBM)

An RBM is a type of artificial neural network and a generative stochastic model. It was first introduced by Paul Smolensky [135] in 1986 under the name "Harmonium," but the concept of a "restricted" Boltzmann machine was developed by Geoffrey Hinton and his students in the mid-2000s. RBMs have a layer of visible units and a layer of hidden units, but no connections within layers—this is the restriction in their name. Each node in the layer is connected to every node in the other layer. The lack of intralayer connections simplifies the learning process. The work by Vairale et al. [136] presents an application of RBMs to develop a personalized fitness recommendation system tailored for individuals diagnosed with thyroid conditions. RBMs are a particular class of generative artificial neural networks characterized by a bidirectional architecture, which operates in an unsupervised manner. This structure comprises a visible layer containing binary variables and a hidden layer, also populated with interconnected binary variables. The learning process within RBMs is primarily conducted through a statistical analysis.

2.5.8. Generative Adversarial Network (GAN)

This type of ML network is composed of two distinct models: a generator and a discriminator. The generator maps a random input vector to an output in the data space, while the discriminator serves as a binary classifier that evaluates both input data from the training set and output data from the generator. GANs have gained widespread use in the diagnosis of diseases, including thyroid nodules [137,138].

2.5.9. Probabilistic Models (PM)

PMs, including Bayesian networks (BNs), are foundational concepts in computer science and statistics. These models represent uncertainty and dependencies among variables. In computer science, PMs are used for tasks such as ML, where they aid decision-making by quantifying uncertainty and modeling complex relationships. A BN, a specific type of PM, uses directed acyclic graphs to represent dependencies between variables. They are valuable for reasoning under uncertainty, making predictions, and handling incomplete information. In statistics, these models facilitate data analysis by incorporating probabilistic reasoning to draw meaningful inferences and estimate parameters, enhancing our understanding of complex systems. BNs have proven effective in the identification of various diseases. For instance, they have been employed to differentiate between benign and malignant thyroid nodules [139,140], as well as in the diagnosis of thyroid cancer, hepatitis, and breast cancer [141].

2.6. Ensemble Methods (EMs)

To address the complexity of cancer data and achieve higher accuracy in detection, the use of ensemble methods is commonly employed in the field. An ensemble method involves dividing the data into subgroups and applying multiple machine learning techniques to each subgroup simultaneously, then synthesizing the results to make a final diagnosis. By combining multiple models, the ensemble method aims to produce an optimal predictive model for thyroid cancer detection. This approach has been shown to be effective in various studies, such as [142], where the authors emphasize the importance of ensemble methods in achieving a more comprehensive understanding of the data and improving the accuracy of the diagnosis.

2.6.1. Bagging (B)

In the realm of thyroid cancer screening, bagging is an ensemble learning technique utilized to improve the accuracy and stability of ML algorithms. This algorithm operates by reducing variance and avoiding overfitting and can be applied to a variety of methods, particularly decision trees. The purpose of bagging is to enhance the performance of weak classifiers in the field of thyroid cancer screening applications.

B1. Bootstrap aggregation (BA): The bootstrap aggregating technique is a widely utilized ensemble method aimed at improving the accuracy of machine learning algorithms, particularly for the purposes of classification, regression, and variance reduction. In [143], this approach was employed for diagnosing thyroid abnormalities.

B2. Feature bagging (FB): In [144], FB is introduced as a method of ensemble learning with the goal of minimizing the correlation between the individual models in the ensemble. FB achieves this by training the models on a randomly selected subset of features, instead of all features in the dataset. The method was applied to distinguish between benign and malignant thyroid cancer cases [145].

2.6.2. Boosting (O)

Meta-algorithms are often used in USL to mitigate the variance and enhance the performance of weak classifiers by transforming them into strong classifiers.

O1. AdaBoost In the study by Pan et al. [146], a new method called AdaBoost was utilized to diagnose thyroid nodules using the standard UCI dataset. The RF and PCA techniques were employed for classification purposes and to maintain data variability, respectively.

O2. Gradient tree boosting (XGBoost): In [147], the XGBoost algorithm was introduced as a fast and efficient implementation of gradient-boosted decision trees. Since its introduction, the XGBoost algorithm has been applied to a range of research topics, including civil engineering [148], time-series classification [149], sport and health monitoring [150], and ischemic stroke readmission [151].

For thyroid cancer detection, the authors in [152] used XGBoost to diagnose benign and malignant thyroid nodules, as a solution to the challenge of obtaining accurate diagnoses with DL models when a large-scale dataset is unavailable.

Table 3 provides a summary of research frameworks for the detection of benign and malignant thyroid cancers, including the category, classifier, detected disease, dataset, objective, and used quantifiable metrics. This table helps to categorize AI methods used for thyroid cancer detection and highlights the current key applications.

Table 3. Summary of research frameworks conducted in the detection of benign and malignant thyroid cancer.

Ref.	Category	Classifier	DD	Dataset	O	SV	APP
[110]	DL	DAE	PTC	TCGA	O1	18,985 features	US
[111]	DL	DAE	PTC	TCGA	O1	510 samples	Omics
[67]	DL	CNN	TC	PD	O1	10,068 images	Omics
[153]	DL	CNN	TC	PD	O1	482 images	Omics
[154]	DL	CNN	PTC, FTC	NA	NA	NA	FNAB
[155]	DL	CNN	PTC	PD	O1	370 microphotographs	FNAB
[156]	DL	CNN	PTC	PD	O3	469 patients	FNAB
[157]	DL	CNN	TC	DDTI	O1	298 patients	US
[158]	DL	CNN	TC	PD	O1	1037 images	US
[159]	DL	CNN	TN	PD	O2	80 patients	US
[160]	DL	CNN	TN	PD	O2	300 images	US
[161]	DL	CNN	TC	PD	O1	459 labeled	US
[162]	DL	CNN	TD	ImageNet	O1	2888 samples	US
[120]	DL	CNN	TC	PD	O1	17,627 patients	US
[121]	DL	CNN	TC	PD	O1	1110 images	US
[123]	DL	CNN	TN	PD	O1, S1	537 images	US
[134]	DL	RNN	TN	PD	O1	13,592 patients	US
[136]	DL	DBM	TD	PD	O1	94 users	Fitness
[138]	DL	GAN	TC	PD	O3	109 images	Surgery
[163]	DL	NA	TC	NA	NA	NA	US
[164]	DL	NA	TC	PD	O1	1358 images	US
[165]	AI	NA	TC	PD	O1	50 patients	Surgery
[166]	AI	NA	TC	PD	O1	89 patients	US
[101]	ANN	ELM	TD	UCI	O1	215 patients	US
[102]	ANN	ELM	TD	UCI	O1	215 patients	US
[103]	ANN	ELM	TD	PD	O1	187 patients	US
[105]	ANN	MLP	TD	PD	O1	7200 samples	US
[106]	ANN	MLP	TD	UCI	O1	7200 patients	US
[109]	ANN	RBF	TD	PD	O1	487 patients	US
[167]	ANN	RBF	TD	PD	O1	447 patients	Cytopathological
[168]	ANN	NA	FTC	PD	O1	57 smears	FNAB
[169]	ANN	NA	FTC	NA	NA	NA	FNAB
[170]	ANN	NA	TC	TCGA	O3	482 samples	Histopathological
[171]	ANN	NA	TC	PD	O1	1264 patients	FNAB
[172]	ANN	NA	TN	PD	O1	276 patients	US
[73]	TCL	KNN	TD	PD	O1	7200 instances	US
[173]	TCL	KNN	FTC	PD	O1, O2	94 patients	Histopathological
[174]	TCL	SVM	FTC	PD	O1	43 nuclei	Histopathological
[175]	TCL	SVM	TN	PD	O1	467 TN	US
[76]	TCL	SVM	TC	PD	O1	92 subjects	US
[176]	TCL	SVM	PTC	TCGA	O1	500 patients	Omics
[177]	DL	DL	PTC	TCGA	O3	115 slides	Omics
[178]	ML	ML	TN	PD	O1	121 patients	Omics
[79]	TCL	DT	TC	UCI	O1	3739 patients	US
[81]	TCL	DT	TC	NA	O1	NA	US
[82]	TCL	DT	TC	UCI	O1	499 patients	US
[83]	TCL	LR	TC	PD	O1	63 patients	US
[84]	TCL	LR	TN	PD	O1	33,530 patients	US
[139]	PM	BN	TD	UCI	O1	93 adult patients	US
[140]	PM	BN	TC	NA	O1	37 patients	US
[96]	C	KM	TC	UCI	O1	215 instances	US
[97]	C	EB	TC	Private data	O1	734 cases	US
[70]	DR	PCA	TC	PD	O1	NA	NA
[144]	B	FB	TN	PD	O1	1480 patients	US

Abbreviation: application (APP), detected disease (DD), objective (O), thyroid cancer (TC), subjects for validation (SV), private data (PD).

3. Thyroid Cancer Datasets

In the field of thyroid carcinoma research, a number of datasets have been developed to facilitate the validation of ML algorithms and models. This is especially important because the creation of such datasets is a major challenge in the area of endocrine ML. In this section, we present an overview of the most significant thyroid databases, which offer a set of standards for evaluating the performance of learning methods and assist in the diagnosis and monitoring of complicated diseases.

- **ThyroidOmics:** This is a dataset developed by the Thyroid Working Group of the CHARGE Consortium that aims to examine the underlying factors and consequences of TD using various omics techniques such as genomics, epigenomics, transcriptomics, proteomics, and metabolomics. The dataset consists of the results of the discovery stage of the genomewide association analysis (GWAS) meta-analysis for thyrotropin (TSH), free thyroxine (FT4), increased TSH (hypothyroidism), and decreased TSH (hyperthyroidism) as reported in [179,180].
- **Thyroid Disease Data Set (TDDS):** The dataset utilized for classifying using ANN is referred to as the Thyroid database and features 3772 training instances and 3428 testing instances, with a combination of 15 categorical and 6 real attributes. The three defined classes in this dataset include normal (not hypothyroid), hyperfunctioning, and subnormal functioning [181].
- **KEEL Thyroid Dataset:** The KEEL dataset provides a set of benchmarks to evaluate the effectiveness of various learning methods. This dataset includes several types of classification, such as standard, multi-instance, imbalanced data, semi-supervised classification, regression, time series, and USL, which can be used as reference points for a performance analysis [182].
- **TNM8 Dataset:** A dataset was created for the purpose of reporting pathologies of thyroid resection specimens associated with carcinoma. The data do not include core needle biopsy specimens or metastasis to the thyroid gland. The dataset also does not encompass noninvasive follicular thyroid neoplasm with papillary-like nuclear features (NIFTP), tumors of uncertain malignancy, thyroid carcinomas originating from struma ovarii, carcinomas originating in thyroglossal duct cysts, sarcomas, or lymphomas.
- **Gene Expression Omnibus (GEO):** The GEO database is a genomics repository that follows the guidelines of the minimum information about a microarray experiment. This database is designed to store gene expression datasets, arrays, and sequences and provides researchers with access to a vast collection of experiment results, gene profiles, and platform records in GEO [183].
- **Surveillance, Epidemiology, and End Results (SEER):** The creators of this dataset aim to supply a collection of clinical characteristics from thyroid carcinoma patients, which includes 34 details such as age, gender, lymph nodes, and others.
- **Digital Database Thyroid Image (DDTI):** The DDTI dataset serves as a valuable resource for researchers and new radiologists looking to develop algorithm-based CAD systems for thyroid nodule analysis. The dataset comprises 99 cases and 134 images, with each patient's data stored in an XML file format [184]. Figure 4 provides an illustration of six samples from each of the thyroid carcinoma tissue types in the DDTI dataset.
- **Cancer Genome Atlas (TCGA):** The TCGA is a comprehensive collection of data gathered from 11,000 patients diagnosed with various types of cancer over a period of 12 years. The data consist of detailed genomic, epigenomic, transcriptomic, and proteomic information, amounting to a total of 2.5 petabytes. This extensive dataset has been instrumental in advancing the research, diagnosis, and treatment of cancer.
- **National Cancer Data Repository (NCDR):** The NCDR serves as a resource for healthcare and research with the goal of capturing all recorded cases of cancer in England. These data are sourced from the office for national statistics [185].
- **Prostate, Lung, Colorectal, and Ovarian (PLCO) dataset** The National Cancer Institute supports the PLCO cancer screening trial, aimed at examining the direct factors that contribute to cancer in both men and women. The trial has records of 155,000 participants, and all studies regarding thyroid cancer incidence and mortality can be found within it [186].

In Table 4, we present examples of public and private TCDs used in thyroid cancer detection.

Table 4. Examples of public and private TCDs used in thyroid cancer detection.

Ref	Year	TCD	IT	IF	Instance	M/F	DA
[44]	2018	BMU	Sonographic	PNG	1077	4309	Public
[172]	2019	TCCC	US	PNG	370	370	Public
[187]	2019	Clinical	US	JPEG	117	2108	Public
[188]	2019	Hospital	US	JPEG	62	12/60	Public
[189]	2020	TIRADS	US	JPEG	5278	NA	Public
[190]	2018	Peking Union	US	JPEG	4309	1179	Private
[120]	2019	Medical Center	US	PNG	1425	2064	Private
[191]	2020	PubMed	CT scans	JPEG	2108	54/253	Private
[156]	2021	ACR	DICOM	DICOM	1629	83/289	Private
[126]	2021	Clinical	US	PNG	40	407	Private

Abbreviations: image types (IT); image format (IF); dataset access (DA); male (M); female (F).
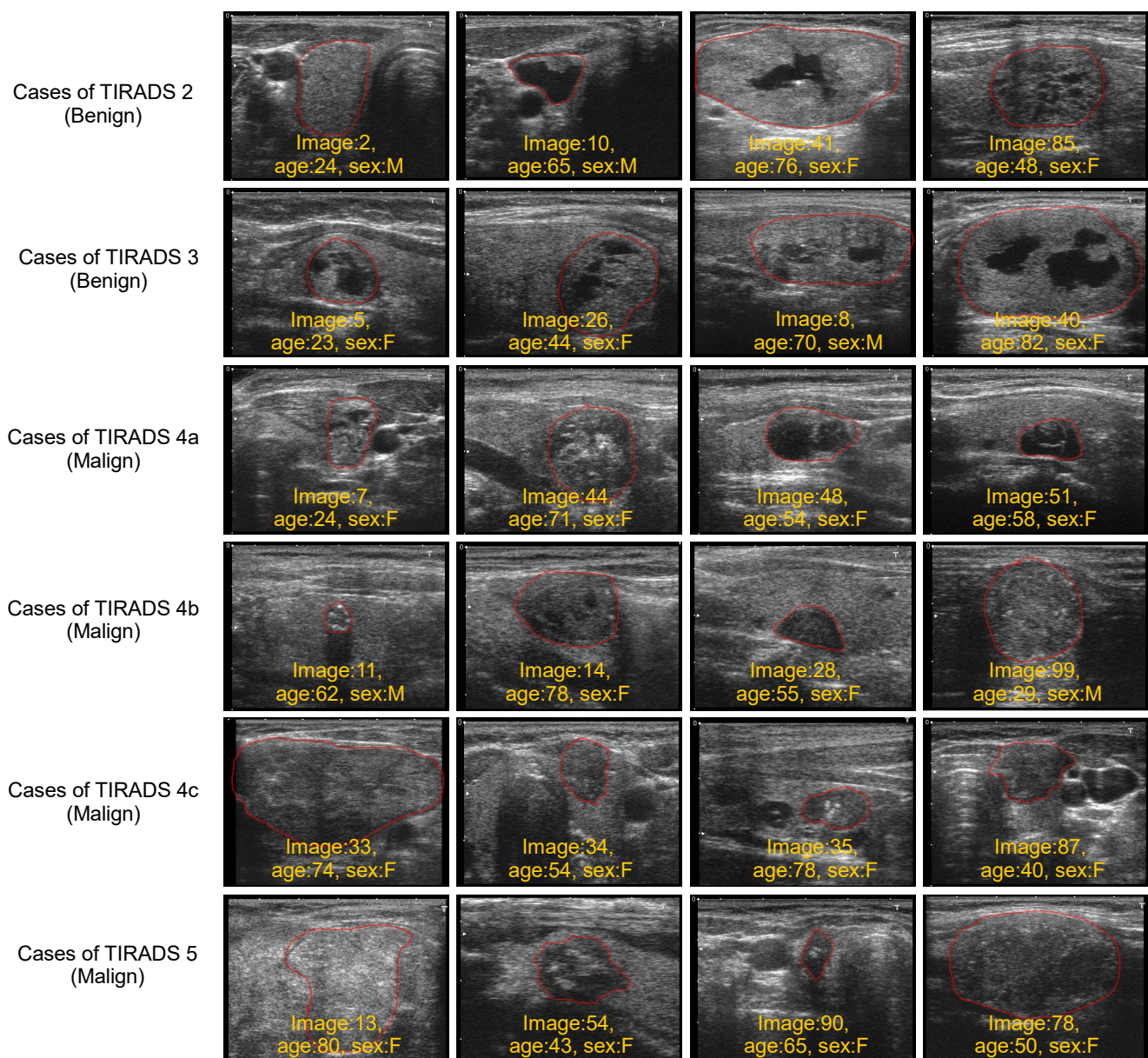
Figure 4. Example of six samples for each class from the DDTI datasets.

The strengths and weaknesses of AI-based thyroid cancer detection techniques are summarized in Table 5.

Table 5. A summary of thyroid cancer detection techniques AI-based, including their strengths and weaknesses.

Ref.	AI Meth.	Achieve. (%)	Advantages	Drawbacks
[192]	DAE	ACC = 92.9	No need for labels for thyroid cancer	Insufficient training data and need relevant data
[193]	CNN	AUC = 85.0	High thyroid cancer detection	Insufficient labels for thyroid cancer and weak in interpretability
[194]	RNN	ACC = 98.2	No need for labels for thyroid cancer	Slow computation and difficulty in training
[195]	MLP	ACC = 95.0	Adaptive learning for thyroid cancer	Limited in its results
[196]	KNN	P = 93.0	High sensitivity to thyroid cancer detection	Insufficient labels for thyroid cancer
[197]	SVM	ACC = 97.0	High sensitivity to thyroid cancer detection	Weak in interpretability and long training time
[198]	DT	AUC = 73.10	Does not require scaling and normalization of data	Unstable
[199]	LR	–	Low-cost training and easier implementation	Difficulty to label data
[200]	B	ACC = 94.88	High detection of thyroid cancer	Loss of interpretability and high computational cost

Abbreviations: area under curve (AUC).

4. Features

In this section, the focus is on showcasing the crucial techniques utilized in the classification process for characteristic extraction and selection. This primarily involves identifying a subset of relevant features that positively impact the classification accuracy and eliminating irrelevant variables.

4.1. Feature Selection Methods (FS)

FS1. Information gain (IG): Information gain (IG) is a straightforward method for classifying thyroid cancer features. This method evaluates the likelihood of having cancer by comparing the entropy before and after the examination. Typically, a higher gain value corresponds to a lower entropy. IG has been used extensively in several applications for the diagnosis of cancerous diseases, such as in filtering informative genes for precise cancer classification [201], selecting breast cancer treatment factors based on the entropy formula [202], analyzing and classifying medical data of breast cancer [203], reducing the dimensionality of genes in multiclass cancer microarray gene expression datasets [204], and filtering irrelevant and redundant genes of cancer [201]. In [205], IG is utilized as a feature selection technique to eliminate redundant and irrelevant symptoms in datasets related to diabetes, breast cancer, and heart disease. Additionally, the IG-SVM approach, combining IG and SVM, has been employed and its results served as input for the LIBSVM classifier [201].

FS2. Correlation-based feature selection (CFS): CFS is a technique frequently used for evaluating the correlation between different cancer features. In various studies, the CFS algorithm has been integrated into attribute selection methods for improved classification, such as in [206], where it was applied to thyroid, hepatitis, and breast cancer data from the UCI ML repository. In [141], the authors proposed a hybrid method that combined learning algorithm tools and feature selection techniques for disease diagnosis. The CFS was utilized in [207] for feature selection in microarray datasets to minimize the data's dimensionality and identify discriminatory genes. A hybrid model incorporating the CFS and a binary particle swarm optimization (BPSO) was proposed in [208] to classify cancer types and was applied to 11 benchmark microarray datasets. The CSVM-RFE, which involves a CFS, was used in [209] to reduce the number of cancer features and eliminate irrelevant ones. In [176], the authors utilized CFS techniques to identify key RNA expression features.

FS3. Relief (R): The relief algorithm, commonly known as RA, is an effective method used in selecting important features by assessing their differentiation quality by assigning scores. This technique calculates the weight of various features based on the correlation between cancer attributes. In a study published in [210], a feature selection method based on the relief algorithm was proposed as a means of improving efficiency.

FS4. Consistency-based subset evaluation (CSE): The study in [211] presents a hybrid classification model for breast cancer, which is based on dividing cancer data into single-

class subsets. The effectiveness of the model is evaluated using the Wisconsin Breast Cancer Dataset (WBCD).

4.2. Feature Extraction Methods (FE)

FE1. Principal components analysis (PCA): The use of PCA has been highlighted in several studies as a method to reduce the dimensionality of data and decorrelate the attributes of cancer features. For instance, in [69], PCA was applied to the dual-tree complex wavelet (DTCW) transform to select the optimum features of thyroid cancer. In [70], PCA was proposed as a tool for classifying different thyroid cancer subtypes such as papillary, follicular, and undifferentiated. The implementation of PCA and linear discriminant analysis was also explored in [212] for classifying Raman spectra of different thyroid cancer subtypes. Finally, in [213], the authors utilized PCA on cDNA microarray data to uncover the biological basis of breast cancers.

FE2. Texture description: Texture analysis is a commonly used method for extracting relevant information in the classification, segmentation, and prediction of thyroid cancer. There are numerous texture analysis techniques in the literature, including wavelet transform, binary descriptors, and statistical descriptors. The discrete wavelet transform (DWT), in particular, has received significant attention for its ability to perfectly decorrelate data. Many studies have utilized wavelets for thyroid cancer detection, such as in [214], where wavelet techniques were employed to identify cancer regions in thyroid, breast, ovarian, and prostate tumors. In [215], texture information was used to diagnose TN malignancy through a two-level 2D wavelet transform. Other works exploring this area can be found in [216,217].

FE3. Active contour (AC): The active contour (AC), first introduced by Kass and Witkin in 1987, is a dynamic structure primarily used in image processing. There are several approaches for solving the problem of contour segmentation using a deformable curve model, which has seen numerous applications in the field of detection of thyroid cancer, as demonstrated in [218–220].

FE4. Local binary patterns (LBP): The LBP are features employed in computer vision to recognize textures or objects in digital images. LBP have been utilized to detect thyroid cancer in [216]. The combination of LBP and DL has also been proposed to classify benign and malignant thyroid nodules in [221,222].

FE5. Gray-level co-occurrence matrix (GLCM): The GLCM is a matrix that represents the distribution of values of pixels that occur together at a specified offset in an image. In [223], GLCM was used to extract features to differentiate between different types of thyroid cancer. In [224], the differences between an individual with Hashimoto's thyroiditis-associated PTC and one with Hashimoto's thyroiditis alone were investigated based on GLCM comparison.

FE6. Independent component analysis (ICA): In an ICA, information is gathered into a set of contributing features for the purpose of feature extraction. ICA is utilized to separate multivariate signals into their individual components. In [225], ICA is used to extract 29 attributes as independent and useful features for classifying data into either hypothyroid or hyperthyroid using an SVM.

A summary of feature selection and extraction methods based on DL conducted in the diagnosis of thyroid cancer are illustrated in Table 6.

Table 6. Summary of feature selection and extraction methods based on DL conducted in the diagnosis of thyroid cancer.

Ref.	Year	Classifier	Features	Contributions
[226]	2017	KNN	FC/IG	- Avoids data redundancy and reduces computation time. The KNN algorithm deals with the missing data, and the ANFIS algorithm is provided with the resultant data as input.
[227]	2017	SVM	FC/CFS	- Extracts the geometric and moment features while some kernels of the SVM classifier classify the extracted features.
[108]	2020	CNN	FC/R	- Combines ML and feature selection algorithms (namely, Fisher's discriminant ratio, Kruskal–Wallis' analysis, and Relief-F) to analyze the SEER database.
[228]	2022	CNN	FE/PCA	- The influence of unbalanced serum Raman data on the prediction results was minimized by using an oversampling algorithm in this study. PCA was used to reduce the data dimension before classifying the data using RF and adaptive boosting.
[229]	2012	O	FE/TD	- Combines CAD and DWT and texture feature extraction. The AdaBoost classifier uses the extracted features to classify images into benign or malignant thyroid images.
[230]	2021	CNN	FE/AC	- Image enhancement, segmentation, and multifeature extraction, encompassing both geometric and texture features. Each characteristic is then classified using an MLP and SVM, resulting in a determination of either benign or malignant.
[189]	2020	SVM	FE/LBP	- Deep features are extracted by a CNN and are combined with handcrafted features, including a histogram of oriented gradient (HOG), and scale-invariant feature transform to create fused features. These fused features are then used for classification by an SVM.
[231]	2019	SVM	FE/GLCM	- Uses a median filter to reduce noise and delineates the contours before extracting features from thyroid regions, including GLCM texture features. SVM, RF, and bootstrap aggregating (bagging) are then used to identify the benign and malignant nodules.
[225]	2019	SVM	FE/ICA	- A multikernel-based SVM is used as a classifier to distinguish the thyroid disease.

5. Standard Assessment Criteria

In this section, we examine the most commonly utilized standard parameters for evaluating the identification of TD. These criteria serve as a measure of the effectiveness of the methods used. Selecting the right metric is crucial when evaluating the performance of machine learning models. Numerous metrics have been proposed to evaluate machine learning models in various applications. Here, we present a summary of popular metrics that are considered suitable for assessing the performance of AI algorithms applied in the detection of thyroid cancer (See Tables 7–9).

Classification and Regression Metrics

Table 7. Summary of classification and regression metrics used in evaluating AI-based thyroid cancer detection schemes.

Metric	Mathematical Formula	Description
Accuracy (ACC)	$\frac{T_P + T_N}{T_P + F_P + T_N + F_N} 100\%$	Gives the correct percent of the total number of positive and negative predictions.
Specificity	$\frac{T_N}{T_N + F_P} 100\%$	It is the ratio of correctly predicted negative samples to the total negative samples.
Sensitivity	$\frac{T_P}{T_P + F_N} 100\%$	It is a quantifiable measure metric of real positive cases that were predicted as true positive cases.
Precision (P)	$\frac{T_P}{T_P + F_P} 100\%$	Measures the proportion of true positive predictions made by the model, out of all the positive predictions made by the model.
F1 score (F1)	$2 \times \frac{Precision \times Recall}{Precision + Recall}$	It is the harmonic mean of precision and sensitivity of the classification.
Error rate (ER)	$\frac{F_N + F_P}{T_P + F_N + F_P + T_N} 100\%$	It is equivalent to one minus accuracy.
Root-mean-square error (RMSE)	$\left(\sqrt{1 - (ER)^2} \right) \times SD$	It is the standard deviation of the predicted error between the training and testing dataset, its lower value means that the classifier is an excellent one.
The negative predictive value (NPV)	$\frac{T_N}{T_N + F_N}$	It is the proportion of negative results in diagnostic tests; a higher value means the accuracy of the diagnosis.
Jaccard similarity index (JSI)	$\frac{\|A \cap B\|}{\|A \cup B\|} = \frac{T_P}{T_P + F_P + F_N}$	It has been proposed by Paul Jaccard to gauge the similarity and variety in samples.
Fallout or false positive rate (FPR)	$\frac{F_P}{F_P + T_N} = 1 - SP$	Measures the proportion of negative samples that are incorrectly classified as positive by the model.
Volumetric overlap error (VOE)	$\frac{F_P + F_N}{T_P + F_P + F_N}$	Evaluates the similarity between the segmented region and the ground-truth region. VOE measures the amount of overlap between the two regions and is defined as the ratio of the volume of the union of the segmented region and the ground-truth region to the volume of their intersection.
Mean absolute error (MAE)	$\frac{1}{N} \sum_{i=1}^{N} \|a_i - p_i\|$	It is the average of the difference between the original values and the predicted values.
Mean squared error (MSE)	$\frac{1}{N} \sum_{i=1}^{N} (y_i - r_i)^2$	It is the average of the square of the difference between the original values and the predicted values.

Statistical Metrics

Table 8. Summary of statistical metrics used in assessing AI-based thyroid cancer detection schemes.

Metric	Mathematical Formula	Description
Standard deviation (SD)	$\sqrt{\sum(x-\mu)^2/N}$	It is a measure of the amount of variation or dispersion in a set of data.
Correlation (Corr)	$(\sum((x-\mu x)\cdot(y-\mu y)))/(\sqrt{(\sum(x-\mu x)^2)}\cdot\sqrt{(\sum(y-\mu y)^2)})$	It describes the degree of association or relationship between two or more variables.
Kappa de Cohen	$k=\frac{\Pr(a)-\Pr(e)}{1-\Pr(e)}$	It measures the degree of concordance between two evaluators, relative to chance.

Computer Vision Metrics

Table 9. Summary of computer vision metrics used in assessing AI-based thyroid cancer detection schemes.

Metric	Mathematical Formula	Description
Peak signal-to-noise ratio (PSNR)	$10\cdot\log_{10}((MAX_I^2)/MSE)$	It measures the ratio of the maximum possible power of a signal to the power of the noise that affects the fidelity of its representation.
Structural similarity index (SSIM)	$MSSIM(x,y)=\frac{1}{L}\sum_{i=1}^{L}SSIM(x_i,y_i)$	It evaluates the similarity between two images or videos by comparing their luminance, contrast, and structural information.
Visual information fidelity (VIF)	$\frac{\sum_j I(C^j;F^j/s^j)}{\sum_j I(C^j;E^j/s^j)}$	It evaluates the quality of a reconstructed or compressed image or video compared to the original signal. It measures the amount of visual information preserved in the processed image or video, taking into account the spatial and frequency characteristics of the image.
Normalized cross-correlation (NCC)	$\frac{\sum_{i=1}^{M}\sum_{i=1}^{N}(I(i,j)-R(i,j))^2}{\sum_{i=1}^{M}\sum_{i=1}^{N}I(i,j)^2}$	Measures the similarity between two images (or videos) by subtracting the mean value of each signal from the signal itself. Then, the signals are normalized by dividing them by their standard deviation. Finally, the cross-correlation between the two normalized signals is calculated.
Structural content (SC)	$\frac{\sum_{i=1}^{M}\sum_{j=1}^{N}I(i,j)^2}{\sum_{i=1}^{M}\sum_{j=1}^{N}R(i,j)^2}$	A higher value of structural content shows that the image is of poor quality.
Weight PSNR	$10\log\left(\frac{(2^n-1)^2}{NVF\times MSE}\right)$	It takes into account the image texture [232].
Noise visibility function (NVF)	$\text{Normalization}\left\{\frac{1}{1+\delta_{bloc}^2}\right\}$	It estimates the texture content in the image. δ_{bloc} is the luminance variance.
Visual signal-to-noise ratio (VSNR)	$10\log_{10}\left(\frac{C^2(I)}{(VD)^2}\right)$	It is based on the specified thresholds of distortions in the image based on the computing of contrast thresholds and a wavelet transform. If the distortions are lower than the threshold, the VSNR is perfect. $C(I)$ is the RMS contrast of the original image I, and VD is the visual distortion [233].
Weighted signal-to-noise ratio (WSNR)	$10\log_{10}\left(\frac{\sum_{u=0}^{M-1}\sum_{v=0}^{N-1}|A(u,v)C(u,v)|^2}{\sum_{u=0}^{M-1}\sum_{v=0}^{N-1}|A(u,v)-B(u,v)C(u,v)|^2}\right)$	It is based on the contrast sensitivity function (CSF). $A(u,v)$, $B(u,v)$, and $C(u,v)$ represent discrete Fourier transforms (2D TFD) [234].
Normalized absolute error (NAE):	$\frac{\sum_{i=1}^{M}\sum_{j=1}^{N}|I(i,j)-R(i,j)|}{\sum_{i=1}^{M}\sum_{j=1}^{N}|I(i,j)|}$	It evaluates the accuracy of an ML model's predictions. It measures the difference between the predicted values and the actual values, as a proportion of the range of the actual values.
Laplacian mean squared error (LMSE)	$\frac{\sum_{i=1}^{M}\sum_{j=1}^{N}[L(I(i,j))-L(R(i,j))]^2}{\sum_{i=1}^{M}\sum_{j=1}^{N}[L(I(i,j))]^2}$	It is a variant of the mean squared error ()! ()!) that uses the Laplacian distribution instead of the Gaussian distribution. $L(I(i,j))$ is the Laplacian operator.

Ranking Metrics

M1. Mean reciprocal rank (MRR): The MRR is a statistic measure for evaluating the mean reciprocal rank of results for a sample of queries [235].

$$MRR=\frac{1}{|Q|}\sum_{i=1}^{|Q|}\frac{1}{rank_i} \tag{1}$$

where $rank_i$ refers to the rank position of the first relevant document for the *i*th query.

M2. The discounted cumulative gain (DCG): the DCG is used to measure the ranking quality [236].

6. Example of Thyroid Cancer Detection Using AI

To explain how thyroid cancer has been considered in the literature and how AI can be used to detect types of cancers, in the following, we present a simple example of TD classification. It has been known that pattern recognition is the process of training a neural network to assign the correct target classes to a set of input patterns. Once trained, the network can be used to classify patterns. In this section, we present an example of thyroid cancer classification as benign, malignant, and normal based on a set of features specified according to the TIRADS. In this example, the dataset (7200 samples) was selected from the UCI Machine Learning Repository [237]. This dataset can be used to create a neural network that classifies patients referred to a clinic as normal, hyperfunctioning, or subnormal functioning. The thyroid inputs and thyroid targets are defined as: (i) TI: a 21×7200 matrix consisting of 7200 patients characterized by 15 binary and 6 continuous patient attributes. (ii) TT: a 3×7200 matrix of 7200 associated class vectors defining which of three classes each input is assigned to. Classes are represented by a one in rows 1, 2, or 3. (1) Normal, not hyperthyroid. (2) Hyperfunctioning. (3) Subnormal functioning.

In this network, the data were divided into 5040 samples, 1080 samples, and 1080 samples used for training, validation, and testing, respectively. The network was trained to reduce the error between thyroid inputs and thyroid targets or until it reached the target goal. If the ER did not decrease and the training did not improve, the training data were halted with the data of the validation set. The testing dataset was used to deduce the values of the targets. Thus, it determined the percentage of learning. For this example, 10 neurons were used in the hidden layer in this model for 21 inputs and 3 outputs. After the simulation of the model, the percent error was 5.337%, 7.407%, and 5.092% for training, validation, and testing, respectively. Thus, in total, it recognized 94.4% and the overall ER was 5.6%. The confusion matrix and the ROC metric are illustrated in Figure 5.
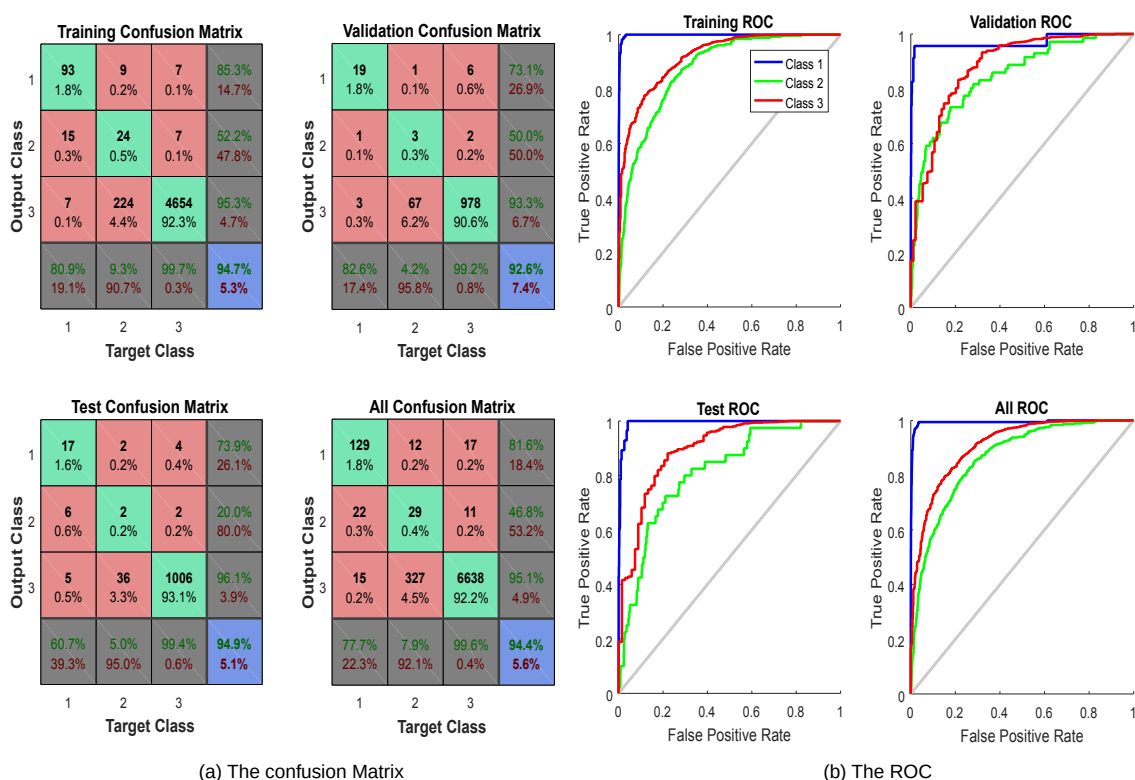

(a) The confusion Matrix (b) The ROC

Figure 5. An example of the confusion matrix and ROC metric for thyroid cancer classification.

Figure 6 illustrates an example of a thyroid segmentation in ultrasound images using K-means (three clusters were chosen for this example) which is one of the most commonly used clustering techniques.
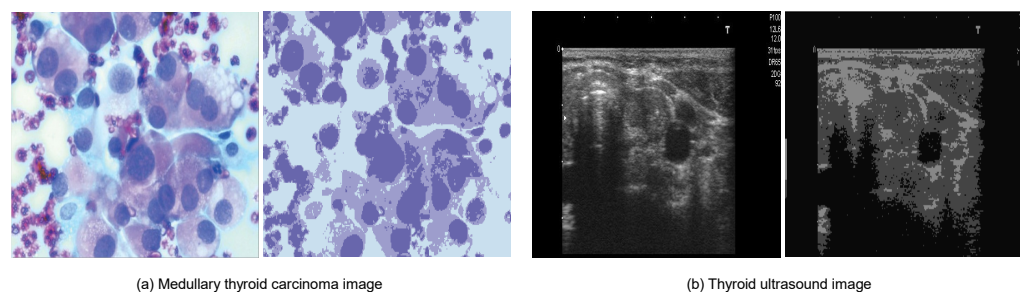

(a) Medullary thyroid carcinoma image   (b) Thyroid ultrasound image

Figure 6. Example of thyroid segmentation based on the K-means method.

7. Critical Analysis and Discussion

As we delve into the core of this paper, it is essential to critically assess and discuss the multitude of facets associated with the application of AI in thyroid carcinoma detection. While the promise of AI has been well articulated in the existing literature, a more nuanced perspective is needed to fully understand its impact on healthcare, both positive and negative. In this section, we undertake a critical analysis of the effectiveness of AI models for thyroid carcinoma detection. Moving beyond the optimistic numbers, we question the robustness of these models in real-world clinical settings and discuss their role in the broader context of clinical decision-making. Furthermore, we explore the potential biases in AI models, understanding how they might inadvertently perpetuate existing inequities in healthcare. A comparative assessment of AI-based and traditional diagnostic methods provides deeper insights into their relative effectiveness. Moreover, acknowledging the challenges to the implementation of AI tools in healthcare, we delve into the infrastructural, regulatory, and cultural barriers that might hinder their widespread adoption. Lastly, we underscore the crucial role of interdisciplinary collaboration in ensuring the successful integration of AI into healthcare.

A summary of the performance of various thyroid cancer frameworks is detailed in Table 10.

Table 10. Evaluation of the performance of various thyroid cancer frameworks in percentages (%).

Ref.	AI Model	Dataset	ACC	SPE	SEN	PPV	F1	NPV	AUC
[238]	CNN	PD	88.00	79.10	98.10	-	-	-	-
[103]	ELM	PD	87.72	94.55	78.89	-	-	-	-
[108]	MLP	PD	87.16	87.05	91.18	16.20	27.50	99.70	-
[142]	SVM	PD	63.27	71.85	38.46	32.43	-	76.87	-
[239]	RF	PD	86.80	87.90	85.20	-	-	-	92.00
[240]	LR	PD	77.80	79.80	70.60	-	-	-	75.00
[231]	B	PD	84.69	86.96	82.69	87.76	-	81.63	88.52
[241]	Ensemble DL	Cytological images	99.71	-	-	-	-	-	-
[100]	VGG-16	Cytological images	97.66	-	-	-	-	-	-
[54]	VGG-16		99.00	86.00	94.00	-	88.00	-	-
[43]	RF	Ultrasound	-	-	-	-	-	-	94.00
[187]	k-SVM	Ultrasound	-	-	-	-	-	-	95.00
[131]	ANN	Ultrasound	-	-	-	-	-	-	69.00
[125]	SVM RF	Ultrasound	-	-	-	-	-	-	95.10
[242]	ANN SVM	Ultrasound	96.00	-	-	-	-	-	-
[243]	RF	Ultrasound	-	-	-	-	-	-	75.00
[244]	CNN	DICOM	83.00	85.00	82.40	-	-	-	-
[28]	CNN	DICOM	-	91.50	-	-	-	-	-
[117]	Fine-tuned DCNN	PD	99.10	-	-	-	-	-	-

Table 10. *Cont.*

Ref.	AI Model	Dataset	ACC	SPE	SEN	PPV	F1	NPV	AUC
[245]	ResNet18-based network	PD	93.80	-	-	-	-	-	-
[246]	Multiple-scale CNN	PD	82.20	-	-	-	-	-	-
[99]	ThyNet	PD	-	-	-	-	-	-	92.10
[247]	Alexnet CNN	PD	86.00	-	-	-	-	-	-
[175]	DNN	ACR TIRADS	87.20	-	-	-	-	-	-
[124]	CNN (BETNET)	Ultrasound	98.30	-	-	-	-	-	-
[248]	ResNet	TIRADS	75.00	-	-	-	-	-	-
[249]	Xception	CT images	89.00	92.00	86.00	-	-	-	-
[120]	DCNN	Sonographic images	89.00	86.00	93.00	-	-	-	-
[250]	Google inception v3	Histopathology images	95.00	-	-	-	-	-	-
[251]	Cascade MaskR-CNN	Ultrasound	94.00	95.00	93.00	-	-	-	-
[252]	VGG16	Ultrasound	-	92.00	70.00	-	-	-	-
[253]	VGG19	Ultrasound	77.60	81.40	72.50	-	-	-	-
[40]	VGG16	Ultrasound	74.00	80.00	63.00	-	-	-	-
[189]	SVM CNN	Ultrasound	92.50	83.10	96.40	-	-	-	-
[254]	CNN	TIRADS	85.10	86.10	81.80	-	-	-	-
[255]	CNN	TIRADS	82.10	85.00	78.00	-	-	-	-
[256]	CNN	TIRADS	80.30	80.10	80.60	-	-	-	-
[257]	CNN	US	83.00	47.00	65.00	-	-	-	-
[258]	CNN	MRI	79.00	80.00	65.00	-	-	-	-
[259]	CNN	US	97.00	84.10	89.50	-	-	-	-
[260]	CNN	CT image	84.00	73.00	93.00	-	-	-	-
[261]	CNN	US	77.00	-	-	-	-	-	-

The reported accuracy, sensitivity, and specificity of AI models in the literature may vary widely based on the dataset used, the quality of the data, and the methodology employed. AI models' effectiveness in a controlled experimental environment may not reflect their performance in a real-world clinical setting. Factors such as noise in the data, incomplete data, and changing clinical conditions can dramatically influence the outcome. Therefore, it is crucial to scrutinize the model's robustness and reliability under various conditions.

Limitations and Open Challenges

Despite the success of AI tools in thyroid cancer diagnosis, their limitations hinder the development of effective solutions, make their application costly, and limit their diffusion. To achieve precise thyroid cancer detection, it is crucial to centralize and securely store all relevant data in one location, unless you opt for federated learning (FL) techniques [262]. Then, algorithms must be developed to identify all forms of thyroid cancer. Every TCD includes a set of training images, test images, nodule plans, and classifications of nodule characteristics of diverse sizes [263]. The datasets must be regularly updated using MRI, CT scans, X-rays, and clinically obtained scans to assess thyroid conditions, and they should also include demographic information such as race, ethnicity, gender, and age. Additionally, it is important to establish a unified and centralized database accessible to all medical centers to test, validate, and apply AI algorithms to existing data [264]. Moreover, the rest of the limitations and open challenges can be summarized as follows:

- Insufficient clean data and accuracy: The lack of comprehensive and annotated datasets regarding the incidence and spread of cancer, specifically thyroid cancer, is a major hindrance to accurate cancer diagnoses and efficient treatment. Medical statistics often do not properly record the number of deaths caused by thyroid cancer, making data collection and validation challenging [265]. This results in a limited quantity of data typically collected from one center, due to the absence of a dedicated thyroid cancer clinical database shared among institutions. The accuracy of AI algorithms in diagnosing thyroid cancer is also limited by the scarcity of available labeled

cases for clinical outcomes [266]. Researchers acknowledge that a large quantity of data is necessary for a neural network to yield accurate results, but caution must be taken in regard to the data added during the learning phase, as it can introduce noise.

- Thyroid gland imaging: In the diagnostic evaluation of thyroid cancer, computed tomography (CT) and MRI are available options, but they are not considered the preferred methods due to their high cost and unavailability in certain cases [55]. Instead, ultrasound is commonly used as an alternative to physical exams, radioisotope scans, or fine-needle aspiration biopsies. During an ultrasound examination, the doctor is able to assess the activity of the gland by observing the echo of the node and determining its echogenicity, size, limits, and the presence of calcifications. However, the results obtained from ultrasound tests are not always accurate enough to differentiate between benign and malignant nodes and the images obtained can be more prone to noise [267].

- DL models' hyperparameters: Choosing the right DL algorithm is crucial in addressing various issues, particularly those related to thyroid cancer diagnosis. Due to the close similarities between benign and malignant tumors, as well as between tumors and other types of lymphocytes, it is challenging to differentiate between them accurately [268]. To achieve this, a significant increase in the number of layers for feature extraction may be required. However, this results in a longer processing time, especially when dealing with large quantities of data, which can impact the timeliness of the diagnosis for cancer patients [54].

- Computation cost and storage space: In the field of algorithms, time computing is a metric that assesses the computational complexity of an algorithm, which predicts the time it takes to run the algorithm by calculating the number of basic operations it performs, as well as its dependence on the size of the input. Typically, time computing is expressed as $O(n)$, where n represents the size of the input, measured in terms of the number of bits required to represent it [269]. Researchers in the AI field, especially those working on thyroid cancer or other types of cancer diagnosis, face the challenge of finding algorithms that are both highly accurate and efficient in terms of processing time. They aim to develop algorithms that can analyze vast quantities of data quickly while still providing accurate results. Moreover, the volume of data used in these algorithms can sometimes exceed the available storage space [54].

- Imbalanced dataset: The distribution of cancer elements within categories related to thyroid tissue cells is often uneven, as these cells often make up a minority of the total tissue cell dataset. As a result, the dataset is highly imbalanced, consisting of both cancer cells and normal cells. This unbalanced distribution of features in cancer cell detection datasets often results in the suboptimal performance of AI algorithms used for the detection [270].

- Sparse labels: Labeling is a crucial aspect of computed tomography (CT) detection, specifically for distinguishing between normal and abnormal cancer cells. However, the process can be time-consuming and costly due to the limited number of available labels. This scarcity results in inconsistent decisions and can negatively impact the accuracy of AI algorithms, which heavily rely on labeled data. This can eventually undermine the trust and credibility of this type of application [270].

- The volume of data: At present, with the advancement in technology, especially in the field of thyroid cancer diagnosis and the growing volume of medical and patient data, researchers are facing challenges in suggesting algorithms that can effectively handle a limited number of samples, noisy samples, unannotated samples, sparse samples, incomplete samples, and high-dimensional samples. This requires AI algorithms that are highly efficient and capable of processing vast quantities of data exchanged between healthcare providers and patients or among specialist physicians [271].

- Error susceptibility: Despite AI being self-sufficient, it is still susceptible to errors. For instance, when training an algorithm with TCDs to diagnose cancerous regions, it can result in biased predictions if the training sets are biased. This can lead to a series of

incorrect results that may go unnoticed for an extended period. If detected, identifying and correcting the source of the problem can be a time-consuming process [272].

- Data form: Despite the numerous advancements in the use of AI for thyroid cancer detection, several limitations persist and pose a challenge to its progress. With the growing demand for various medical imaging technologies that result in vast quantities of data needed for AI algorithms, coordinating and organizing this information has become a daunting task. This can largely be attributed to the absence of proper labeling, annotation, or segmentation of the data, making it difficult to manage effectively [273].

- Unexplainable AI: The utilization of AI in the medical field can sometimes yield results that are unclear and lack proper justification, known as a "black box". This leaves doctors unsure about the accuracy of the results and may lead to erroneous decisions and treatments for patients with thyroid cancer. Essentially, AI can behave like a black box and fail to provide understandable explanations for its outputs [274].

- Lack of cancer detection platform: One of the major barriers to detecting various cancers, particularly thyroid cancer, is the limited availability of platforms for reproducing and examining previous results. This shortage represents a significant weakness and hinders the comparison of AI algorithm performance, making it challenging to improve their efficacy [159]. The presence of online platforms with comprehensive datasets, cutting-edge algorithms, and expert recommendations is vital in aiding doctors, researchers, developers, and specialists to make informed decisions with a low margin of error. Such platforms also provide a crucial supplement to clinical diagnoses by allowing for a more comprehensive experimentation and comparison [275].

- The digitization and loss data: The digitization of medical records has become a necessity, particularly in the realm of cancer diagnosis, due to the widespread adoption of various technologies such as whole-slide images. These latter serve as digital versions of glass slides, facilitating the application of AI techniques for pathological analysis [276]. Despite its benefits, digitization in the medical field is confronted with certain limitations, such as the risk of significant information loss during the quantification and inaccuracies that may arise from data compression utilized in autoencoder algorithms. Hence, it is crucial to be mindful in selecting the right digitization technology to preserve the information and maintain the originality of the data [277,278].

- Contrast: The absence of sufficient contrast in the tissues neighboring the TG complicates the process of accurately analyzing and diagnosing thyroid cancer.

8. Future Research Directions

We also highlight the future trajectory of AI in thyroid carcinoma detection, discussing emerging trends and technologies while considering their ethical implications. The ethical considerations do not end there, as we further examine issues related to data privacy, accountability, and equity. This section highlights promising research trends that will have a major effect on enhancing thyroid cancer detection in the future.

8.1. Explainable Artificial Intelligence (XAI)

The use of AI systems in decision-making is crucial, but they can be complex and difficult to understand. To address this issue, the field of XAI has emerged, which aims to provide transparency in AI models. The need for XAI is especially important in health applications where the interpretation of results is crucial. The use of XAI has been demonstrated in the analysis of incurable diseases affecting the TG, as seen in several studies such as [279–283]. The difference between AI and XAI is illustrated in Figure 7. In [171], the authors present an XAI model for the detection of thyroid cancer, which improves the confidence of medical practitioners in the predictions. Unlike traditional AI algorithms, XAI models provide evidence to support their conclusions and avoid the limitations of

"black box" algorithms. By using XAI, clinicians can make more informed decisions with greater confidence.
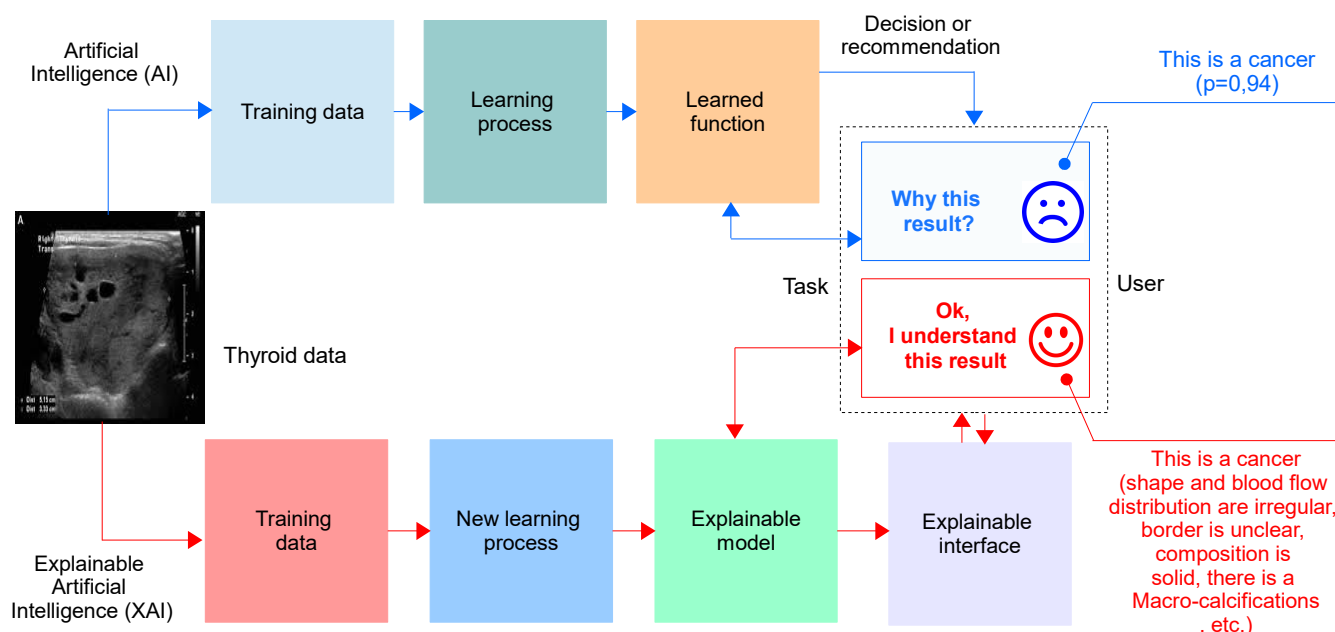

Figure 7. XAI diagram block.

8.2. Edge, Fog, and Cloud Computing for Implementation

The edge network is a combination of edge computing and AI that processes algorithms based on AI near the source of data [284]. This allows for better performance and lower costs for applications that require heavy information processing and reduces the need for long-distance communication between the patient and the doctor. The proximity of the information and storage capabilities to the end-user in the health sector allows for direct and immediate access [285]. To further enhance performance, the detection of thyroid cancer in edge networks relies on the use of fog computing, which is a decentralized computing architecture located between the cloud and the data-producing devices. This architecture allows for the flexible placement of computing and storage resources in logical locations, improving performance [286]. To ensure the proper operation of the AI-based thyroid cancer detection system, it utilizes cloud computing as an access point. This guarantees that the stored data, servers, databases, networks, and programs are accessible and shared among specialized doctors, as long as it is connected to the Internet. Such a hybrid system has proven to be effective for medical applications, including the detection of thyroid cancer, as seen in various studies including [287–297].

8.3. Reinforcement Learning (RL)

RL, a subfield of ML, allows agents to make decisions in interactive environments through trial and error, observation, and learning (as depicted in Figure 8). In recent years, there has been a significant interest in using RL for detecting incurable diseases and providing explanations to aid medical decision-making. For example, RL is used in [298] to classify cancer data, and deep RL is used in [299] to segment lymph node sets. The authors generate pseudo-ground-truths using RECIST-slices and achieve the simultaneous optimization of lymph-node bounding boxes through the interaction between a segmentation network and a policy network.
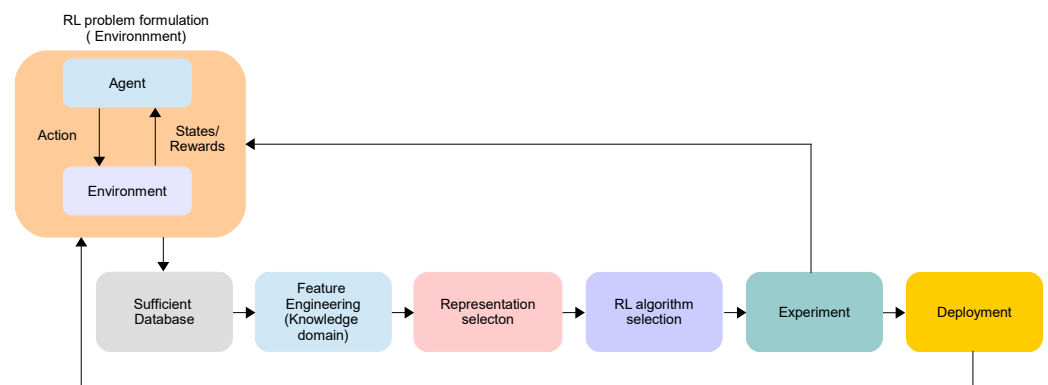
Figure 8. Deep RL procedure.

8.4. Transfer Learning (TL)

TL is a valuable solution to the overfitting and precision challenges faced by diagnosis systems [300–302]. This technique leverages stored knowledge from a specific problem to address other issues such as reducing training time and data volume [271,303]. Its use in the diagnosis of the TG is demonstrated in Figure 9. For instance, the Enhance-Net model, as introduced in [304], could serve as a source model for enhancing the performance of a target DL model designed for real-time medical images. Furthermore, in [158], the authors tackle the challenge of capturing appropriate features of benign and malignant nodules using CNNs. They transfer the knowledge learned from natural data to an ultrasound image dataset to produce hybrid semantic deep features. The TL technique has also been successfully applied to classify thyroid nodules images in [164]. Other related works can be found in [162,252,305–307].
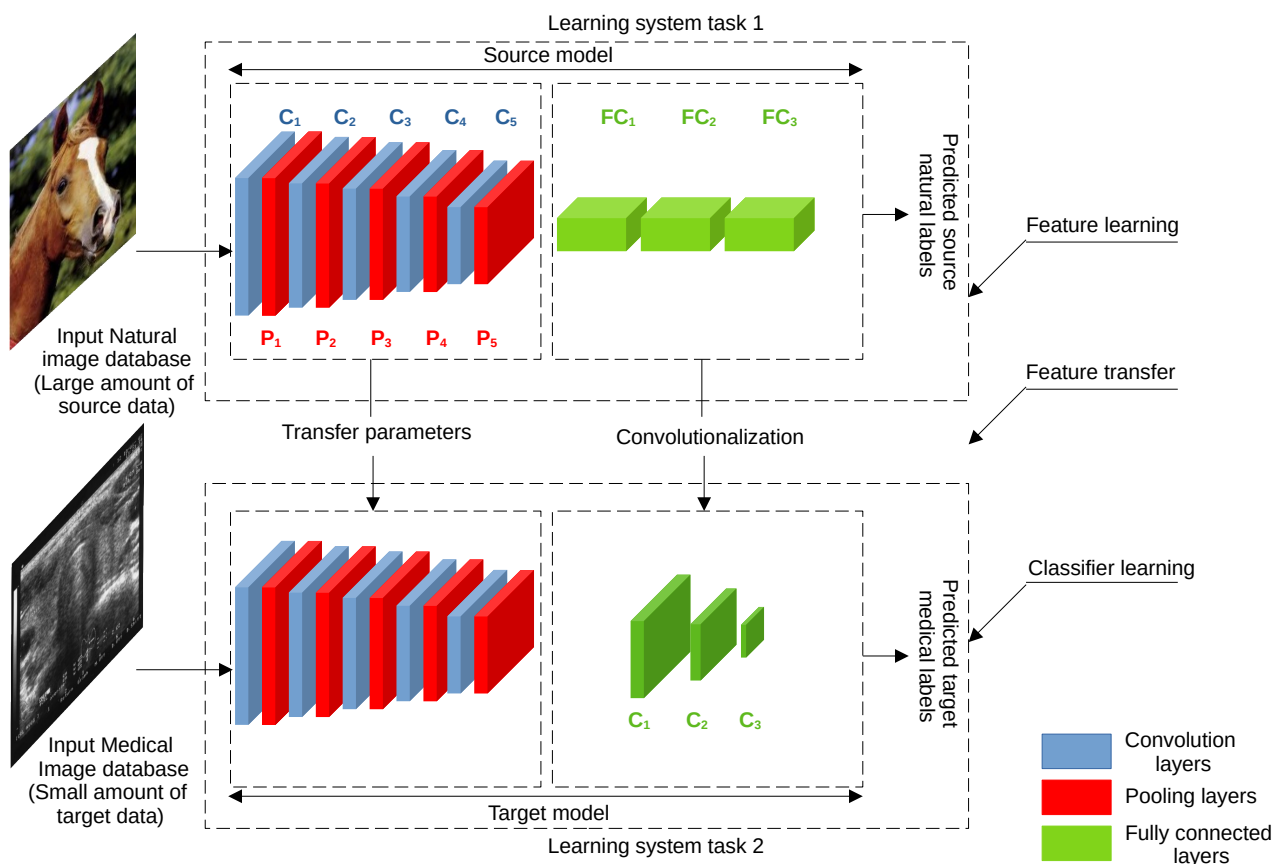
Figure 9. Deep transfer learning for thyroid diagnosis.

8.5. Panoptic Segmentation (PS)

The challenge of accurately separating and dividing objects with diverse and overlapping appearances remains an issue, particularly in the medical field. To address this, many researchers have put forth proposals for a comprehensive and cohesive segmentation of various details [308,309]. The focus has been on PS, which combines both instance and semantic segmentation to identify and separate objects. In semantic segmentation, the goal is to classify each pixel into specific classes, while in instance segmentation, the focus is on segmenting individual object instances. AI has been incorporated into this model through supervised or unsupervised instance segmentation learning, making it well suited for medical applications (Figure 10). This has been demonstrated in works such as [310,311].
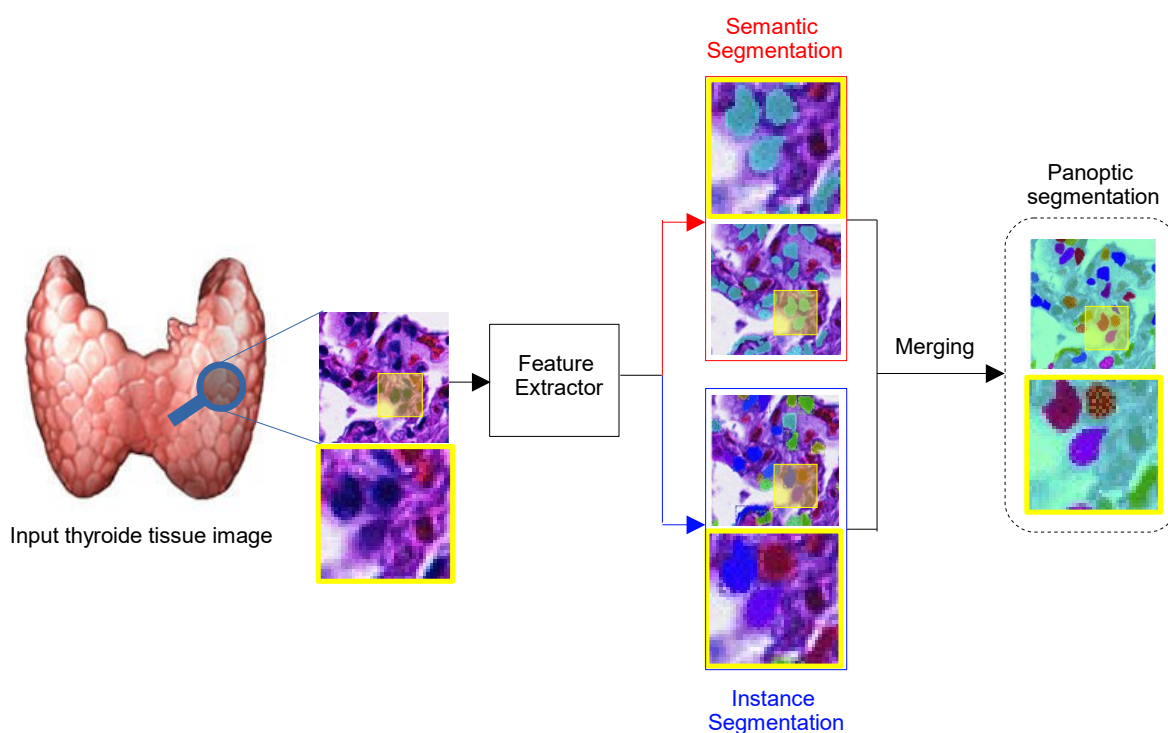
Figure 10. PS architecture.

8.6. Internet of Medical Imaging Things (IoMIT)

The IoMIT has recently gained widespread attention in the medical field, as it seeks to enhance healthcare delivery and reduce treatment costs through the exchange of health data between patients and doctors using connected devices with wireless communication (Figure 11). One example of this integration can be found in [312], which proposes an AI-based solution for the early detection of thyroid cancer in the IoMT, utilizing CNN to improve the differentiation between benign and malignant nodules, ultimately saving lives. Other relevant studies related to the IoMIT have also been conducted, such as [313,314].

8.7. Three-Dimensional Thyroid Cancer Detection (3D-TCD)

The conventional 2D ultrasound is widely used for diagnosing thyroid nodules, but its static images may not accurately reflect the nodule's structures. Hence, the use of 3D ultrasound has gained attention as it provides a more comprehensive view of the lesion by reconstructing its features and enabling a better differentiation between different diagnoses [315]. With the ability to examine complex growth patterns and margins and to give shape from multiple angles and levels, 3D ultrasound can provide a more accurate evaluation of the morphological features of thyroid nodules in comparison to 2D images. This has been confirmed through comparative studies between 3D and 2D ultrasound images [316–318].
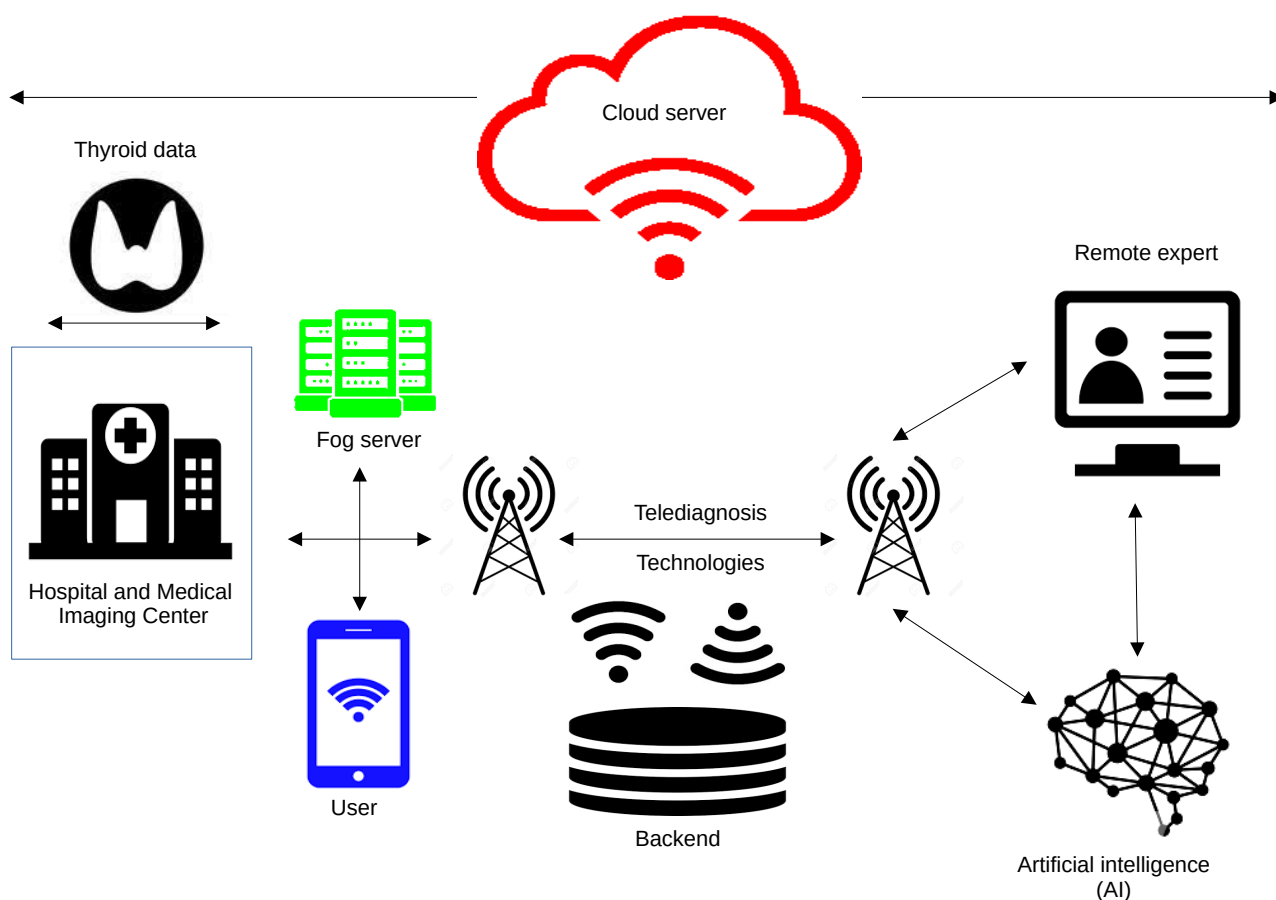
Figure 11. Example of a hybrid network system based on AI for thyroid cancer detection.

8.8. AI in Thyroid Surgery (AI-TS)

In light of the challenges faced in surgical procedures, the use of AI-powered robots in surgical practices is becoming increasingly essential. AI has the potential to address numerous clinical issues by analyzing and sharing massive quantities of data to support decisions with a level of accuracy comparable to that of healthcare professionals [319]. Companies are incorporating AI into surgical practices by training AI-based systems and providing robots that assist surgeons in operating rooms, supply surgical materials, handle contaminated materials and medical waste, remotely monitor patients, and collect and organize patient data such as electronic medical records, vital signs, laboratory results, and video footage [320]. As such, it is important for surgeons to have a strong understanding of AI in order to grasp its impact on healthcare. While AI-powered robotic surgery may still be some time away, collaboration across various fields can accelerate AI's capabilities and improve surgical care [321–328].

8.9. Wavelet-Based AI

Recently, the wavelet transform, specifically the first and second-generation ones, has gained recognition for its ability to detect various forms of cancer, especially when integrated with AI. This combination has become crucial in the medical field, providing doctors and surgeons with a tool to accurately diagnose diseases more efficiently and quickly [329,330]. The proposed method is based on preprocessing the dataset through DWT and then evaluating the performance of AI in classifying different types of tumors that can impact organs in the body (as explained in Figure 12). This model holds great potential for the detection of thyroid cancer and researchers are encouraged to test different wavelets available in the literature to further improve its effectiveness [331].
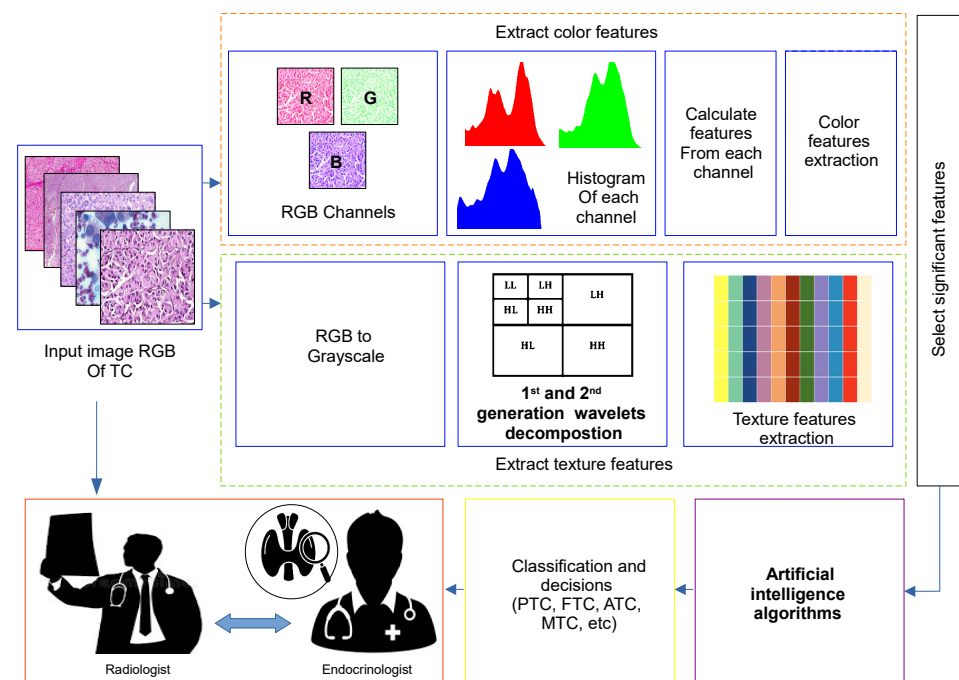
Figure 12. Applications of AI-based on wavelet in the detection of thyroid cancer.

8.10. Learning with Reduced Data

One of the hurdles in implementing AI in the medical sector is acquiring adequate data and annotations. AI's capability to minimize the need for labeled data in making an accurate diagnosis is crucial [332]. This can be achieved through various learning methods such as semi-supervised learning, supervised learning, USL, or alternative approaches that necessitate a smaller quantity of annotated data (Figure 13) [333].
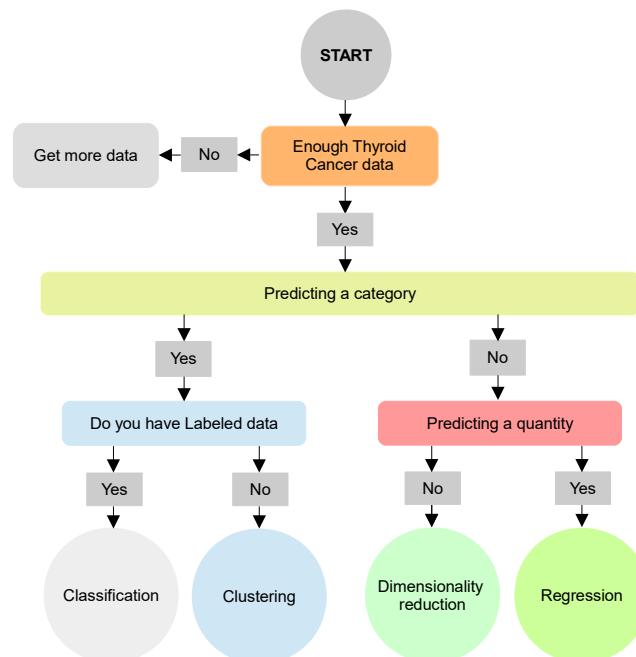
Figure 13. Diagram of the choice of AI-algorithms for thyroid cancer detection.

8.11. Recommender Systems (RSs)

The abundance of data collected from online medical platforms and electronic health records can make it challenging for thyroid cancer patients to access relevant and accurate

information [334]. The high cost of healthcare data also poses difficulties for doctors to track patients and manage a large patient volume with various treatment options. Given these challenges, the implementation of recommender systems (RSs) has been proposed to improve decision-making in healthcare and ease the workload for both patients and oncologists [335,336]. The use of RS in digital health provides personalized recommendations, an accurate analysis of big data, and stronger privacy protection through integration with AI and machine learning technologies [337] as depicted in Figure 14.
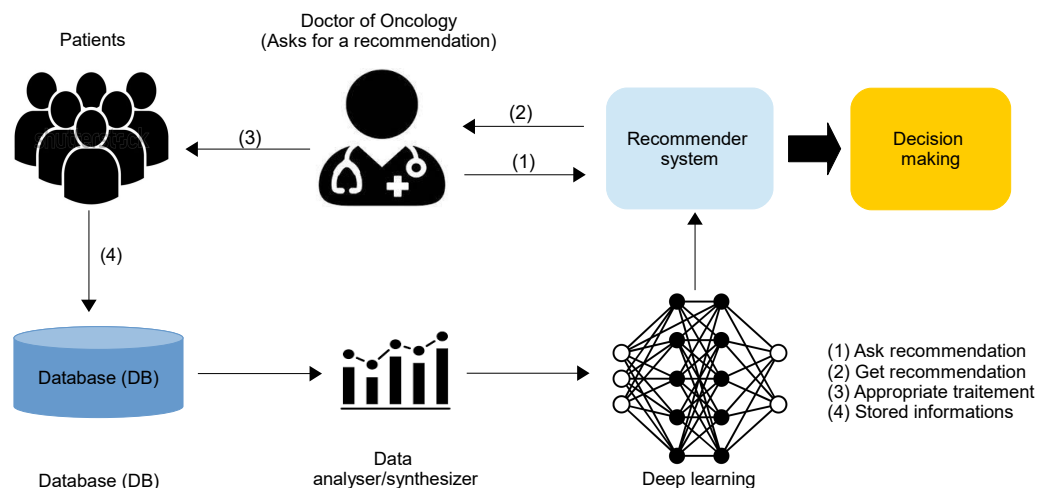
Figure 14. RSs for thyroid cancer detection.

8.12. Federated Learning (FL):

FL has become very popular in the field of healthcare applications [338]. The surrounding conditions greatly affect human health and cause negative effects on the economy. Diseases of the thyroid gland are among the most common health problems that have become noticeable among various groups of society in recent times. ML can play a vital role in such medical conditions, as the collected data can be exploited to train an ML model that can predict critical conditions. Emphasizing that patient data across different medical centers should be handled privately, the FL setup is the natural choice for such applications, as depicted in Figure 15. Therefore, in [339], the authors compared the performance of FL against five conventional deep learning methods (VGG19, ResNet50, ResNext50, SE-ResNet50, and SE-ResNext50) for analyzing and detecting TCDs.
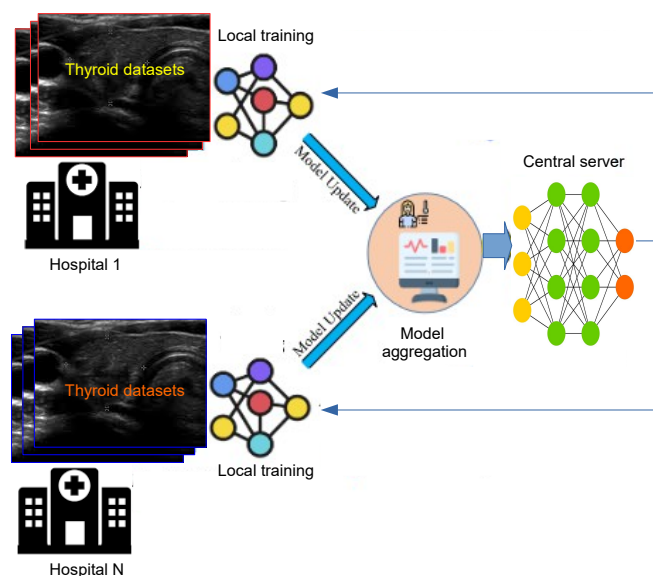
Figure 15. FL for healthcare.

8.13. Generative Chatbots

Most recently, the realm of AI has witnessed significant advancements, particularly in the development of generative chatbots and large language models such as GPT variants [340]. These state-of-the-art models, trained on vast quantities of data, are adept at generating humanlike text and engaging in coherent conversations, going beyond mere predefined responses. As their capability has expanded, so too has their potential for application across various domains, healthcare being one of the prominent ones. In the healthcare sector, these sophisticated models are being explored for patient engagement, preliminary symptom checks, providing health-related information, and even assisting professionals with medical research and data analysis [3]. The integration of such technology holds the promise of streamlining healthcare processes, enhancing patient experience, and augmenting the capabilities of healthcare professionals, albeit with the necessary precautions and ethical considerations in place [341].

Using generative chatbots or models such as ChatGPT to diagnose thyroid cancer (or any medical condition) directly would be inappropriate and potentially dangerous. However, they can be incorporated into healthcare settings in auxiliary roles [342]. Typically, chatbots can gather preliminary information from patients, including their symptoms, family history, and lifestyle habits. These data can provide a better understanding of the patient's concerns before they meet a healthcare professional. Moreover, they can be programmed to provide information about thyroid cancer, such as risk factors, symptoms, and preventive measures [343]. Patients can learn about the disease and its potential signs, allowing them to approach healthcare providers if they find any matching symptoms. Furthermore, while they cannot replace professional diagnostic tools, they can be designed to guide users through a series of questions that could highlight potential risk factors or symptoms, encouraging them to consult a medical professional for a more comprehensive evaluation [344].

On the other hand, once a diagnosis has been made, chatbots can provide patients with information on treatment options, side effects, diet recommendations, and answer frequently asked questions. Additionally, they can (i) remind patients to take their medications, attend follow-up appointments, or perform regular self-examinations or monitoring, (ii) offer support in terms of relaxation techniques, provide resources for further psychological support, or even just offer a nonjudgmental "listening ear", and (iii) assist doctors and other healthcare professionals by providing instant information about thyroid cancer, recent research, or treatment options, acting as a dynamic reference tool [345].

9. Conclusions

In this research, a comprehensive overview of DNNs was presented, spotlighting their ascendant trend in recent years owing to their superior accuracy compared to other methodologies. An array of algorithms and training structures, inclusive of their benefits and constraints, was delineated. DNNs are manifestly pivotal in myriad real-world applications, particularly lauded for their generalizability and tolerance to noise.

Notwithstanding these advancements, barriers persist in fully adopting DNNs in thyroid cancer detection. A paramount obstacle is the absence of clean datasets and platforms. To cultivate efficient and formidable cancer detection models capable of discerning more advanced malignancies, these data constraints warrant meticulous attention.

Future research needs to be oriented towards circumventing these impediments and enhancing thyroid cancer detection's caliber. Furthermore, this study underscores the urgency for amplified research endeavors in thyroid cancer identification, especially given the diagnostic precision coveted by medical practitioners. While the detection of various cancers in two or three dimensions is a burgeoning research area, the deficiency in expertise with diverse geometric transformations and the requisite dimensional databases curtails the precision in diagnosing terminal illnesses. Hence, pioneering methodologies to discern disparate magnitudes of cancerous nodules become indispensable. Such innova-

tions can exponentially augment treatment velocity, diagnostic accuracy, enable proactive epidemiological surveillance, and subsequently mitigate mortality rates.

Emerging technologies, namely explainable AI, edge computing, RL, PS, and RSs, have unfurled novel research horizons in thyroid cancer detection. These innovations are proving invaluable for clinicians by streamlining the diagnostic process, curtailing detection time frames, and fortifying patient confidentiality. As a trajectory for future endeavors, our focus will pivot towards a deeper probe into the contributions of these avant-garde technologies. Our ambition is to foster a seismic paradigm shift in cancer detection by ideating state-of-the-art, privacy-centric technologies for thyroid cancer patient identification and broader applications, such as telehealth.

Author Contributions: Conceptualization, Y.H. (Yassine Habchi); methodology, Y.H. (Yassine Habchi), Y.H. (Yassine Himeur) and A.B.; software, Y.H. (Yassine Habchi); validation, Y.H. (Yassine Habchi), Y.H. (Yassine Himeur) and A.B.; formal analysis, Y.H. (Yassine Habchi), Y.H. (Yassine Himeur) and H.K.; investigation, A.O.; data curation, Y.H. (Yassine Habchi); writing—original draft preparation, Y.H. (Yassine Habchi); writing—review and editing, Y.H. (Yassine Himeur), H.K., A.B., S.A., A.C., A.O. and W.M.; visualization, Y.H. (Yassine Habchi) and A.C.; supervision, Y.H. (Yassine Himeur) A.B. and W.M. All authors have read and agreed to the published version of the manuscript.

Institutional Review Board Statement: Not applicable.

Data Availability Statement: Not applicable.

Conflicts of Interest: The authors declare no conflict of interest.

Abbreviations

AC	Active contour
AI	Artificial intelligence
ANN	Artificial neural network
ATC	Anaplastic thyroid carcinoma
BA	Bootstrap aggregation
Bi-LSTM	Bidirectional LSTM
BN	Bayesian network
CAD	Computer-aided diagnosis
CFS	Correlation-based feature selection
CNN	Convolutional neural network
CT	Computed tomography
DAE	Denoising autoencoder
DCG	Discounted cumulative gain
DCNN	Deep convolutional neural network
DDTI	Digital Database Thyroid Image
DL	Deep learning
DNN	Deep neural network
DR	Dimensionality reduction
DT	Decision trees
DTCW	Double-tree complex wavelet transform
DWT	Discrete wavelet transfer
ELM	Extreme learning machine
ER	Error rate
FB	Feature bagging
FL	Federated learning
FNAB	Fine-needle aspiration biopsy

FTC	Follicular thyroid carcinoma
GAN	Generative adversarial network
GEO	Gene expression omnibus
GLCM	Gray-level co-occurrence matrix
HOG	Histogram of oriented gradient
ICA	Independent component analysis
IG	Information gain
IoMIT	Internet of medical imaging things
KM	K-means
KNN	K-nearest neighbors
LBP	Local binary patterns
LR	Logistic regression
LSTM	lLong short-term memory
ML	Machine learning
MLP	Multilayer perceptron
MRI	Magnetic resonance imaging
MRM	MicroRNA regulatory module
MRR	Mean reciprocal rank
MSE	Mean squared error
MTC	Medullary thyroid carcinoma
NCDR	National Cancer Data Repository
PCA	Principal component analysis
PLCO	Prostate, Lung, Colorectal, and Ovarian
PM	Probabilistic models
PS	Panoptic segmentation
PSNR	Peak signal to noise ratio
PTC	Papillary carcinoma
RBF	Radial basis function
RBM	Restricted Boltzmann machine
RF	Random forest
RL	Reinforcement learning
RMSE	Root-mean-square error
RNN	Recurrent neural network
RS	Recommender systems
SEER	Surveillance, Epidemiology, and End Results
SL	Supervised learning
SVM	Support vector machine
TCD	Thyroid cancer dataset
TCGA	The Cancer Genome Atlas
TCL	Traditional classification
TD	Thyroid disease
TDDS	Thyroid Disease Data Set
TG	Thyroid gland
TIRADS	Thyroid Imaging, Reporting, and Data System
TI-RADS	Thyroid Imaging, Reporting, and Data System
TL	Transfer learning
TN	Thyroid nodules
USL	Unsupervised learning
XAI	Explainable AI
XAI	Explainable artificial intelligence
XGBoost	Gradient tree boosting

References

1. Himeur, Y.; Al-Maadeed, S.; Varlamis, I.; Al-Maadeed, N.; Abualsaud, K.; Mohamed, A. Face mask detection in smart cities using deep and transfer learning: Lessons learned from the COVID-19 pandemic. *Systems* **2023**, *11*, 107. [CrossRef]
2. Himeur, Y.; Al-Maadeed, S.; Almaadeed, N.; Abualsaud, K.; Mohamed, A.; Khattab, T.; Elharrouss, O. Deep visual social distancing monitoring to combat COVID-19: A comprehensive survey. *Sustain. Cities Soc.* **2022**, *85*, 104064. [CrossRef]

3. Sohail, S.S.; Farhat, F.; Himeur, Y.; Nadeem, M.; Madsen, D.Ø.; Singh, Y.; Atalla, S.; Mansoor, W. Decoding ChatGPT: A Taxonomy of Existing Research, Current Challenges, and Possible Future Directions. *J. King Saud Univ. Comput. Inf. Sci.* **2023**, *35*, 101675.

4. Himeur, Y.; Elnour, M.; Fadli, F.; Meskin, N.; Petri, I.; Rezgui, Y.; Bensaali, F.; Amira, A. AI-big data analytics for building automation and management systems: A survey, actual challenges and future perspectives. *Artif. Intell. Rev.* **2023**, *56*, 4929–5021. [CrossRef]

5. Calisto, F.M.; Nunes, N.; Nascimento, J.C. Modeling adoption of intelligent agents in medical imaging. *Int. J. Hum. Comput. Stud.* **2022**, *168*, 102922. [CrossRef]

6. Deng, Y.; Li, H.; Wang, M.; Li, N.; Tian, T.; Wu, Y.; Xu, P.; Yang, S.; Zhai, Z.; Zhou, L.; et al. Global burden of thyroid cancer from 1990 to 2017. *JAMA Netw. Open* **2020**, *3*, e208759. [CrossRef]

7. Hammouda, D.; Aoun, M.; Bouzerar, K.; Namaoui, M.; Rezzik, L.; Meguerba, O.; Belaidi, A.; Kherroubi, S. *Registre des Tumeurs d'Alger*; Ministere de la Sante et de la Population Institut National de Sante Publique: Paris, France, 2006.

8. Abid, L. Le cancer de la thyroide en Algérie. In *Guide de la Santé en Algérie: Actualité Pathologie*; Santedz: Alger, Algeria, 2008.

9. NIPH. Available online: http://www.insp.dz/index.php/Non-categorise/registre-des-tumeurs-d-alger.html (accessed on 17 January 2021).

10. Siegel, R.L.; Miller, K.D.; Jemal, A. Cancer statistics, 2019. *CA Cancer J. Clin.* **2019**, *69*, 7–34. [CrossRef]

11. Hitu, L.; Gabora, K.; Bonci, E.A.; Piciu, A.; Hitu, A.C.; Ștefan, P.A.; Piciu, D. MicroRNA in Papillary Thyroid Carcinoma: A Systematic Review from 2018 to June 2020. *Cancers* **2020**, *12*, 3118. [CrossRef]

12. Castellana, M.; Piccardo, A.; Virili, C.; Scappaticcio, L.; Grani, G.; Durante, C.; Giovanella, L.; Trimboli, P. Can ultrasound systems for risk stratification of thyroid nodules identify follicular carcinoma? *Cancer Cytopathol.* **2020**, *128*, 250–259. [CrossRef]

13. Ferrari, S.M.; Elia, G.; Ragusa, F.; Ruffilli, I.; La Motta, C.; Paparo, S.R.; Patrizio, A.; Vita, R.; Benvenga, S.; Materazzi, G.; et al. Novel treatments for anaplastic thyroid carcinoma. *Gland. Surg.* **2020**, *9*, S28. [CrossRef]

14. Giovanella, L.; Treglia, G.; Iakovou, I.; Mihailovic, J.; Verburg, F.A.; Luster, M. EANM practice guideline for PET/CT imaging in medullary thyroid carcinoma. *Eur. J. Nucl. Med. Mol. Imaging* **2020**, *47*, 61–77. [CrossRef]

15. Carling, T.; Udelsman, R. Thyroid cancer. *Annu. Rev. Med.* **2014**, *65*, 125–137. [CrossRef] [PubMed]

16. Yang, R.; Zou, X.; Zeng, H.; Zhao, Y.; Ma, X. Comparison of Diagnostic Performance of Five Different Ultrasound TI-RADS Classification Guidelines for Thyroid Nodules. *Front. Oncol.* **2020**, *10*, 598225. [CrossRef] [PubMed]

17. Kobayashi, K.; Fujimoto, T.; Ota, H.; Hirokawa, M.; Yabuta, T.; Masuoka, H.; Fukushima, M.; Higashiyama, T.; Kihara, M.; Ito, Y.; et al. Calcifications in thyroid tumors on ultrasonography: Calcification types and relationship with histopathological type. *Ultrasound Int. Open* **2018**, *4*, E45. [CrossRef] [PubMed]

18. Tessler, F.N.; Middleton, W.D.; Grant, E.G.; Hoang, J.K.; Berland, L.L.; Teefey, S.A.; Cronan, J.J.; Beland, M.D.; Desser, T.S.; Frates, M.C.; et al. ACR thyroid imaging, reporting and data system (TI-RADS): White paper of the ACR TI-RADS committee. *J. Am. Coll. Radiol.* **2017**, *14*, 587–595. [CrossRef]

19. Tessler, F.N.; Middleton, W.D.; Grant, E.G. Thyroid imaging reporting and data system (TI-RADS): A user's guide. *Radiology* **2018**, *287*, 29–36. [CrossRef]

20. Genomic Data Commons Data Portal. Available online: https://portal.gdc.cancer.gov/ (accessed on 10 January 2021).

21. TI-RADS Calculator. Available online: http://tiradscalculator.com/ (accessed on 10 January 2021).

22. AI TI-RADS Calculator. Available online: https://deckard.duhs.duke.edu/~ai-ti-rads/ (accessed on 10 January 2021).

23. Schlumberger, M.; Tahara, M.; Wirth, L.J.; Robinson, B.; Brose, M.S.; Elisei, R.; Habra, M.A.; Newbold, K.; Shah, M.H.; Hoff, A.O.; et al. Lenvatinib versus placebo in radioiodine-refractory thyroid cancer. *N. Engl. J. Med.* **2015**, *372*, 621–630. [CrossRef] [PubMed]

24. Wettasinghe, M.C.; Rosairo, S.; Ratnatunga, N.; Wickramasinghe, N.D. Diagnostic accuracy of ultrasound characteristics in the identification of malignant thyroid nodules. *BMC Res. Notes* **2019**, *12*, 193. [CrossRef]

25. Nayak, R.; Nawar, N.; Webb, J.; Fatemi, M.; Alizad, A. Impact of imaging cross-section on visualization of thyroid microvessels using ultrasound: Pilot study. *Sci. Rep.* **2020**, *10*, 415. [CrossRef]

26. Singh Ospina, N.; Maraka, S.; Espinosa DeYcaza, A.; O'Keeffe, D.; Brito, J.P.; Gionfriddo, M.R.; Castro, M.R.; Morris, J.C.; Erwin, P.; Montori, V.M. Diagnostic accuracy of thyroid nodule growth to predict malignancy in thyroid nodules with benign cytology: Systematic review and meta-analysis. *Clin. Endocrinol.* **2016**, *85*, 122–131. [CrossRef]

27. Kumar, V.; Webb, J.; Gregory, A.; Meixner, D.D.; Knudsen, J.M.; Callstrom, M.; Fatemi, M.; Alizad, A. Automated segmentation of thyroid nodule, gland, and cystic components from ultrasound images using deep learning. *IEEE Access* **2020**, *8*, 63482–63496. [CrossRef] [PubMed]

28. Ma, J.; Wu, F.; Jiang, T.; Zhao, Q.; Kong, D. Ultrasound image-based thyroid nodule automatic segmentation using convolutional neural networks. *Int. J. Comput. Assist. Radiol. Surg.* **2017**, *12*, 1895–1910. [CrossRef] [PubMed]

29. Song, J.S.A.; Hart, R.D. Fine-needle aspiration biopsy of thyroid nodules: Determining when it is necessary. *Can. Fam. Physician* **2018**, *64*, 127.

30. Hahn, S.Y.; Shin, J.H.; Oh, Y.L.; Park, K.W.; Lim, Y. Comparison between fine needle Aspiration and core needle Biopsy for the Diagnosis of thyroid Nodules: Effective Indications according to US Findings. *Sci. Rep.* **2020**, *10*, 4969. [CrossRef]

31. Ullah, H.; Saba, T.; Islam, N.; Abbas, N.; Rehman, A.; Mehmood, Z.; Anjum, A. An ensemble classification of exudates in color fundus images using an evolutionary algorithm based optimal features selection. *Microsc. Res. Tech.* **2019**, *82*, 361–372. [CrossRef]

32. Saba, T.; Bokhari, S.T.F.; Sharif, M.; Yasmin, M.; Raza, M. Fundus image classification methods for the detection of glaucoma: A review. *Microsc. Res. Tech.* **2018**, *81*, 1105–1121. [CrossRef] [PubMed]

33. Mughal, B.; Muhammad, N.; Sharif, M.; Rehman, A.; Saba, T. Removal of pectoral muscle based on topographic map and shape-shifting silhouette. *BMC Cancer* **2018**, *18*, 778. [CrossRef] [PubMed]

34. Morais, M.; Calisto, F.M.; Santiago, C.; Aleluia, C.; Nascimento, J.C. Classification of Breast Cancer in Mri with Multimodal Fusion. In Proceedings of the 2023 IEEE 20th International Symposium on Biomedical Imaging (ISBI), Cartagena de Indias, Colombia, 18–21 April 2023; IEEE: Piscataway, NJ, USA, 2023; pp. 1–4.

35. Diogo, P.; Morais, M.; Calisto, F.M.; Santiago, C.; Aleluia, C.; Nascimento, J.C. Weakly-Supervised Diagnosis and Detection of Breast Cancer Using Deep Multiple Instance Learning. In Proceedings of the 2023 IEEE 20th International Symposium on Biomedical Imaging (ISBI), Cartagena de Indias, Colombia, 18–21 April 2023; IEEE: Piscataway, NJ, USA, 2023; pp. 1–4.

36. Wang, X.; Zhang, J.; Yang, S.; Xiang, J.; Luo, F.; Wang, M.; Zhang, J.; Yang, W.; Huang, J.; Han, X. A generalizable and robust deep learning algorithm for mitosis detection in multicenter breast histopathological images. *Med. Image Anal.* **2023**, *84*, 102703. [CrossRef] [PubMed]

37. Mughal, B.; Sharif, M.; Muhammad, N.; Saba, T. A novel classification scheme to decline the mortality rate among women due to breast tumor. *Microsc. Res. Tech.* **2018**, *81*, 171–180. [CrossRef]

38. Abbas, N.; Saba, T.; Mehmood, Z.; Rehman, A.; Islam, N.; Ahmed, K.T. An automated nuclei segmentation of leukocytes from microscopic digital images. *Pak. J. Pharm. Sci.* **2019**, *32*, 2123–2138.

39. Abbas, N.; Saba, T.; Rehman, A.; Mehmood, Z.; Javaid, N.; Tahir, M.; Khan, N.U.; Ahmed, K.T.; Shah, R. Plasmodium species aware based quantification of malaria parasitemia in light microscopy thin blood smear. *Microsc. Res. Tech.* **2019**, *82*, 1198–1214. [CrossRef] [PubMed]

40. Wang, Y.; Yue, W.; Li, X.; Liu, S.; Guo, L.; Xu, H.; Zhang, H.; Yang, G. Comparison study of radiomics and deep learning-based methods for thyroid nodules classification using ultrasound images. *IEEE Access* **2020**, *8*, 52010–52017. [CrossRef]

41. Qin, P.; Wu, K.; Hu, Y.; Zeng, J.; Chai, X. Diagnosis of benign and malignant thyroid nodules using combined conventional ultrasound and ultrasound elasticity imaging. *IEEE J. Biomed. Health Inform.* **2019**, *24*, 1028–1036. [CrossRef]

42. Wu, H.; Deng, Z.; Zhang, B.; Liu, Q.; Chen, J. Classifier model based on machine learning algorithms: Application to differential diagnosis of suspicious thyroid nodules via sonography. *Am. J. Roentgenol.* **2016**, *207*, 859–864. [CrossRef] [PubMed]

43. Zhang, B.; Tian, J.; Pei, S.; Chen, Y.; He, X.; Dong, Y.; Zhang, L.; Mo, X.; Huang, W.; Cong, S.; et al. Machine learning–assisted system for thyroid nodule diagnosis. *Thyroid* **2019**, *29*, 858–867. [CrossRef]

44. Sollini, M.; Cozzi, L.; Chiti, A.; Kirienko, M. Texture analysis and machine learning to characterize suspected thyroid nodules and differentiated thyroid cancer: Where do we stand? *Eur. J. Radiol.* **2018**, *99*, 1–8. [CrossRef]

45. Yang, C.Q.; Gardiner, L.; Wang, H.; Hueman, M.T.; Chen, D. Creating prognostic systems for well-differentiated thyroid cancer using machine learning. *Front. Endocrinol.* **2019**, *10*, 288. [CrossRef] [PubMed]

46. Abbad Ur Rehman, H.; Lin, C.Y.; Mushtaq, Z. Effective K-Nearest Neighbor Algorithms Performance Analysis of Thyroid Disease. *J. Chin. Inst. Eng.* **2021**, *44*, 77–87. [CrossRef]

47. Taylor, J.N.; Mochizuki, K.; Hashimoto, K.; Kumamoto, Y.; Harada, Y.; Fujita, K.; Komatsuzaki, T. High-resolution Raman microscopic detection of follicular thyroid cancer cells with unsupervised machine learning. *J. Phys. Chem. B* **2019**, *123*, 4358–4372. [CrossRef]

48. Chandio, J.A.; Mallah, G.A.; Shaikh, N.A. Decision Support System for Classification Medullary Thyroid Cancer. *IEEE Access* **2020**, *8*, 145216–145226. [CrossRef]

49. Lee, J.H.; Chai, Y.J. A deep-learning model to assist thyroid nodule diagnosis and management. *Lancet Digit. Health* **2021**, *3*, e410 [CrossRef] [PubMed]

50. Buda, M.; Wildman-Tobriner, B.; Hoang, J.K.; Thayer, D.; Tessler, F.N.; Middleton, W.D.; Mazurowski, M.A. Management of thyroid nodules seen on US images: Deep learning may match performance of radiologists. *Radiology* **2019**, *292*, 695–701. [CrossRef] [PubMed]

51. Liu, Y.; Liang, J.; Peng, S.; Wang, W.; Xiao, H. A deep-learning model to assist thyroid nodule diagnosis and management–Authors' reply. *Lancet Digit. Health* **2021**, *3*, e411–e412. [CrossRef]

52. Iesato, A.; Nucera, C. Role of regulatory non-coding RNAs in aggressive thyroid cancer: Prospective applications of neural network analysis. *Molecules* **2021**, *26*, 3022. [CrossRef]

53. Sharifi, Y.; Bakhshali, M.A.; Dehghani, T.; DanaiAshgzari, M.; Sargolzaei, M.; Eslami, S. Deep learning on ultrasound images of thyroid nodules. *Biocybern. Biomed. Eng.* **2021**, *41*, 636–655. [CrossRef]

54. Lin, Y.J.; Chao, T.K.; Khalil, M.A.; Lee, Y.C.; Hong, D.Z.; Wu, J.J.; Wang, C.W. Deep learning fast screening approach on cytological whole slides for thyroid cancer diagnosis. *Cancers* **2021**, *13*, 3891. [CrossRef]

55. Ha, E.J.; Baek, J.H. Applications of machine learning and deep learning to thyroid imaging: Where do we stand? *Ultrasonography* **2021**, *40*, 23. [CrossRef] [PubMed]

56. Wu, X.L.; Li, M.; Cui, X.W.; Xu, G. Deep multimodal learning for lymph node metastasis prediction of primary thyroid cancer. *Phys. Med. Biol.* **2022**, *67*, 035008. [CrossRef]

57. Pavithra, S.; Yamuna, G.; Arunkumar, R. Deep Learning Method for Classifying Thyroid Nodules Using Ultrasound Images. In Proceedings of the 2022 International Conference on Smart Technologies and Systems for Next Generation Computing (ICSTSN), Villupuram, India, 25–26 March 2022; IEEE: Piscataway, NJ, USA, 2022; pp. 1–6.

58. Paul, R.; Juliano, A.; Faquin, W.; Chan, A.W. An Artificial Intelligence Ultrasound Platform for Screening and Staging of Thyroid Cancer. *Int. J. Radiat. Oncol. Biol. Phys.* **2022**, *112*, e8. [CrossRef]

59. Ilyas, M.; Malik, H.; Adnan, M.; Bashir, U.; Bukhari, W.A.; Khan, M.I.A.; Ahmad, A. Deep Learning based Classification of Thyroid Cancer using Different Medical Imaging Modalities: A Systematic Review. *Vfast Trans. Softw. Eng.* **2022**, *9*, 1–17.

60. Liu, C.; Huang, Y.; Ozolek, J.A.; Hanna, M.G.; Singh, R.; Rohde, G.K. SetSVM: An approach to set classification in nuclei-based cancer detection. *IEEE J. Biomed. Health Inform.* **2018**, *23*, 351–361. [CrossRef]

61. Zhang, S.; Du, H.; Jin, Z.; Zhu, Y.; Zhang, Y.; Xie, F.; Zhang, M.; Jiao, Z.; Tian, X.; Zhang, J.; et al. Integrating Clinical Knowledge in a Thyroid Nodule Classification Model Based on. In Proceedings of the 2019 IEEE International Ultrasonics Symposium (IUS), Glasgow, UK, 6–9 October 2019; IEEE: Piscataway, NJ, USA, 2019; pp. 2334–2336.

62. Zhang, H.; Zhao, C.; Guo, L.; Li, X.; Luo, Y.; Lu, J.; Xu, H. Diagnosis of Thyroid Nodules in Ultrasound Images Using Two Combined Classification Modules. In Proceedings of the 2019 12th International Congress on Image and Signal Processing, BioMedical Engineering and Informatics (CISP-BMEI), Suzhou, China, 19–21 October 2019; IEEE: San Francisco, CA, USA, 2019; pp. 1–5.

63. Chen, D.; Zhang, J.; Li, W. Thyroid Nodule Classification Using Two Levels Attention-Based Bi-Directional LSTM with Ultrasound Reports. In Proceedings of the 2018 9th International Conference on Information Technology in Medicine and Education (ITME), Hangzhou, China, 19–21 October 2018; IEEE: San Francisco, CA, USA, 2018; pp. 309–312.

64. Ma, X.; Sun, B.; Liu, W.; Sui, D.; Chen, J.; Tian, Z. AMSeg: A Novel Adversarial Architecture based Multi-scale Fusion Framework for Thyroid Nodule Segmentation. *IEEE Access* **2023**, *11*, 72911–72924. [CrossRef]

65. Yadav, N.; Dass, R.; Virmani, J. Assessment of encoder-decoder-based segmentation models for thyroid ultrasound images. *Med. Biol. Eng. Comput.* **2023**, *61*, 2159–2195. [CrossRef]

66. Jajroudi, M.; Baniasadi, T.; Kamkar, L.; Arbabi, F.; Sanei, M.; Ahmadzade, M. Prediction of survival in thyroid cancer using data mining technique. *Technol. Cancer Res. Treat.* **2014**, *13*, 353–359. [CrossRef]

67. Sajeev, V.; Vyshnavi, A.H.; Namboori, P.K. Thyroid Cancer Prediction Using Gene Expression Profile, Pharmacogenomic Variants And Quantum Image Processing in Deep Learning Platform—A Theranostic Approach. In Proceedings of the 2020 International Conference for Emerging Technology (INCET), Belgaum, India, 5–7 June 2020; IEEE: Piscataway, NJ, USA, 2020; pp. 1–5.

68. Tarkov, M.; Chiglintsev, E. Data space dimensionality reduction in the problem of diagnosing a thyroid disease. *Bull. Novosib. Comput. Cent. Ser. Comput. Sci.* **2012**, *33*, 79–84.

69. Shankarlal, B.; Sathya, P. Performance Analysis of Thyroid Tumor Detection and Segmentation Using PCA-Based Random Classification Method. In *Innovations in Electrical and Electronics Engineering*; Springer: New York, NY, USA, 2020; pp. 833–841.

70. Soulaymani, A.; Aschawa, H. Epidemiological Study of Thyroid Carcinoma Using Principal Component Analysis. *J. Clin. Epigenetics* **2018**, *4*, 9.

71. Liu, N.; Fenster, A.; Tessier, D.; Gou, S.; Chong, J. Self-supervised learning enhanced ultrasound video thyroid nodule tracking. In *Medical Imaging 2023: Image Processing*; SPIE: Stockholm, Sweden, 2023; Volume 12464, pp. 683–687.

72. Hou, Y.; Sang, Q. Boosting Ultrasonic Image Classification via Self-Supervised Representation Learning. In Proceedings of the 2023 3rd International Conference on Computer, Control and Robotics (ICCCR), Shanghai, China, 24–26 March 2023; IEEE: Piscataway, NJ, USA, 2023; pp. 116–120.

73. Chandel, K.; Kunwar, V.; Sabitha, S.; Choudhury, T.; Mukherjee, S. A comparative study on thyroid disease detection using K-nearest neighbor and Naive Bayes classification techniques. *CSI Trans. ICT* **2016**, *4*, 313–319. [CrossRef]

74. Liu, D.Y.; Chen, H.L.; Yang, B.; Lv, X.E.; Li, L.N.; Liu, J. Design of an enhanced fuzzy k-nearest neighbor classifier based computer aided diagnostic system for thyroid disease. *J. Med. Syst.* **2012**, *36*, 3243–3254. [CrossRef]

75. Geetha, K.; Baboo, S.S. An empirical model for thyroid disease classification using evolutionary multivariate Bayseian prediction method. *Glob. J. Comput. Sci. Technol.* **2016**, *16*, 1–10.

76. Ma, J.; Luo, S.; Dighe, M.; Lim, D.J.; Kim, Y. Differential diagnosis of thyroid nodules with ultrasound elastography based on support vector machines. In Proceedings of the 2010 IEEE International Ultrasonics Symposium, San Diego, CA, USA, 11–14 October 2010; IEEE: Piscataway, NJ, USA, 2010; pp. 1372–1375.

77. Chang, C.Y.; Chen, S.J.; Tsai, M.F. Application of support-vector-machine-based method for feature selection and classification of thyroid nodules in ultrasound images. *Pattern Recognit.* **2010**, *43*, 3494–3506. [CrossRef]

78. Dogantekin, E.; Dogantekin, A.; Avci, D. An expert system based on Generalized Discriminant Analysis and Wavelet Support Vector Machine for diagnosis of thyroid diseases. *Expert Syst. Appl.* **2011**, *38*, 146–150. [CrossRef]

79. Yadav, D.C.; Pal, S. Prediction of thyroid disease using decision tree ensemble method. *Hum.-Intell. Syst. Integr.* **2020**, *2*, 89–95. [CrossRef]

80. Hao, Y.; Zuo, W.; Shi, Z.; Yue, L.; Xue, S.; He, F. Prognosis of thyroid disease using MS-apriori improved decision tree. In Proceedings of the International Conference on Knowledge Science, Engineering and Management, Changchun, China, 17–19 August 2018; Springer: New York, NY, USA, 2018; pp. 452–460.

81. Dharmarajan, K.; Balasree, K.; Arunachalam, A.; Abirmai, K. Thyroid Disease Classification Using Decision Tree and SVM. *Exec. Ed.* **2020**, *11*, 3234.

82. Yadav, D.C.; Pal, S. Decision tree ensemble techniques to predict thyroid disease. *Int. J. Recent Technol. Eng.* **2019**, *8*, 8242–8246. [CrossRef]

83. Zhao, R.N.; Zhang, B.; Yang, X.; Jiang, Y.X.; Lai, X.J.; Zhang, X.Y. Logistic regression analysis of contrast-enhanced ultrasound and conventional ultrasound characteristics of sub-centimeter thyroid nodules. *Ultrasound Med. Biol.* **2015**, *41*, 3102–3108. [CrossRef] [PubMed]

84. Yazdani-Charati, J.; Akha, O.; Khosravi, F. Factors Affecting Thyroid Cancer in Patients with Thyroid Nodules Using Logistic Regression in Interval Censored Data. *Int. J. Cancer Manag.* **2018**, *11*, e9111. [CrossRef]

85. Kate, M.D.; Kale, V. Check for updates The Role of Machine Learning in Thyroid Cancer Diagnosis. In Proceedings of the International Conference on Applications of Machine Intelligence and Data Analytics (ICAMIDA 2022), Aurangabad, India, 22–24 December 2022; Springer Nature: London, UK, 2023; Volume 105, p. 276.

86. Nobile, M.S.; Capitoli, G.; Sowirono, V.; Clerici, F.; Piga, I.; van Abeelen, K.; Magni, F.; Pagni, F.; Galimberti, S.; Cazzaniga, P.; et al. Unsupervised neural networks as a support tool for pathology diagnosis in MALDI-MSI experiments: A case study on thyroid biopsies. *Expert Syst. Appl.* **2023**, *215*, 119296. [CrossRef]

87. Manogaran, G.; Vijayakumar, V.; Varatharajan, R.; Kumar, P.M.; Sundarasekar, R.; Hsu, C.H. Machine learning based big data processing framework for cancer diagnosis using hidden Markov model and GM clustering. *Wirel. Pers. Commun.* **2018**, *102*, 2099–2116. [CrossRef]

88. Agrawal, U.; Soria, D.; Wagner, C.; Garibaldi, J.; Ellis, I.O.; Bartlett, J.M.; Cameron, D.; Rakha, E.A.; Green, A.R. Combining clustering and classification ensembles: A novel pipeline to identify breast cancer profiles. *Artif. Intell. Med.* **2019**, *97*, 27–37. [CrossRef]

89. de Souto, M.C.; Costa, I.G.; de Araujo, D.S.; Ludermir, T.B.; Schliep, A. Clustering cancer gene expression data: A comparative study. *BMC Bioinform.* **2008**, *9*, 497. [CrossRef]

90. Anas, M.; Gupta, K.; Ahmad, S. Skin cancer classification using K-means clustering. *Int. J. Tech. Res. Appl.* **2017**, *5*, 62–65.

91. Khan, A.R.; Khan, S.; Harouni, M.; Abbasi, R.; Iqbal, S.; Mehmood, Z. Brain tumor segmentation using K-means clustering and deep learning with synthetic data augmentation for classification. *Microsc. Res. Tech.* **2021**, *84*, 1389–1399. [CrossRef] [PubMed]

92. Yu, X.; Yu, G.; Wang, J. Clustering cancer gene expression data by projective clustering ensemble. *PLoS ONE* **2017**, *12*, e0171429. [CrossRef] [PubMed]

93. Chandel, K.; Kunwar, V.; Sabitha, A.S.; Bansal, A.; Choudhury, T. Analysing thyroid disease using density-based clustering technique. *Int. J. Bus. Intell. Data Min.* **2020**, *17*, 273–297. [CrossRef]

94. Katikireddy Srinivas, D.K. Performa analysis of clustering of thyroid drug data using fuzzy and m-clust. *J. Crit. Rev.* **2020**, *7*, 2128–2141.

95. Venkataramana, B.; Padmasree, L.; Rao, M.S.; Latha, D.; Ganesan, G. Comparative Study on performance of Fuzzy clustering algorithms on Liver and Thyroid Data. *J. Fuzzy Set Valued Anal.* **2018**, *2018*, 9240389. [CrossRef]

96. Mahurkar, K.K.; Gaikwad, D. Normalization using Improvised K-Means applied in diagnosing thyroid disease with ANN. In Proceedings of the 2017 International Conference on Trends in Electronics and Informatics (ICEI), Tirunelveli, India, 11–12 May 2017; IEEE: Piscataway, NJ, USA, 2017; pp. 579–583.

97. Yang, Y.; Song, Y.; Cao, B. An Information Entropy-based Method to Detect microRNA Regulatory Module. *IPSJ Trans. Bioinform.* **2019**, *12*, 1–8. [CrossRef]

98. Canton, S.P.; Dadashzadeh, E.; Yip, L.; Forsythe, R.; Handzel, R. Automatic Detection of Thyroid and Adrenal Incidentals Using Radiology Reports and Deep Learning. *J. Surg. Res.* **2021**, *266*, 192–200. [CrossRef]

99. Peng, S.; Liu, Y.; Lv, W.; Liu, L.; Zhou, Q.; Yang, H.; Ren, J.; Liu, G.; Wang, X.; Zhang, X.; et al. Deep learning-based artificial intelligence model to assist thyroid nodule diagnosis and management: A multicentre diagnostic study. *Lancet Digit. Health* **2021**, *3*, e250–e259. [CrossRef]

100. Guan, Q.; Wang, Y.; Du, J.; Qin, Y.; Lu, H.; Xiang, J.; Wang, F. Deep learning based classification of ultrasound images for thyroid nodules: A large scale of pilot study. *Ann. Transl. Med.* **2019**, *7*, 137. [CrossRef]

101. Li, L.N.; Ouyang, J.H.; Chen, H.L.; Liu, D.Y. A computer aided diagnosis system for thyroid disease using extreme learning machine. *J. Med. Syst.* **2012**, *36*, 3327–3337. [CrossRef]

102. Ma, C.; Guan, J.; Zhao, W.; Wang, C. An efficient diagnosis system for Thyroid disease based on enhanced Kernelized Extreme Learning Machine Approach. In Proceedings of the International Conference on Cognitive Computing, San Francisco, CA, USA, 2–7 July 2018; Springer: New York, NY, USA, 2018; pp. 86–101.

103. Xia, J.; Chen, H.; Li, Q.; Zhou, M.; Chen, L.; Cai, Z.; Fang, Y.; Zhou, H. Ultrasound-based differentiation of malignant and benign thyroid Nodules: An extreme learning machine approach. *Comput. Methods Programs Biomed.* **2017**, *147*, 37–49. [CrossRef] [PubMed]

104. Pavithra, R.; Parthiban, L. Optimal Deep Learning with Kernel Extreme Learning Machine Based Thyroid Disease Diagnosis and Classification Model. *J. Comput. Theor. Nanosci.* **2021**, *18*, 639–649.

105. Rao, B.N.; Reddy, D.L.S.; Bhaskar, G. Thyroid Diagnosis Using Multilayer Perceptron. In Proceedings of the International Conference on E-Business and Telecommunications, Prague, Czech Republic, 26–28 July 2019; Springer: New York, NY, USA, 2019; pp. 452–459.

106. Hosseinzadeh, M.; Ahmed, O.H.; Ghafour, M.Y.; Safara, F.; Ali, S.; Vo, B.; Chiang, H.S. A multiple multilayer perceptron neural network with an adaptive learning algorithm for thyroid disease diagnosis in the internet of medical things. *J. Supercomput.* **2020**, *77*, 1–22. [CrossRef]

107. Isa, I.; Saad, Z.; Omar, S.; Osman, M.; Ahmad, K.; Sakim, H.M. Suitable MLP network activation functions for breast cancer and thyroid disease detection. In Proceedings of the 2010 Second International Conference on Computational Intelligence, Modelling and Simulation, Bali, Indonesia, 28–30 September 2010; IEEE: Piscataway, NJ, USA, 2010; pp. 39–44.

108. Mourad, M.; Moubayed, S.; Dezube, A.; Mourad, Y.; Park, K.; Torreblanca-Zanca, A.; Torrecilla, J.S.; Cancilla, J.C.; Wang, J. Machine Learning and feature Selection Applied to SeeR Data to Reliably Assess thyroid cancer prognosis. *Sci. Rep.* **2020**, *10*, 5176. [CrossRef]

109. Erol, R.; Oğulata, S.N.; Şahin, C.; Alparslan, Z.N. A radial basis function neural network (RBFNN) approach for structural classification of thyroid diseases. *J. Med. Syst.* **2008**, *32*, 215–220. [CrossRef]

110. Ferreira, M.F.; Camacho, R.; Teixeira, L.F. Autoencoders as weight initialization of deep classification networks applied to papillary thyroid carcinoma. In Proceedings of the 2018 IEEE International Conference on Bioinformatics and Biomedicine (BIBM), Madrid, Spain, 3–6 December 2018; IEEE: Piscataway, NJ, USA, 2018; pp. 629–632.

111. Teixeira, V.; Camacho, R.; Ferreira, P.G. Learning influential genes on cancer gene expression data with stacked denoising autoencoders. In Proceedings of the 2017 IEEE International Conference on Bioinformatics and Biomedicine (BIBM), Kansas City, MO, USA, 13–16 November 2017; IEEE: Piscataway, NJ, USA, 2017; pp. 1201–1205.

112. Liu, T.; Guo, Q.; Lian, C.; Ren, X.; Liang, S.; Yu, J.; Niu, L.; Sun, W.; Shen, D. Automated detection and classification of thyroid nodules in ultrasound images using clinical-knowledge-guided convolutional neural networks. *Med. Image Anal.* **2019**, *58*, 101555. [CrossRef]

113. Ha, E.J.; Baek, J.H.; Na, D.G. Deep convolutional neural network models for the diagnosis of thyroid cancer. *Lancet Oncol.* **2019**, *20*, e130. [CrossRef]

114. Zhang, Q.; Hu, J.; Zhou, S. The Detection of Hyperthyroidism by the Modified LeNet-5 Network. *Indian J. Pharm. Sci.* **2020**, *82*, 108–114. [CrossRef]

115. Qiao, T.; Liu, S.; Cui, Z.; Yu, X.; Cai, H.; Zhang, H.; Sun, M.; Lv, Z.; Li, D. Deep learning for intelligent diagnosis in thyroid scintigraphy. *J. Int. Med. Res.* **2021**, *49*, 0300060520982842. [CrossRef]

116. Cox, J.; Rubin, S.; Adams, J.; Pereira, C.; Dighe, M.; Alessio, A. Hyperparameter selection for ResNet classification of malignancy from thyroid ultrasound images. In *Medical Imaging 2020: Computer-Aided Diagnosis. International Society for Optics and Photonics*; SPIE: New York, NY, USA, 2020; Volume 11314, p. 1131447.

117. Chi, J.; Walia, E.; Babyn, P.; Wang, J.; Groot, G.; Eramian, M. Thyroid nodule classification in ultrasound images by fine-tuning deep convolutional neural network. *J. Digit. Imaging* **2017**, *30*, 477–486. [CrossRef]

118. Tekchandani, H.; Verma, S.; Londhe, N.D.; Jain, R.R.; Tiwari, A. Severity Assessment of Cervical Lymph Nodes using Modified VGG-Net, and Squeeze and Excitation Concept. In Proceedings of the 2021 IEEE 11th Annual Computing and Communication Workshop and Conference (CCWC), Virtual, 27–30 January 2021; IEEE: Piscataway, NJ, USA, 2021; pp. 709–714.

119. Ke, L.; Deng, Y.; Xia, W.; Qiang, M.; Chen, X.; Liu, K.; Jing, B.; He, C.; Xie, C.; Guo, X.; et al. Development of a self-constrained 3D DenseNet model in automatic detection and segmentation of nasopharyngeal carcinoma using magnetic resonance images. *Oral Oncol.* **2020**, *110*, 104862. [CrossRef] [PubMed]

120. Li, X.; Zhang, S.; Zhang, Q.; Wei, X.; Pan, Y.; Zhao, J.; Xin, X.; Qin, C.; Wang, X.; Li, J.; et al. Diagnosis of thyroid cancer using deep convolutional neural network models applied to sonographic images: A retrospective, multicohort, diagnostic study. *Lancet Oncol.* **2019**, *20*, 193–201. [CrossRef] [PubMed]

121. Xie, S.; Yu, J.; Liu, T.; Chang, Q.; Niu, L.; Sun, W. Thyroid Nodule Detection in Ultrasound Images with Convolutional Neural Networks. In Proceedings of the 2019 14th IEEE Conference on Industrial Electronics and Applications (ICIEA), Xi'an, China, 19–21 June 2019; IEEE: Piscataway, NJ, USA, 2019; pp. 1442–1446.

122. Koh, J.; Lee, E.; Han, K.; Kim, E.K.; Son, E.J.; Sohn, Y.M.; Seo, M.; Kwon, M.R.; Yoon, J.H.; Lee, J.H.; et al. Diagnosis of thyroid nodules on ultrasonography by a deep convolutional neural network. *Sci. Rep.* **2020**, *10*, 15245. [CrossRef] [PubMed]

123. Liang, X.; Yu, J.; Liao, J.; Chen, Z. Convolutional Neural Network for Breast and Thyroid Nodules Diagnosis in Ultrasound Imaging. *BioMed Res. Int.* **2020**, *2020*, 1763803. [CrossRef]

124. Zhu, J.; Zhang, S.; Yu, R.; Liu, Z.; Gao, H.; Yue, B.; Liu, X.; Zheng, X.; Gao, M.; Wei, X. An efficient deep convolutional neural network model for visual localization and automatic diagnosis of thyroid nodules on ultrasound images. *Quant. Imaging Med. Surg.* **2021**, *11*, 1368. [CrossRef]

125. Zhao, C.K.; Ren, T.T.; Yin, Y.F.; Shi, H.; Wang, H.X.; Zhou, B.Y.; Wang, X.R.; Li, X.; Zhang, Y.F.; Liu, C.; et al. A comparative analysis of two machine learning-based diagnostic patterns with thyroid imaging reporting and data system for thyroid nodules: Diagnostic performance and unnecessary biopsy rate. *Thyroid* **2021**, *31*, 470–481. [CrossRef]

126. Han, M.; Ha, E.; Park, J. Computer-aided diagnostic system for thyroid nodules on ultrasonography: Diagnostic performance based on the thyroid imaging reporting and data system classification and dichotomous outcomes. *Am. J. Neuroradiol.* **2021**, *42*, 559–565. [CrossRef]

127. Liu, Z.; Zhong, S.; Liu, Q.; Xie, C.; Dai, Y.; Peng, C.; Chen, X.; Zou, R. Thyroid nodule recognition using a joint convolutional neural network with information fusion of ultrasound images and radiofrequency data. *Eur. Radiol.* **2021**, *31*, 5001–5011. [CrossRef]

128. Wei, Q.; Zeng, S.E.; Wang, L.P.; Yan, Y.J.; Wang, T.; Xu, J.W.; Zhang, M.Y.; Lv, W.Z.; Cui, X.W.; Dietrich, C.F. The value of S-Detect in improving the diagnostic performance of radiologists for the differential diagnosis of thyroid nodules. *Med. Ultrason.* **2020**, *22*, 415–423. [CrossRef]

129. Stib, M.T.; Pan, I.; Merck, D.; Middleton, W.D.; Beland, M.D. Thyroid Nodule Malignancy Risk Stratification Using a Convolutional Neural Network. *Ultrasound Q.* **2020**, *36*, 164–172. [CrossRef] [PubMed]

130. Ye, H.; Hang, J.; Chen, X.; Xu, D.; Chen, J.; Ye, X.; Zhang, D. An intelligent platform for ultrasound diagnosis of thyroid nodules. *Sci. Rep.* **2020**, *10*, 13223. [CrossRef] [PubMed]

131. Shin, I.; Kim, Y.J.; Han, K.; Lee, E.; Kim, H.J.; Shin, J.H.; Moon, H.J.; Youk, J.H.; Kim, K.G.; Kwak, J.Y. Application of machine learning to ultrasound images to differentiate follicular neoplasms of the thyroid gland. *Ultrasonography* **2020**, *39*, 257. [CrossRef] [PubMed]

132. Park, V.Y.; Han, K.; Seong, Y.K.; Park, M.H.; Kim, E.K.; Moon, H.J.; Yoon, J.H.; Kwak, J.Y. Diagnosis of thyroid nodules: Performance of a deep learning convolutional neural network model vs. radiologists. *Sci. Rep.* **2019**, *9*, 110335. [CrossRef] [PubMed]

133. Xia, S.; Yao, J.; Zhou, W.; Dong, Y.; Xu, S.; Zhou, J.; Zhan, W. A computer-aided diagnosing system in the evaluation of thyroid nodules–experience in a specialized thyroid center. *World J. Surg. Oncol.* **2019**, *17*, 210. [CrossRef]

134. Chen, D.; Shi, C.; Wang, M.; Pan, Q. Thyroid Nodule Classification Using Hierarchical Recurrent Neural Network with Multiple Ultrasound Reports. In Proceedings of the International Conference on Neural Information Processing, Guangzhou, China, 14–18 November 2017; Springer: New York, NY, USA, 2017; pp. 765–773.

135. Smolensky, P.; McClelland, J.L. *Information Processing in Dynamical Systems: Foundations of Harmony Theory*; MIT Press: Cambridge, MA, USA, 1986.

136. Vairale, V.S.; Shukla, S. Physical Fitness Recommender Framework for Thyroid Patients using Restricted Boltzmann Machines. *Int. J. Intell. Eng. Syst.* **2020**, *13*, 247–256. [CrossRef]

137. Yang, W.; Zhao, J.; Qiang, Y.; Yang, X.; Dong, Y.; Du, Q.; Shi, G.; Zia, M.B. DScGANS: Integrate domain knowledge in training dual-path semi-supervised conditional generative adversarial networks and s3vm for ultrasonography thyroid nodules classification. In Proceedings of the International Conference on Medical Image Computing and Computer-Assisted Intervention, Shenzhen, China, 13–17 October 2019 Springer: New York, NY, USA, 2019; pp. 558–566.

138. Yoo, T.K.; Choi, J.Y.; Kim, H.K. A generative adversarial network approach to predicting postoperative appearance after orbital decompression surgery for thyroid eye disease. *Comput. Biol. Med.* **2020**, *118*, 103628. [CrossRef]

139. Liu, Y.I.; Kamaya, A.; Desser, T.S.; Rubin, D.L. A bayesian network for differentiating benign from malignant thyroid nodules using sonographic and demographic features. *Am. J. Roentgenol.* **2011**, *196*, W598–W605. [CrossRef]

140. Liu, Y.I.; Kamaya, A.; Desser, T.S.; Rubin, D.L. A controlled vocabulary to represent sonographic features of the thyroid and its application in a Bayesian network to predict thyroid nodule malignancy. *Summit Transl. Bioinform.* **2009**, *2009*, 68.

141. Ashraf, M.; Chetty, G.; Tran, D.; Sharma, D. Hybrid approach for diagnosing thyroid, hepatitis, and breast cancer based on correlation based feature selection and Naïve bayes. In Proceedings of the International Conference on Neural Information Processing, Doha, Qatar, 12–15 November 2012; Springer: New York, NY, USA, 2012; pp. 272–280.

142. Chandran, V.; Sumithra, M.; Karthick, A.; George, T.; Deivakani, M.; Elakkiya, B.; Subramaniam, U.; Manoharan, S. Diagnosis of Cervical Cancer based on Ensemble Deep Learning Network using Colposcopy Images. *BioMed Res. Int.* **2021**, *2021*, 5584004. [CrossRef]

143. Awujoola Olalekan, J.; Ogwueleka, F.; Odion, P. Effective and Accurate Bootstrap Aggregating (Bagging) Ensemble Algorithm Model for Prediction and Classification of Hypothyroid Disease. *Int. J. Comput. Appl.* **2020**, *975*, 8887.

144. Chen, D.; Hu, J.; Zhu, M.; Tang, N.; Yang, Y.; Feng, Y. Diagnosis of thyroid nodules for ultrasonographic characteristics indicative of malignancy using random forest. *BioData Min.* **2020**, *13*, 14. [CrossRef] [PubMed]

145. Himeur, Y.; Ghanem, K.; Alsalemi, A.; Bensaali, F.; Amira, A. Artificial intelligence based anomaly detection of energy consumption in buildings: A review, current trends and new perspectives. *Appl. Energy* **2021**, *287*, 116601. [CrossRef]

146. Pan, Q.; Zhang, Y.; Zuo, M.; Xiang, L.; Chen, D. Improved ensemble classification method of thyroid disease based on random forest. In Proceedings of the 2016 8th International Conference on Information Technology in Medicine and Education (ITME), Fuzhou, China, 23–25 December 2016; IEEE: Piscataway, NJ, USA, 2016; pp. 567–571.

147. Chen, T.; Guestrin, C. Xgboost: A scalable tree boosting system. In Proceedings of the 22nd ACM Sigkdd International Conference on Knowledge Discovery and Data Mining, San Francisco, CA, USA, 13–17 August 2016; pp. 785–794.

148. Lim, S.; Chi, S. Xgboost application on bridge management systems for proactive damage estimation. *Adv. Eng. Inform.* **2019**, *41*, 100922. [CrossRef]

149. Ji, C.; Zou, X.; Hu, Y.; Liu, S.; Lyu, L.; Zheng, X. XG-SF: An XGBoost classifier based on shapelet features for time series classification. *Procedia Comput. Sci.* **2019**, *147*, 24–28. [CrossRef]

150. Guo, J.; Yang, L.; Bie, R.; Yu, J.; Gao, Y.; Shen, Y.; Kos, A. An XGBoost-based physical fitness evaluation model using advanced feature selection and Bayesian hyper-parameter optimization for wearable running monitoring. *Comput. Netw.* **2019**, *151*, 166–180. [CrossRef]

151. Xu, Y.; Yang, X.; Huang, H.; Peng, C.; Ge, Y.; Wu, H.; Wang, J.; Xiong, G.; Yi, Y. Extreme gradient boosting model has a better performance in predicting the risk of 90-day readmissions in patients with ischaemic stroke. *J. Stroke Cerebrovasc. Dis.* **2019**, *28*, 104441. [CrossRef]

152. Chen, Y.; Li, D.; Zhang, X.; Jin, J.; Shen, Y. Computer aided diagnosis of thyroid nodules based on the devised small-datasets multi-view ensemble learning. *Med. Image Anal.* **2020**, *67*, 101819. [CrossRef]

153. Thomas, J.; Haertling, T. AIBx, artificial intelligence model to risk stratify thyroid nodules. *Thyroid* **2020**, *30*, 878–884. [CrossRef]

154. Kezlarian, B.; Lin, O. Artificial Intelligence in Thyroid Fine Needle Aspiration Biopsies. *Acta Cytol.* **2020**, *65*, 324–329. [CrossRef]

155. Sanyal, P.; Mukherjee, T.; Barui, S.; Das, A.; Gangopadhyay, P. Artificial intelligence in cytopathology: A neural network to identify papillary carcinoma on thyroid fine-needle aspiration cytology smears. *J. Pathol. Inform.* **2018**, *9*, 43. [CrossRef] [PubMed]

156. Yoon, J.; Lee, E.; Koo, J.S.; Yoon, J.H.; Nam, K.H.; Lee, J.; Jo, Y.S.; Moon, H.J.; Park, V.Y.; Kwak, J.Y. Artificial intelligence to predict the BRAFV600E mutation in patients with thyroid cancer. *PLoS ONE* **2020**, *15*, e0242806. [CrossRef]

157. Nguyen, D.T.; Kang, J.K.; Pham, T.D.; Batchuluun, G.; Park, K.R. Ultrasound image-based diagnosis of malignant thyroid nodule using artificial intelligence. *Sensors* **2020**, *20*, 1822. [CrossRef] [PubMed]

158. Liu, T.; Xie, S.; Yu, J.; Niu, L.; Sun, W. Classification of thyroid nodules in ultrasound images using deep model based transfer learning and hybrid features. In Proceedings of the 2017 IEEE International Conference on Acoustics, Speech and Signal Processing (ICASSP), New Orleans, LA, USA, 5–9 March 2017; IEEE: Piscataway, NJ, USA, 2017; pp. 919–923.

159. Abdolali, F.; Kapur, J.; Jaremko, J.L.; Noga, M.; Hareendranathan, A.R.; Punithakumar, K. Automated thyroid nodule detection from ultrasound imaging using deep convolutional neural networks. *Comput. Biol. Med.* **2020**, *122*, 103871. [CrossRef] [PubMed]

160. Li, X.; Wang, S.; Wei, X.; Zhu, J.; Yu, R.; Zhao, M.; Yu, M.; Liu, Z.; Liu, S. Fully convolutional networks for ultrasound image segmentation of thyroid nodules. In Proceedings of the 2018 IEEE 20th International Conference on High Performance Computing and Communications; IEEE 16th International Conference on Smart City; IEEE 4th International Conference on Data Science and Systems (HPCC/SmartCity/DSS), Exeter, UK, 28–30 June 2018; IEEE: Piscataway, NJ, USA, 2018; pp. 886–890.

161. Kim, E.; Corte-Real, M.; Baloch, Z. A deep semantic mobile application for thyroid cytopathology. In *Medical Imaging 2016: PACS and Imaging Informatics: Next Generation and Innovations. International Society for Optics and Photonics*; SPIE: Bellingham, WA, USA, 2016; Volume 9789, p. 97890A.

162. Ma, L.; Ma, C.; Liu, Y.; Wang, X. Thyroid diagnosis from SPECT images using convolutional neural network with optimization. *Comput. Intell. Neurosci.* **2019**, *2019*, 6212759. [CrossRef]

163. Chai, Y.; Song, J.; Shear, M. Artificial Intelligence for thyroid nodule ultrasound image analysis. *Ann. Thyroid.* **2020**, *5*, 8. [CrossRef]

164. Song, J.; Chai, Y.J.; Masuoka, H.; Park, S.W.; Kim, S.J.; Choi, J.Y.; Kong, H.J.; Lee, K.E.; Lee, J.; Kwak, N.; et al. Ultrasound image analysis using deep learning algorithm for the diagnosis of thyroid nodules. *Medicine* **2019**, *98*, e15133. [CrossRef]

165. Barczyński, M.; Stopa-Barczyńska, M.; Wojtczak, B.; Czarniecka, A.; Konturek, A. Clinical validation of S-DetectTM mode in semi-automated ultrasound classification of thyroid lesions in surgical office. *Gland. Surg.* **2020**, *9*, S77. [CrossRef]

166. Choi, Y.J.; Baek, J.H.; Park, H.S.; Shim, W.H.; Kim, T.Y.; Shong, Y.K.; Lee, J.H. A computer-aided diagnosis system using artificial intelligence for the diagnosis and characterization of thyroid nodules on ultrasound: Initial clinical assessment. *Thyroid* **2017**, *27*, 546–552. [CrossRef]

167. Fragopoulos, C.; Pouliakis, A.; Meristoudis, C.; Mastorakis, E.; Margari, N.; Chroniaris, N.; Koufopoulos, N.; Delides, A.G.; Machairas, N.; Ntomi, V.; et al. Radial Basis Function Artificial Neural Network for the Investigation of Thyroid Cytological Lesions. *J. Thyroid. Res.* **2020**, *2020*, 5464787. [CrossRef]

168. Savala, R.; Dey, P.; Gupta, N. Artificial neural network model to distinguish follicular adenoma from follicular carcinoma on fine needle aspiration of thyroid. *Diagn. Cytopathol.* **2018**, *46*, 244–249. [CrossRef] [PubMed]

169. Li, L.R.; Du, B.; Liu, H.Q.; Chen, C. Artificial Intelligence for Personalized Medicine in Thyroid Cancer: Current Status and Future Perspectives. *Front. Oncol.* **2021**, *10*, 3360. [CrossRef] [PubMed]

170. Zhao, Y.; Zhao, L.; Mao, T.; Zhong, L. Assessment of risk based on variant pathways and establishment of an artificial neural network model of thyroid cancer. *BMC Med. Genet.* **2019**, *20*, 92. [CrossRef]

171. Wildman-Tobriner, B.; Buda, M.; Hoang, J.K.; Middleton, W.D.; Thayer, D.; Short, R.G.; Tessler, F.N.; Mazurowski, M.A. Using artificial intelligence to revise ACR TI-RADS risk stratification of thyroid nodules: Diagnostic accuracy and utility. *Radiology* **2019**, *292*, 112–119. [CrossRef] [PubMed]

172. Wang, L.; Yang, S.; Yang, S.; Zhao, C.; Tian, G.; Gao, Y.; Chen, Y.; Lu, Y. Automatic thyroid nodule recognition and diagnosis in ultrasound imaging with the YOLOv2 neural network. *World J. Surg. Oncol.* **2019**, *17*, 12. [CrossRef]

173. Ozolek, J.A.; Tosun, A.B.; Wang, W.; Chen, C.; Kolouri, S.; Basu, S.; Huang, H.; Rohde, G.K. Accurate diagnosis of thyroid follicular lesions from nuclear morphology using supervised learning. *Med. Image Anal.* **2014**, *18*, 772–780. [CrossRef]

174. Wang, W.; Ozolek, J.A.; Rohde, G.K. Detection and classification of thyroid follicular lesions based on nuclear structure from histopathology images. *Cytom. Part A J. Int. Soc. Adv. Cytom.* **2010**, *77*, 485–494. [CrossRef]

175. Zhu, Y.; Sang, Q.; Jia, S.; Wang, Y.; Deyer, T. Deep neural networks could differentiate Bethesda class III versus class IV/V/VI. *Ann. Transl. Med.* **2019**, *7*, 231. [CrossRef]

176. Bhalla, S.; Kaur, H.; Kaur, R.; Sharma, S.; Raghava, G.P. Expression based biomarkers and models to classify early and late-stage samples of Papillary Thyroid Carcinoma. *PLoS ONE* **2020**, *15*, e0231629. [CrossRef]

177. Dolezal, J.M.; Trzcinska, A.; Liao, C.Y.; Kochanny, S.; Blair, E.; Agrawal, N.; Keutgen, X.M.; Angelos, P.; Cipriani, N.A.; Pearson, A.T. Deep learning prediction of BRAF-RAS gene expression signature identifies noninvasive follicular thyroid neoplasms with papillary-like nuclear features. *Mod. Pathol.* **2020**, *34*, 862–874. [CrossRef]

178. Daniels, K.; Gummadi, S.; Zhu, Z.; Wang, S.; Patel, J.; Swendseid, B.; Lyshchik, A.; Curry, J.; Cottrill, E.; Eisenbrey, J. Machine learning by ultrasonography for genetic risk stratification of thyroid nodules. *JAMA Otolaryngol.–Head Neck Surg.* **2020**, *146*, 36–41. [CrossRef]

179. Teumer, A.; Chaker, L.; Groeneweg, S.; Li, Y.; Di Munno, C.; Barbieri, C.; Schultheiss, U.T.; Traglia, M.; Ahluwalia, T.S.; Akiyama, M.; et al. Genome-wide analyses identify a role for SLC17A4 and AADAT in thyroid hormone regulation. *Nat. Commun.* **2018**, *9*, 4455. [CrossRef] [PubMed]

180. The ThyroidOmics Consortium. Available online: https://transfer.sysepi.medizin.uni-greifswald.de/thyroidomics/ (accessed on 1 March 2021).

181. Thyroid Disease Data Set. Available online: https://archive.ics.uci.edu/ml/datasets/thyroid+disease (accessed on 1 March 2021).

182. Knowledge Extraction Based on Evolutionary Learning. Available online: https://sci2s.ugr.es/keel/dataset.php?cod=67 (accessed on 1 March 2021).

183. Gene Expression Omnibus. Available online: https://www.ncbi.nlm.nih.gov/geo/ (accessed on 1 March 2021).

184. The Digital Database of Thyroid Ultrasound Images. Available online: http://cimalab.intec.co/?lang=en&mod=project&id=31 (accessed on 1 March 2021).

185. The National Cancer Registration and Analysis Service. Available online: http://www.ncin.org.uk/about_ncin/ (accessed on 1 March 2021).

186. The Prostate, Lung, Colorectal and Ovarian (PLCO) Cancer Screening Trial. Available online: https://prevention.cancer.gov/major-programs/prostate-lung-colorectal-and-ovarian-cancer-screening-trial (accessed on 1 March 2021).

187. Ouyang, F.S.; Guo, B.L.; Ouyang, L.Z.; Liu, Z.W.; Lin, S.J.; Meng, W.; Huang, X.Y.; Chen, H.X.; Qiu-Gen, H.; Yang, S.M. Comparison between linear and nonlinear machine-learning algorithms for the classification of thyroid nodules. *Eur. J. Radiol.* **2019**, *113*, 251–257. [CrossRef]

188. Moon, J.H.; Steinhubl, S.R. Digital medicine in thyroidology: A new era of managing thyroid disease. *Endocrinol. Metab.* **2019**, *34*, 124–131. [CrossRef]

189. Sun, C.; Zhang, Y.; Chang, Q.; Liu, T.; Zhang, S.; Wang, X.; Guo, Q.; Yao, J.; Sun, W.; Niu, L. Evaluation of a deep learning-based computer-aided diagnosis system for distinguishing benign from malignant thyroid nodules in ultrasound images. *Med. Phys.* **2020**, *47*, 3952–3960. [CrossRef]

190. Wang, Y.; Wei, K.; Wan, P. A method of ultrasonic image recognition for thyroid papillary carcinoma based on deep convolution neural network. *NeuroQuantology* **2018**, *16*, 757–768. [CrossRef]

191. Xu, L.; Gao, J.; Wang, Q.; Yin, J.; Yu, P.; Bai, B.; Pei, R.; Chen, D.; Yang, G.; Wang, S.; et al. Computer-aided diagnosis systems in diagnosing malignant thyroid nodules on ultrasonography: A systematic review and meta-analysis. *Eur. Thyroid. J.* **2020**, *9*, 186–193. [CrossRef] [PubMed]

192. Li, Z.; Yang, K.; Zhang, L.; Wei, C.; Yang, P.; Xu, W. Classification of Thyroid Nodules with Stacked Denoising Sparse Autoencoder. *Int. J. Endocrinol.* **2020**, *2020*, 9015713. [CrossRef]

193. Ko, S.Y.; Lee, J.H.; Yoon, J.H.; Na, H.; Hong, E.; Han, K.; Jung, I.; Kim, E.K.; Moon, H.J.; Park, V.Y.; et al. Deep convolutional neural network for the diagnosis of thyroid nodules on ultrasound. *Head Neck* **2019**, *41*, 885–891. [CrossRef]

194. Lee, C.; Kim, Y.; Kim, Y.S.; Jang, J. Automatic disease annotation from radiology reports using artificial intelligence implemented by a recurrent neural network. *Am. J. Roentgenol.* **2019**, *212*, 734–740. [CrossRef]

195. Sharifi, A.; Alizadeh, K. Comparison of the Particle Swarm Optimization with the Genetic Algorithms as a Training for Multilayer Perceptron Technique to Diagnose Thyroid Functional Disease. *Shiraz E-Med. J.* **2021**, *22*, 100351. [CrossRef]

196. Vairale, V.S.; Shukla, S. Recommendation of Food Items for Thyroid Patients Using Content-Based KNN Method. In *Data Science and Security*; Springer: New York, NY, USA, 2021; pp. 71–77.

197. Shen, Y.; Lai, Y.; Xu, D.; Xu, L.; Song, L.; Zhou, J.; Song, C.; Wang, J. Diagnosis of thyroid neoplasm using support vector machine algorithms based on platelet RNA-seq. *Endocrine* **2020**, *72*, 758–783. [CrossRef] [PubMed]

198. Wu, Y.; Rao, K.; Liu, J.; Han, C.; Gong, L.; Chong, Y.; Liu, Z.; Xu, X. Machine Learning Algorithms for the Prediction of Central Lymph Node Metastasis in Patients with Papillary Thyroid Cancer. *Front. Endocrinol.* **2020**, *11*, 816. [CrossRef]

199. McDow, A.D.; Roman, B.R.; Saucke, M.C.; Jensen, C.B.; Zaborek, N.; Jennings, J.L.; Davies, L.; Brito, J.P.; Pitt, S.C. Factors associated with physicians' recommendations for managing low-risk papillary thyroid cancer. *Am. J. Surg.* **2020**, *222*, 111–118. [CrossRef] [PubMed]

200. Li, D.; Yang, D.; Zhang, J. ARB: Knowledge Discovery and Disease Diagnosis on Thyroid Disease Diagnosis integrating Association Rule with Bagging Algorithm. *Eng. Lett.* **2020**, *28*, 390–399.

201. Gao, L.; Ye, M.; Lu, X.; Huang, D. Hybrid method based on information gain and support vector machine for gene selection in cancer classification. *Genom. Proteom. Bioinform.* **2017**, *15*, 389–395. [CrossRef] [PubMed]

202. Fahrudin, T.M.; Syarif, I.; Barakbah, A.R. Data mining approach for breast cancer patient recovery. *EMITTER Int. J. Eng. Technol.* **2017**, *5*, 36–71. [CrossRef]

203. Hamsagayathri, P.; Sampath, P. Performance analysis of breast cancer classification using decision tree classifiers. *Int. J. Curr. Pharm. Res.* **2017**, *9*, 19–25. [CrossRef]

204. Chinnaswamy, A.; Srinivasan, R. Hybrid information gain based fuzzy roughset feature selection in cancer microarray data. In Proceedings of the 2017 Innovations in Power and Advanced Computing Technologies (i-PACT), Vellore, India, 21–22 April 2017; IEEE: San Francisco, CA, USA, 2017; pp. 1–6.

205. Mishra, S.; Mallick, P.K.; Tripathy, H.K.; Bhoi, A.K.; González-Briones, A. Performance Evaluation of a Proposed Machine Learning Model for Chronic Disease Datasets Using an Integrated Attribute Evaluator and an Improved Decision Tree Classifier. *Appl. Sci.* **2020**, *10*, 8137. [CrossRef]

206. Ashraf, M.; Chetty, G.; Tran, D. Feature selection techniques on thyroid, hepatitis, and breast cancer datasets. *Int. J. Data Min. Intell. Inf. Technol. Appl.* **2013**, *3*, 1.

207. Al-Batah, M.; Zaqaibeh, B.; Alomari, S.A.; Alzboon, M.S. Gene Microarray Cancer Classification using Correlation Based Feature Selection Algorithm and Rules Classifiers. *Int. J. Online Biomed. Eng.* **2019**, *15*, 62–73. [CrossRef]

208. Jain, I.; Jain, V.K.; Jain, R. Correlation feature selection based improved-binary particle swarm optimization for gene selection and cancer classification. *Appl. Soft Comput.* **2018**, *62*, 203–215. [CrossRef]

209. Rustam, Z.; Maghfirah, N. Correlated based SVM-RFE as feature selection for cancer classification using microarray databases. In Proceedings of the AIP Conference Proceedings, 3rd International Symposium on Current Progress in Mathematics and Sciences 2017, ISCPMS 2017, Bali, Indonesia, 26–27 July 2017; AIP Publishing LLC: Melville, NY, USA, 2018; Volume 2023, p. 020235.

210. Cui, L.; Ge, L.; Gan, H.; Liu, X.; Zhang, Y. Ovarian Cancer Identification Based on Feature Weighting for High-throughput Mass Spectrometry Data. *J. Syst. Biol.* **2018**, *1*, 1.

211. Onan, A. A fuzzy-rough nearest neighbor classifier combined with consistency-based subset evaluation and instance selection for automated diagnosis of breast cancer. *Expert Syst. Appl.* **2015**, *42*, 6844–6852. [CrossRef]

212. O'Dea, D.; Bongiovanni, M.; Sykiotis, G.P.; Ziros, P.G.; Meade, A.D.; Lyng, F.M.; Malkin, A. Raman spectroscopy for the preoperative diagnosis of thyroid cancer and its subtypes: An in vitro proof-of-concept study. *Cytopathology* **2019**, *30*, 51–60. [CrossRef]

213. Selaru, F.M.; Yin, J.; Olaru, A.; Mori, Y.; Xu, Y.; Epstein, S.H.; Sato, F.; Deacu, E.; Wang, S.; Sterian, A.; et al. An unsupervised approach to identify molecular phenotypic components influencing breast cancer features. *Cancer Res.* **2004**, *64*, 1584–1588. [CrossRef]

214. Sudarshan, V.K.; Mookiah, M.R.K.; Acharya, U.R.; Chandran, V.; Molinari, F.; Fujita, H.; Ng, K.H. Application of wavelet techniques for cancer diagnosis using ultrasound images: A review. *Comput. Biol. Med.* **2016**, *69*, 97–111. [CrossRef] [PubMed]

215. Haji, S.O.; Yousif, R.Z. A Novel Run-length based wavelet features for Screening Thyroid Nodule Malignancy. *Braz. Arch. Biol. Technol.* **2019**, *62*, e19170821. [CrossRef]

216. Yu, B.; Wang, Z.; Zhu, R.; Feng, X.; Qi, M.; Li, J.; Zhao, R.; Huang, L.; Xin, R.; Li, F.; et al. The transverse ultrasonogram of thyroid papillary carcinoma has a better prediction accuracy than the longitudinal one. *IEEE Access* **2019**, *7*, 100763–100770. [CrossRef]

217. Nguyen, D.T.; Pham, T.D.; Batchuluun, G.; Yoon, H.S.; Park, K.R. Artificial intelligence-based thyroid nodule classification using information from spatial and frequency domains. *J. Clin. Med.* **2019**, *8*, 1976. [CrossRef]

218. Poudel, P.; Illanes, A.; Arens, C.; Hansen, C.; Friebe, M. Active contours extension and similarity indicators for improved 3D segmentation of thyroid ultrasound images. In Proceedings of the Medical Imaging 2017: Imaging Informatics for Healthcare, Research, and Applications. International Society for Optics and Photonics, Orlando, FL, USA, 11–16 February 2017; Volume 10138, p. 1013803.

219. Poudel, P.; Hansen, C.; Sprung, J.; Friebe, M. 3D segmentation of thyroid ultrasound images using active contours. *Curr. Dir. Biomed. Eng.* **2016**, *2*, 467–470. [CrossRef]

220. Nugroho, H.A.; Nugroho, A.; Choridah, L. Thyroid nodule segmentation using active contour bilateral filtering on ultrasound images. In Proceedings of the 2015 International Conference on Quality in Research (QiR), Lombok, Indonesia, 10–13 August 2015; IEEE: Washington, DC, USA, 2015; pp. 43–46.

221. Xie, J.; Guo, L.; Zhao, C.; Li, X.; Luo, Y.; Jianwei, L. A Hybrid Deep Learning and Handcrafted Features based Approach for Thyroid Nodule Classification in Ultrasound Images. In *Journal of Physics: Conference Series, Proceedings of the 2020 3rd International Conference on Computer Information Science and Artificial Intelligence (CISAI), Inner Mongolia, China, 25–27 September 2020*; IOP Publishing: Bristol, UK, 2020; Volume 1693, p. 012160.

222. Mei, X.; Dong, X.; Deyer, T.; Zeng, J.; Trafalis, T.; Fang, Y. Thyroid nodule benignty prediction by deep feature extraction. In Proceedings of the 2017 IEEE 17th International Conference on Bioinformatics and Bioengineering (BIBE), Washington, DC, USA, 23–25 October 2017; IEEE: Washington, DC, USA, 2017; pp. 241–245.

223. Song, G.; Xue, F.; Zhang, C. A model using texture features to differentiate the nature of thyroid nodules on sonography. *J. Ultrasound Med.* **2015**, *34*, 1753–1760. [CrossRef] [PubMed]

224. Dinčić, M.; Todorović, J.; Ostojić, J.N.; Kovačević, S.; Dunđerović, D.; Lopičić, S.; Spasić, S.; Radojević-Škodrić, S.; Stanisavljević, D.; Ilić, A.Ž. The fractal and GLCM textural parameters of chromatin may be potential biomarkers of papillary thyroid carcinoma in Hashimoto's thyroiditis specimens. *Microsc. Microanal.* **2020**, *26*, 717–730. [CrossRef]

225. Kalaimani, I. Analysis for the Prediction of Thyroid Disease by Using ICA and Optimal Kernel SVM Approach. *Int. J. Emerg. Technol. Innov. Eng.* **2019**, *5*, 39–55.

226. Ahmad, W.; Huang, L.; Ahmad, A.; Shah, F.; Iqbal, A.; Saeed, A. Thyroid diseases forecasting using a hybrid decision support system based on ANFIS, k-NN and information gain method. *J. Appl. Environ. Biol. Sci.* **2017**, *7*, 78–85.

227. Zulfanahri; Nugroho, H.A.; Nugroho, A.; Frannita, E.L.; Ardiyanto, I. Classification of thyroid ultrasound images based on shape features analysis. In Proceedings of the 2017 10th Biomedical Engineering International Conference (BMEiCON), Hokkaido, Japan, 31 August–2 September 2017; IEEE: Washington, DC, USA, 2017; pp. 1–5.

228. Song, H.; Dong, C.; Zhang, X.; Wu, W.; Chen, C.; Ma, B.; Chen, F.; Chen, C.; Lv, X. Rapid identification of papillary thyroid carcinoma and papillary microcarcinoma based on serum Raman spectroscopy combined with machine learning models. *Photodiagn. Photodyn. Ther.* **2022**, *37*, 102647. [CrossRef]

229. Acharya, U.R.; Faust, O.; Sree, S.V.; Molinari, F.; Suri, J.S. ThyroScreen system: High resolution ultrasound thyroid image characterization into benign and malignant classes using novel combination of texture and discrete wavelet transform. *Comput. Methods Programs Biomed.* **2012**, *107*, 233–241. [CrossRef]

230. Nugroho, H.A.; Zulfanahri; Frannita, E.L.; Ardiyanto, I.; Choridah, L. Computer aided diagnosis for thyroid cancer system based on internal and external characteristics. *J. King Saud Univ.-Comput. Inf. Sci.* **2021**, *33*, 329–339.

231. Liu, C.; Chen, S.; Yang, Y.; Shao, D.; Peng, W.; Wang, Y.; Chen, Y.; Wang, Y. The value of the computer-aided diagnosis system for thyroid lesions based on computed tomography images. *Quant. Imaging Med. Surg.* **2019**, *9*, 642. [CrossRef]

232. Erfurt, J.; Helmrich, C.R.; Bosse, S.; Schwarz, H.; Marpe, D.; Wiegand, T. A study of the perceptually weighted peak signal-to-noise ratio (WPSNR) for image compression. In Proceedings of the 2019 IEEE International Conference on Image Processing (ICIP), Taipei, Taiwan, 22–29 September 2019; IEEE: Washington, DC, USA, 2019; pp. 2339–2343.

233. Chandler, D.M.; Hemami, S.S. VSNR: A wavelet-based visual signal-to-noise ratio for natural images. *IEEE Trans. Image Process.* **2007**, *16*, 2284–2298. [CrossRef]

234. Zhou, W.; Wang, Z.; Xie, W. Weighted signal-to-noise ratio robust design for a new double sampling npx chart. *Comput. Ind. Eng.* **2020**, *139*, 106124. [CrossRef]

235. Lasseck, M. Audio-based Bird Species Identification with Deep Convolutional Neural Networks. In Proceedings of the CLEF (Working Notes), Avignon, France, 10–14 September 2018.

236. Agarwal, A.; Zaitsev, I.; Joachims, T. Counterfactual learning-to-rank for additive metrics and deep models. *arXiv* **2018**, arXiv:1805.00065.

237. Murphy, P.M. UCI Repository of Machine Learning Databases. 1994. Available online: https://archive.ics.uci.edu/ (accessed on 1 March 2021).

238. Bai, Z.; Chang, L.; Yu, R.; Li, X.; Wei, X.; Yu, M.; Liu, Z.; Gao, J.; Zhu, J.; Zhang, Y.; et al. Thyroid nodules risk stratification through deep learning based on ultrasound images. *Med. Phys.* **2020**, *47*, 6355–6365. [CrossRef] [PubMed]

239. Colakoglu, B.; Alis, D.; Yergin, M. Diagnostic value of machine learning-based quantitative texture analysis in differentiating benign and malignant thyroid nodules. *J. Oncol.* **2019**, *2019*, 6328329. [CrossRef] [PubMed]

240. Park, V.Y.; Lee, E.; Lee, H.S.; Kim, H.J.; Yoon, J.; Son, J.; Song, K.; Moon, H.J.; Yoon, J.H.; Kim, G.R.; et al. Combining radiomics with ultrasound-based risk stratification systems for thyroid nodules: An approach for improving performance. *Eur. Radiol.* **2021**, *31*, 2405–2413. [CrossRef]

241. Duc, N.T.; Lee, Y.M.; Park, J.H.; Lee, B. An ensemble deep learning for automatic prediction of papillary thyroid carcinoma using fine needle aspiration cytology. *Expert Syst. Appl.* **2022**, *188*, 115927. [CrossRef]

242. Vadhiraj, V.V.; Simpkin, A.; O'Connell, J.; Singh Ospina, N.; Maraka, S.; O'Keeffe, D.T. Ultrasound image classification of thyroid nodules using machine learning techniques. *Medicina* **2021**, *57*, 527. [CrossRef]

243. Gild, M.L.; Chan, M.; Gajera, J.; Lurie, B.; Gandomkar, Z.; Clifton-Bligh, R.J. Risk stratification of indeterminate thyroid nodules using ultrasound and machine learning algorithms. *Clin. Endocrinol.* **2022**, *96*, 646–652. [CrossRef]

244. Ma, J.; Wu, F.; Zhu, J.; Xu, D.; Kong, D. A pre-trained convolutional neural network based method for thyroid nodule diagnosis. *Ultrasonics* **2017**, *73*, 221–230. [CrossRef]

245. Zhu, Y.; Fu, Z.; Fei, J. An image augmentation method using convolutional network for thyroid nodule classification by transfer learning. In Proceedings of the 2017 3rd IEEE international conference on computer and communications (ICCC), Chengdu, China, 13–16 December 2017; IEEE: Washington, DC, USA, 2017; pp. 1819–1823.

246. Gao, L.; Liu, R.; Jiang, Y.; Song, W.; Wang, Y.; Liu, J.; Wang, J.; Wu, D.; Li, S.; Hao, A.; et al. Computer-aided system for diagnosing thyroid nodules on ultrasound: A comparison with radiologist-based clinical assessments. *Head Neck* **2018**, *40*, 778–783. [CrossRef]

247. Zuo, D.; Han, L.; Chen, K.; Li, C.; Hua, Z.; Lin, J. Extraction of calcification in ultrasonic images based on convolution neural network. *Sheng Xue Gong Cheng Xue Zhi/J. Biomed. Eng./Shengwu Yixue Gongchengxue Zazhi* **2018**, *35*, 679–687.

248. Kim, Y.J.; Choi, Y.; Hur, S.J.; Park, K.S.; Kim, H.J.; Seo, M.; Lee, M.K.; Jung, S.L.; Jung, C.K. Deep convolutional neural network for classification of thyroid nodules on ultrasound: Comparison of the diagnostic performance with that of radiologists. *Eur. J. Radiol.* **2022**, *152*, 110335. [CrossRef]

249. Lee, J.H.; Ha, E.J.; Kim, J.H. Application of deep learning to the diagnosis of cervical lymph node metastasis from thyroid cancer with CT. *Eur. Radiol.* **2019**, *29*, 5452–5457. [CrossRef] [PubMed]

250. Tsou, P.; Wu, C.J. Mapping driver mutations to histopathological subtypes in papillary thyroid carcinoma: Applying a deep convolutional neural network. *J. Clin. Med.* **2019**, *8*, 1675. [CrossRef] [PubMed]

251. Lu, Y.; Yang, Y.; Chen, W. Application of deep learning in the prediction of benign and malignant thyroid nodules on ultrasound images. *IEEE Access* **2020**, *8*, 221468–221480. [CrossRef]

252. Kwon, S.W.; Choi, I.J.; Kang, J.Y.; Jang, W.I.; Lee, G.H.; Lee, M.C. Ultrasonographic thyroid nodule classification using a deep convolutional neural network with surgical pathology. *J. Digit. Imaging* **2020**, *33*, 1202–1208. [CrossRef]

253. Chan, W.K.; Sun, J.H.; Liou, M.J.; Li, Y.R.; Chou, W.Y.; Liu, F.H.; Chen, S.T.; Peng, S.J. Using deep convolutional neural networks for enhanced ultrasonographic image diagnosis of differentiated thyroid cancer. *Biomedicines* **2021**, *9*, 1771. [CrossRef]

254. Kim, G.; Lee, E.; Kim, H.; Yoon, J.; Park, V.; Kwak, J. Convolutional neural network to stratify the malignancy risk of thyroid nodules: Diagnostic performance compared with the American college of radiology thyroid imaging reporting and data system implemented by experienced radiologists. *Am. J. Neuroradiol.* **2021**, *42*, 1513–1519. [CrossRef]

255. Wu, G.G.; Lv, W.Z.; Yin, R.; Xu, J.W.; Yan, Y.J.; Chen, R.X.; Wang, J.Y.; Zhang, B.; Cui, X.W.; Dietrich, C.F. Deep learning based on ACR TI-RADS can improve the differential diagnosis of thyroid nodules. *Front. Oncol.* **2021**, *11*, 575166. [CrossRef]

256. Jin, Z.; Zhu, Y.; Zhang, S.; Xie, F.; Zhang, M.; Zhang, Y.; Tian, X.; Zhang, J.; Luo, Y.; Cao, J. Ultrasound computer-aided diagnosis (CAD) based on the thyroid imaging reporting and data system (TI-RADS) to distinguish benign from malignant thyroid nodules and the diagnostic performance of radiologists with different diagnostic experience. *Med. Sci. Monit. Int. Med. J. Exp. Clin. Res.* **2020**, *26*, e918452-1. [CrossRef]

257. Wang, X.; Agyekum, E.A.; Ren, Y.; Zhang, J.; Zhang, Q.; Sun, H.; Zhang, G.; Xu, F.; Bo, X.; Lv, W.; et al. A radiomic nomogram for the ultrasound-based evaluation of extrathyroidal extension in papillary thyroid carcinoma. *Front. Oncol.* **2021**, *11*, 625646. [CrossRef] [PubMed]

258. Wei, R.; Wang, H.; Wang, L.; Hu, W.; Sun, X.; Dai, Z.; Zhu, J.; Li, H.; Ge, Y.; Song, B. Radiomics based on multiparametric MRI for extrathyroidal extension feature prediction in papillary thyroid cancer. *BMC Med. Imaging* **2021**, *21*, 20. [CrossRef] [PubMed]

259. Zhou, H.; Jin, Y.; Dai, L.; Zhang, M.; Qiu, Y.; Wang, K.; Tian, J.; Zheng, J. Differential diagnosis of benign and malignant thyroid nodules using deep learning radiomics of thyroid ultrasound images. *Eur. J. Radiol.* **2020**, *127*, 108992. [CrossRef] [PubMed]

260. Gu, J.; Zhu, J.; Qiu, Q.; Wang, Y.; Bai, T.; Yin, Y. Prediction of immunohistochemistry of suspected thyroid nodules by use of machine learning–based radiomics. *Am. J. Roentgenol.* **2019**, *213*, 1348–1357. [CrossRef]

261. Park, V.Y.; Han, K.; Lee, E.; Kim, E.K.; Moon, H.J.; Yoon, J.H.; Kwak, J.Y. Association between radiomics signature and disease-free survival in conventional papillary thyroid carcinoma. *Sci. Rep.* **2019**, *9*, 4501. [CrossRef] [PubMed]

262. Himeur, Y.; Varlamis, I.; Kheddar, H.; Amira, A.; Atalla, S.; Singh, Y.; Bensaali, F.; Mansoor, W. Federated Learning for Computer Vision. *arXiv* **2023**, arXiv:2308.13558.

263. Shah, A.A.; Malik, H.A.M.; Muhammad, A.; Alourani, A.; Butt, Z.A. Deep learning ensemble 2D CNN approach towards the detection of lung cancer. *Sci. Rep.* **2023**, *13*, 2987. [CrossRef]

264. Salazar-Vega, J.; Ortiz-Prado, E.; Solis-Pazmino, P.; Gómez-Barreno, L.; Simbaña-Rivera, K.; Henriquez-Trujillo, A.R.; Brito, J.P.; Toulkeridis, T.; Coral-Almeida, M. Thyroid Cancer in Ecuador, a 16 years population-based analysis (2001–2016). *BMC Cancer* **2019**, *19*, 294. [CrossRef]

265. Elmore, L.W.; Greer, S.F.; Daniels, E.C.; Saxe, C.C.; Melner, M.H.; Krawiec, G.M.; Cance, W.G.; Phelps, W.C. Blueprint for cancer research: Critical gaps and opportunities. *CA Cancer J. Clin.* **2021**, *71*, 107–139. [CrossRef]

266. Park, S.H.; Choi, J.; Byeon, J.S. Key principles of clinical validation, device approval, and insurance coverage decisions of artificial intelligence. *Korean J. Radiol.* **2021**, *22*, 442. [CrossRef]

267. Zhu, Y.C.; AlZoubi, A.; Jassim, S.; Jiang, Q.; Zhang, Y.; Wang, Y.B.; Ye, X.D.; Hongbo, D. A generic deep learning framework to classify thyroid and breast lesions in ultrasound images. *Ultrasonics* **2021**, *110*, 106300. [CrossRef] [PubMed]

268. Wang, C.W.; Lin, K.Y.; Lin, Y.J.; Khalil, M.A.; Chu, K.L.; Chao, T.K. A soft label deep learning to assist breast cancer target therapy and thyroid cancer diagnosis. *Cancers* **2022**, *14*, 5312. [CrossRef]

269. Al-Qurayshi, Z.; Randolph, G.W.; Kandil, E. Cost-effectiveness of computed tomography nodal scan in patients with papillary thyroid carcinoma. *Oral Oncol.* **2021**, *118*, 105326. [CrossRef] [PubMed]

270. Yao, J.; Lei, Z.; Yue, W.; Feng, B.; Li, W.; Ou, D.; Feng, N.; Lu, Y.; Xu, J.; Chen, W.; et al. DeepThy-Net: A Multimodal Deep Learning Method for Predicting Cervical Lymph Node Metastasis in Papillary Thyroid Cancer. *Adv. Intell. Syst.* **2022**, *4*, 2200100. [CrossRef]

271. Sayed, A.N.; Himeur, Y.; Bensaali, F. From time-series to 2d images for building occupancy prediction using deep transfer learning. *Eng. Appl. Artif. Intell.* **2023**, *119*, 105786. [CrossRef]

272. Karsa, A.; Punwani, S.; Shmueli, K. An optimized and highly repeatable MRI acquisition and processing pipeline for quantitative susceptibility mapping in the head-and-neck region. *Magn. Reson. Med.* **2020**, *84*, 3206–3222. [CrossRef]

273. Kim, S.; Bang, J.I.; Boo, D.; Kim, B.; Choi, I.Y.; Ko, S.; Yoo, I.R.; Kim, K.; Kim, J.; Joo, Y.; et al. Second primary malignancy risk in thyroid cancer and matched patients with and without radioiodine therapy analysis from the observational health data sciences and informatics. *Eur. J. Nucl. Med. Mol. Imaging* **2022**, *49*, 3547–3556. [CrossRef]

274. Sardianos, C.; Varlamis, I.; Chronis, C.; Dimitrakopoulos, G.; Alsalemi, A.; Himeur, Y.; Bensaali, F.; Amira, A. The emergence of explainability of intelligent systems: Delivering explainable and personalized recommendations for energy efficiency. *Int. J. Intell. Syst.* **2021**, *36*, 656–680. [CrossRef]

275. Masuda, T.; Nakaura, T.; Funama, Y.; Sugino, K.; Sato, T.; Yoshiura, T.; Baba, Y.; Awai, K. Machine learning to identify lymph node metastasis from thyroid cancer in patients undergoing contrast-enhanced CT studies. *Radiography* **2021**, *27*, 920–926. [CrossRef]

276. Dov, D.; Kovalsky, S.; Cohen, J.; Range, D.; Henao, R.; Carin, L. Thyroid cancer malignancy prediction from whole slide cytopathology images. *arXiv* **2019**, arXiv:1904.00839.

277. Dov, D.; Kovalsky, S.Z.; Cohen, J.; Range, D.E.; Henao, R.; Carin, L. *AI-Assisted Thyroid Malignancy Prediction from Whole-Slide Images*; Stanford University: Palo Alto, CA, USA, 2019.

278. Halicek, M.; Shahedi, M.; Little, J.V.; Chen, A.Y.; Myers, L.L.; Sumer, B.D.; Fei, B. Head and neck cancer detection in digitized whole-slide histology using convolutional neural networks. *Sci. Rep.* **2019**, *9*, 14043. [CrossRef]

279. Lamy, J.B.; Sekar, B.; Guezennec, G.; Bouaud, J.; Séroussi, B. Explainable artificial intelligence for breast cancer: A visual case-based reasoning approach. *Artif. Intell. Med.* **2019**, *94*, 42–53. [CrossRef] [PubMed]

280. Kobylińska, K.; Mikołajczyk, T.; Adamek, M.; Orłowski, T.; Biecek, P. Explainable machine learning for modeling of early postoperative mortality in lung cancer. In *Artificial Intelligence in Medicine: Knowledge Representation and Transparent and Explainable Systems*; Springer: New York, NY, USA, 2019; pp. 161–174.

281. Pintelas, E.; Liaskos, M.; Livieris, I.E.; Kotsiantis, S.; Pintelas, P. Explainable Machine Learning Framework for Image Classification Problems: Case Study on Glioma Cancer Prediction. *J. Imaging* **2020**, *6*, 37. [CrossRef]

282. Lamy, J.B.; Sekar, B.D.; Guezennec, G.; Bouaud, J.; Séroussi, B. *Intelligence Artificielle Explicable Pour le Cancer du Sein: Une Approche Visuelle de Raisonnement à Partir de cas*; EGC: Bruxelles, Belgique, 2020; pp. 457–466.

283. Poceviciute, M.; Eilertsen, G.; Lundström, C. Survey of XAI in Digital Pathology. *Artif. Intell. Mach. Learn. Digit. Pathol. State-Art Future Challenges* **2020**, *12090*, 56.

284. Sayed, A.N.; Bensaali, F.; Himeur, Y.; Houchati, M. Edge-Based Real-Time Occupancy Detection System through a Non-Intrusive Sensing System. *Energies* **2023**, *16*, 2388. [CrossRef]

285. Alsalemi, A.; Himeur, Y.; Bensaali, F.; Amira, A. An innovative edge-based internet of energy solution for promoting energy saving in buildings. *Sustain. Cities Soc.* **2022**, *78*, 103571. [CrossRef]

286. Sayed, A.; Himeur, Y.; Alsalemi, A.; Bensaali, F.; Amira, A. Intelligent edge-based recommender system for internet of energy applications. *IEEE Syst. J.* **2021**, *16*, 5001–5010. [CrossRef]

287. Charteros, E.; Koutsopoulos, I. Edge Computing for Having an Edge on Cancer Treatment: A Mobile App for Breast Image Analysis. In Proceedings of the 2020 IEEE International Conference on Communications Workshops (ICC Workshops), Dublin, Ireland, 7–11 June 2020; IEEE: Washington, DC, USA, 2020; pp. 1–6.

288. Sufian, A.; Ghosh, A.; Sadiq, A.S.; Smarandache, F. A survey on deep transfer learning to edge computing for mitigating the COVID-19 pandemic. *J. Syst. Archit.* **2020**, *108*, 101830. [CrossRef]

289. Chen, J.; Li, K.; Rong, H.; Bilal, K.; Yang, N.; Li, K. A disease diagnosis and treatment recommendation system based on big data mining and cloud computing. *Inf. Sci.* **2018**, *435*, 124–149. [CrossRef]

290. Chai, X. Diagnosis Method of Thyroid Disease Combining Knowledge Graph and Deep Learning. *IEEE Access* **2020**, *8*, 149787–149795. [CrossRef]

291. Jagtap, P.; Jagdale, P.; Gawade, S.; Javalkar, P. Online Healthcare System Using the Concept of Cloud Computing. *Int. J. Sci. Res. Sci. Eng. Technol. IJSRSET* **2016**, *2*, 943–946.

292. Anuradha, M.; Jayasankar, T.; Prakash, N.; Sikkandar, M.Y.; Hemalakshmi, G.; Bharatiraja, C.; Britto, A.S.F. IoT enabled cancer prediction system to enhance the authentication and security using cloud computing. *Microprocess. Microsyst.* **2021**, *80*, 103301. [CrossRef]

293. Kečo, D.; Subasi, A.; Kevric, J. Cloud computing-based parallel genetic algorithm for gene selection in cancer classification. *Neural Comput. Appl.* **2018**, *30*, 1601–1610. [CrossRef]

294. Rajan, J.P.; Rajan, S.E.; Martis, R.J.; Panigrahi, B.K. Fog computing employed computer aided cancer classification system using deep neural network in internet of things based healthcare system. *J. Med. Syst.* **2020**, *44*, 34. [CrossRef] [PubMed]

295. Mutlag, A.A.; Abd Ghani, M.K.; Arunkumar, N.A.; Mohammed, M.A.; Mohd, O. Enabling technologies for fog computing in healthcare IoT systems. *Future Gener. Comput. Syst.* **2019**, *90*, 62–78. [CrossRef]

296. Hartmann, M.; Hashmi, U.S.; Imran, A. Edge computing in smart health care systems: Review, challenges, and research directions. *Trans. Emerg. Telecommun. Technol.* **2019**, *33*, e3710. [CrossRef]

297. Corchado Rodríguez, J.M. AI, Blockchain and Edge Computing for Industrial Predictive Maintenance. In Proceedings of the 9th Workshop on Service Oriented, Holonic and Multi-Agent Manufacturing Systems for Industry of the Future, SOHOMA 2019, Valencia, Spain, 3–4 October 2019.

298. Balaprakash, P.; Egele, R.; Salim, M.; Wild, S.; Vishwanath, V.; Xia, F.; Brettin, T.; Stevens, R. Scalable reinforcement-learning-based neural architecture search for cancer deep learning research. In Proceedings of the International Conference for High Performance Computing, Networking, Storage and Analysis, Denver, CO, USA, 17–22 November 2019; pp. 1–33.

299. Li, Z.; Xia, Y. Deep reinforcement learning for weakly-supervised lymph node segmentation in ct images. *IEEE J. Biomed. Health Inform.* **2020**, *25*, 774–783. [CrossRef]

300. Kerdjidj, O.; Himeur, Y.; Sohail, S.S.; Amira, A.; Fadli, F.; Atalla, S.; Mansoor, W.; Copiaco, A.; Daradkeh, M.; Gawanmeh, A.; et al. Uncovering the Potential of Indoor Localization: Role of Deep and Transfer Learning. *Preprints* **2023**, 2023062249. [CrossRef]

301. Kheddar, H.; Himeur, Y.; Awad, A.I. Deep Transfer Learning Applications in Intrusion Detection Systems: A Comprehensive Review. *arXiv* **2023**, arXiv:2304.10550.

302. Himeur, Y.; Al-Maadeed, S.; Kheddar, H.; Al-Maadeed, N.; Abualsaud, K.; Mohamed, A.; Khattab, T. Video surveillance using deep transfer learning and deep domain adaptation: Towards better generalization. *Eng. Appl. Artif. Intell.* **2023**, *119*, 105698. [CrossRef]

303. Kheddar, H.; Himeur, Y.; Al-Maadeed, S.; Amira, A.; Bensaali, F. Deep transfer learning for automatic speech recognition: Towards better generalization. *Knowl. Based Syst.* **2023**, *277*, 110851. [CrossRef]

304. Narayan, V.; Mall, P.K.; Alkhayyat, A.; Abhishek, K.; Kumar, S.; Pandey, P. Enhance-Net: An Approach to Boost the Performance of Deep Learning Model Based on Real-Time Medical Images. *J. Sensors* **2023**, *2023*, 8276738. [CrossRef]

305. Yu, J.; Deng, Y.; Liu, T.; Zhou, J.; Jia, X.; Xiao, T.; Zhou, S.; Li, J.; Guo, Y.; Wang, Y.; et al. Lymph node metastasis prediction of papillary thyroid carcinoma based on transfer learning radiomics. *Nat. Commun.* **2020**, *11*, 4807. [CrossRef]

306. Wang, Y.; Guan, Q.; Lao, I.; Wang, L.; Wu, Y.; Li, D.; Ji, Q.; Wang, Y.; Zhu, Y.; Lu, H.; et al. Using deep convolutional neural networks for multi-classification of thyroid tumor by histopathology: A large-scale pilot study. *Ann. Transl. Med.* **2019**, *7*, 468. [CrossRef] [PubMed]

307. Sundar, K.S.; Sai, S.S.S. Exploring Transfer Learning, Fine-tuning of Thyroid Ultrasound Images. In Proceedings of the 1st Conference on Medical Imaging with Deep Learning (MIDL 2018), Amsterdam, The Netherlands, 4–6 July 2018.

308. Liu, D.; Zhang, D.; Song, Y.; Zhang, C.; Zhang, F.; O'Donnell, L.; Cai, W. Nuclei Segmentation via a Deep Panoptic Model with Semantic Feature Fusion. In Proceedings of the IJCAI, 2019 International Joint Conference on Artificial Intelligence, Macao, China, 10–16 August 2019; pp. 861–868.

309. Elharrouss, O.; Al-Maadeed, S.; Subramanian, N.; Ottakath, N.; Almaadeed, N.; Himeur, Y. Panoptic segmentation: A review. *arXiv* **2021**, arXiv:2111.10250.

310. Yu, X.; Lou, B.; Zhang, D.; Winkel, D.; Arrahmane, N.; Diallo, M.; Meng, T.; von Busch, H.; Grimm, R.; Kiefer, B.; et al. Deep Attentive Panoptic Model for Prostate Cancer Detection Using Biparametric MRI Scans. In Proceedings of the International Conference on Medical Image Computing and Computer-Assisted Intervention, Lima, Peru, 4–8 October 2020; Springer: New York, NY, USA, 2020; pp. 594–604.

311. Cai, W.; Xiong, Z.; Sun, X.; Rosin, P.L.; Jin, L.; Peng, X. Panoptic Segmentation-Based Attention for Image Captioning. *Appl. Sci.* **2020**, *10*, 391. [CrossRef]

312. Ivanova, D. Artificial Intelligence in Internet of Medical Imaging Things: The Power of Thyroid Cancer Detection. In Proceedings of the 2018 International Conference on Information Technologies (InfoTech), Varna, Bulgaria, 20–21 September 2018; IEEE: Washington, DC, USA, 2018; pp. 1–4.

313. Borovska, P.; Ivanova, D.; Draganov, I. Internet of Medical Imaging Things and Analytics in Support of Precision Medicine for the Case Study of Thyroid Cancer Early Diagnostics. *Serdica J. Comput. Bulg. Acad. Sci. Inst. Math. Inform.* **2018**, *12*, 47–64.

314. Ivanova, D. Internet of Medical Imaging Things and the Application of Information Technologies for Early Detection of Thyroid Cancer. *Silico Intellect* **2017**, *1*, 20–25.

315. Seifert, P.; Ullrich, S.L.; Kühnel, C.; Gühne, F.; Drescher, R.; Winkens, T.; Freesmeyer, M. Optimization of Thyroid Volume Determination by Stitched 3D-Ultrasound Data Sets in Patients with Structural Thyroid Disease. *Biomedicines* **2023**, *11*, 381. [CrossRef]

316. Li, W.B.; Zhang, B.; Zhu, Q.L.; Jiang, Y.X.; Sun, J.; Yang, M.; Li, J.C. Comparison between thin-slice 3-D volumetric ultrasound and conventional ultrasound in the differentiation of benign and malignant thyroid lesions. *Ultrasound Med. Biol.* **2015**, *41*, 3096–3101. [CrossRef]

317. Lyshchik, A.; Drozd, V.; Reiners, C. Accuracy of three-dimensional ultrasound for thyroid volume measurement in children and adolescents. *Thyroid* **2004**, *14*, 113–120. [CrossRef]

318. Ying, M.; Yung, D.M.; Ho, K.K. Two-dimensional ultrasound measurement of thyroid gland volume: A new equation with higher correlation with 3-D ultrasound measurement. *Ultrasound Med. Biol.* **2008**, *34*, 56–63. [CrossRef]

319. Pakkasjärvi, N.; Luthra, T.; Anand, S. Artificial Intelligence in Surgical Learning. *Surgeries* **2023**, *4*, 86–97. [CrossRef]

320. Bodenstedt, S.; Wagner, M.; Müller-Stich, B.P.; Weitz, J.; Speidel, S. Artificial intelligence-assisted surgery: Potential and challenges. *Visc. Med.* **2020**, *36*, 450–455. [CrossRef]

321. Zhou, X.Y.; Guo, Y.; Shen, M.; Yang, G.Z. Artificial intelligence in surgery. *arXiv* **2019**, arXiv:2001.00627.

322. Zhou, X.Y.; Guo, Y.; Shen, M.; Yang, G.Z. Application of artificial intelligence in surgery. *Front. Med.* **2020**, *14*, 417–430. [CrossRef] [PubMed]

323. Berikol, G.B.; Berikol, G.; Bozdereli, D. Artificial intelligence in neuro, head, and neck surgery. In *Artificial Intelligence in Precision Health*; Elsevier: Amsterdam, The Netherlands, 2020; pp. 393–404.

324. Tan, L.; Tivey, D.; Kopunic, H.; Babidge, W.; Langley, S.; Maddern, G. Part 1: Artificial intelligence technology in surgery. *ANZ J. Surg.* **2020**, *90*, 2409–2414. [CrossRef]

325. Habal, M.B. Brave New Surgical Innovations: The Impact of Bioprinting, Machine Learning, and Artificial Intelligence in Craniofacial Surgery. *J. Craniofac. Surg.* **2020**, *31*, 889–890. [CrossRef] [PubMed]

326. Lee, D.; Yu, H.W.; Kwon, H.; Kong, H.J.; Lee, K.E.; Kim, H.C. Evaluation of Surgical Skills during Robotic Surgery by Deep Learning-Based Multiple Surgical Instrument Tracking in Training and Actual Operations. *J. Clin. Med.* **2020**, *9*, 1964. [CrossRef] [PubMed]

327. Voglis, S.; van Niftrik, C.H.; Staartjes, V.E.; Brandi, G.; Tschopp, O.; Regli, L.; Serra, C. Feasibility of machine learning based predictive modelling of postoperative hyponatremia after pituitary surgery. *Pituitary* **2020**, *23*, 543–551. [CrossRef] [PubMed]

328. Navarrete-Welton, A.J.; Hashimoto, D.A. Current applications of artificial intelligence for intraoperative decision support in surgery. *Front. Med.* **2020**, *14*, 369381. [CrossRef] [PubMed]

329. Melarkode, N.; Srinivasan, K.; Qaisar, S.M.; Plawiak, P. AI-Powered Diagnosis of Skin Cancer: A Contemporary Review, Open Challenges and Future Research Directions. *Cancers* **2023**, *15*, 1183. [CrossRef]

330. Kumar, Y.; Koul, A.; Singla, R.; Ijaz, M.F. Artificial intelligence in disease diagnosis: A systematic literature review, synthesizing framework and future research agenda. *J. Ambient. Intell. Humaniz. Comput.* **2022**, *14*, 8459–8486. [CrossRef]

331. Abdolali, F.; Shahroudnejad, A.; Hareendranathan, A.R.; Jaremko, J.L.; Noga, M.; Punithakumar, K. A systematic review on the role of artificial intelligence in sonographic diagnosis of thyroid cancer: Past, present and future. *Front. Biomed. Technol.* **2020**, *7*, 266–280. [CrossRef]

332. Petersson, L.; Larsson, I.; Nygren, J.M.; Nilsen, P.; Neher, M.; Reed, J.E.; Tyskbo, D.; Svedberg, P. Challenges to implementing artificial intelligence in healthcare: A qualitative interview study with healthcare leaders in Sweden. *BMC Health Serv. Res.* **2022**, *22*, 850. [CrossRef]

333. Sarker, I.H. Ai-based modeling: Techniques, applications and research issues towards automation, intelligent and smart systems. *SN Comput. Sci.* **2022**, *3*, 158. [CrossRef]

334. Himeur, Y.; Alsalemi, A.; Al-Kababji, A.; Bensaali, F.; Amira, A.; Sardianos, C.; Dimitrakopoulos, G.; Varlamis, I. A survey of recommender systems for energy efficiency in buildings: Principles, challenges and prospects. *Inf. Fusion* **2021**, *72*, 1–21. [CrossRef]

335. Areeb, Q.M.; Nadeem, M.; Sohail, S.S.; Imam, R.; Doctor, F.; Himeur, Y.; Hussain, A.; Amira, A. Filter bubbles in recommender systems: Fact or fallacy—A systematic review. *Wiley Interdisc. Rev. Data Min. Knowl. Discov.* **2023**, e1512. [CrossRef]

336. Varlamis, I.; Sardianos, C.; Chronis, C.; Dimitrakopoulos, G.; Himeur, Y.; Alsalemi, A.; Bensaali, F.; Amira, A. Smart fusion of sensor data and human feedback for personalized energy-saving recommendations. *Appl. Energy* **2022**, *305*, 117775. [CrossRef]

337. Atalla, S.; Daradkeh, M.; Gawanmeh, A.; Khalil, H.; Mansoor, W.; Miniaoui, S.; Himeur, Y. An Intelligent Recommendation System for Automating Academic Advising Based on Curriculum Analysis and Performance Modeling. *Mathematics* **2023**, *11*, 1098. [CrossRef]

338. Antunes, R.S.; André da Costa, C.; Küderle, A.; Yari, I.A.; Eskofier, B. Federated learning for healthcare: Systematic review and architecture proposal. *ACM Trans. Intell. Syst. Technol. (TIST)* **2022**, *13*, 1–23. [CrossRef]

339. Lee, H.; Chai, Y.J.; Joo, H.; Lee, K.; Hwang, J.Y.; Kim, S.M.; Kim, K.; Nam, I.C.; Choi, J.Y.; Yu, H.W.; et al. Federated learning for thyroid ultrasound image analysis to protect personal information: Validation study in a real health care environment. *JMIR Med. Informatics* **2021**, *9*, e25869. [CrossRef] [PubMed]

340. Sohail, S.S.; Madsen, D.Ø.; Himeur, Y.; Ashraf, M. Using ChatGPT to Navigate Ambivalent and Contradictory Research Findings on Artificial Intelligence. *Front. Artif. Intell.* **2023**, *6*, 1195797. [CrossRef] [PubMed]

341. Farhat, F.; Silva, E.S.; Hassani, H.; Madsen, D.Ø.; Sohail, S.S.; Himeur, Y.; Alam, M.A.; Zafar, A. Analyzing the scholarly footprint of ChatGPT: Mapping the progress and identifying future trends. *Preprints* **2023**, 2023062100. [CrossRef]

342. Sohail, S.S.; Farhat, F.; Himeur, Y.; Nadeem, M.; Madsen, D.Ø.; Singh, Y.; Atalla, S.; Mansoor, W. The future of gpt: A taxonomy of existing chatgpt research, current challenges, and possible future directions. *Curr. Challenges, Possible Future Dir.* **2023**. [CrossRef]

343. Haver, H.L.; Ambinder, E.B.; Bahl, M.; Oluyemi, E.T.; Jeudy, J.; Yi, P.H. Appropriateness of Breast Cancer Prevention and Screening Recommendations Provided by ChatGPT. *Radiology* **2023**, *307*, e230424. [CrossRef]

344. Cao, J.J.; Kwon, D.H.; Ghaziani, T.T.; Kwo, P.; Tse, G.; Kesselman, A.; Kamaya, A.; Tse, J.R. Accuracy of Information Provided by ChatGPT Regarding Liver Cancer Surveillance and Diagnosis. *Am. J. Roentgenol.* **2023**, *221*, 556–559. [CrossRef]

345. Sorin, V.; Klang, E.; Sklair-Levy, M.; Cohen, I.; Zippel, D.B.; Balint Lahat, N.; Konen, E.; Barash, Y. Large language model (ChatGPT) as a support tool for breast tumor board. *NPJ Breast Cancer* **2023**, *9*, 44. [CrossRef]